



LEHIGH
UNIVERSITY

Library &
Technology
Services

The Preserve: Lehigh Library Digital Collections

Interpenetrating Polymer Networks Of Poly(ethyl Acrylate) And Poly(methylmethacrylate-co- styrene): Morphology And Dynamic Mechanical Behavior.

Citation

HUELCK, VOLKER. *Interpenetrating Polymer Networks Of Poly(ethyl Acrylate) And Poly(methylmethacrylate-Co-styrene): Morphology And Dynamic Mechanical Behavior*. 1971, <https://preserve.lehigh.edu/lehigh-scholarship/graduate-publications-theses-dissertations/theses-dissertations-332>.

Find more at <https://preserve.lehigh.edu/>

This document is brought to you for free and open access by Lehigh Preserve. It has been accepted for inclusion by an authorized administrator of Lehigh Preserve. For more information, please contact preserve@lehigh.edu.

72-9294

HUELCK, Volker, 1940-

INTERPENETRATING POLYMER NETWORKS OF POLY(ETHYL
ACRYLATE) AND POLY(METHYL METHACRYLATE-CO-
STYRENE): MORPHOLOGY AND DYNAMIC MECHANICAL
BEHAVIOR.

Lehigh University, Ph.D., 1971
Engineering, chemical

University Microfilms, A XEROX Company, Ann Arbor, Michigan

INTERPENETRATING POLYMER NETWORKS OF POLY(ETHYL
ACRYLATE) AND POLY(METHYL METHACRYLATE-CO-
STYRENE): MORPHOLOGY AND DYNAMIC
MECHANICAL BEHAVIOR

by

Volker Huelck

A Dissertation

Presented to the Graduate Committee

of Lehigh University

in Candidacy for the Degree of

Doctor of Philosophy

in

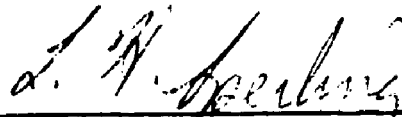
Chemical Engineering

Lehigh University

1971

Approved and recommended for acceptance as a dissertation
in partial fulfillment of the requirements for the degree of
Doctor of Philosophy.

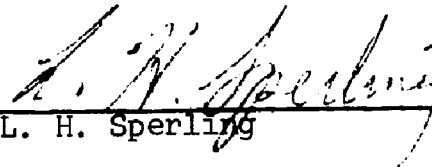
July 14, 1971



Professor in Charge, L. H. Sperling

Accepted, July 14, 1971


Special committee directing the
doctoral work of Mr. Volker Huelck



L. H. Sperling Chairman



J. A. Manson



E. P. Ostocka



G. W. Poehlein



D. A. Thomas

PLEASE NOTE:

**Some Pages have indistinct
print. Filmed as received.**

UNIVERSITY MICROFILMS

DEDICATION

I wish to dedicate this thesis to my wife

Wiltrud D. H. Huelck-Freese

ACKNOWLEDGEMENT

The author wishes to express his gratitude to Dr. L. H. Sperling for his valuable guidance throughout the course of this investigation. Grateful acknowledgements go also to Drs. J. A. Manson and D. A. Thomas for their beneficial discussions and contributions. This sincere appreciation is extended to Dr. M. Matsuo, who served very kindly as a visiting member of the research committee, and to Drs. E. P. Otocka and G. W. Poehlein for their helpful suggestions. The discussions with Mrs. E. Chiu are also greatly appreciated.

The author is indebted to the National Science Foundation for providing the financial support for this academic endeavor.

TABLE OF CONTENTS

| | <u>page</u> |
|---|-------------|
| Abstract | 1 |
| I. General Introduction | 2 |
| II. Background and Review of Two-Phase Polymeric Systems | 5 |
| A. Thermodynamic Considerations | 5 |
| B. Methods of Preparation of Two-Phase Polymers | 9 |
| 1. Melt Blending | |
| 2. Solution Mixing | |
| 3. Graft Copolymers | |
| 4. Block Copolymers | |
| C. Dynamic Mechanical Behavior of Two-Phase Polymers | 13 |
| D. Morphology of Two-Phase Polymers via Electron Microscopy | 20 |
| E. Domain Formation | 25 |
| III. Interpenetrating Polymer Networks | 28 |
| A. History of IPN's | 28 |
| B. Statement of the Problem | 36 |
| IV. Experimental | 37 |
| A. Materials | 37 |
| B. Synthesis | 38 |

| | <u>page</u> |
|------------------------------------|-------------|
| C. Mechanical Experiments | 45 |
| 1. GEHMAN Torsion Stiffness Tester | |
| 2. Viscoelastometer (Rheovibron) | |
| D. Electron Microscopy | 49 |
| V. Experimental Results | 51 |
| A. Creep Data | 52 |
| B. Dynamic Mechanical Behavior | 57 |
| 1. Leathery Series | |
| 2. Elastomeric Series | |
| 3. Plastic Series | |
| 4. Inverse Series | |
| C. Electron Micrographs | 79 |
| 1. Leathery Series | |
| 2. Elastomeric Series | |
| 3. Plastic Series | |
| 4. Inverse Series | |
| VI. Discussion | 102 |
| A. Creep Behavior | 102 |
| 1. Glass Transition Behavior | |
| 2. Rubbery Plateau Considerations | |
| 3. Relaxation Behavior | |
| 4. Grafting Effects | |

| | <u>page</u> |
|---|-------------|
| B. Dynamic Mechanical Behavior | 116 |
| 1. Change in Compatibility within Series L, E and P | |
| 2. Comparison Normal-Inverse IPN's | |
| C. Micromorphology | 120 |
| 1. OsO ₄ Staining Technique | |
| 2. Micromorphological Features | |
| D. General Discussion | 129 |
| 1. E'-Morphology Considerations | |
| 2. E" Considerations | |
| E. Dynamic Mechanical Behavior-Structure Relationship | 145 |
| 1. Compatibility | |
| 2. Phase Inversion | |
| 3. Evidence of Interpenetration | |
| VII. Conclusions | 152 |
| VIII. Recommendations | 154 |
| IX. Appendix | 156 |
| X. Bibliography | 160 |
| Vita | 168 |

LIST OF FIGURES

| <u>No.</u> | | <u>page</u> |
|------------|---|-------------|
| 1. | Schematic illustration of an IPN snythesis | 30 |
| 2. | 3 x shear modulus vs. temperature for 3 IPN's G1 (●), G3(+) and G5 (o) (data from (92)) | 53 |
| 3. | 3 x shear modulus vs. time for IPN G5 (from (92)) | 56 |
| 4. | Temperature dependence of E' and E'' of IPN L1 | 58 |
| 5. | Temperature dependence of E' and E'' of IPN L4 | 59 |
| 6. | Temperature dependence of E' and E'' of IPN L5 | 60 |
| 7. | Temperature dependence of E' and E'' of IPN L6 | 61 |
| 8. | Temperature dependence of E' and E'' of IPN E1 | 63 |
| 9. | Temperature dependence of E' and E'' of IPN E2 | 64 |
| 10. | Temperature dependence of E' and E'' of IPN E3 | 65 |
| 11. | Temperature dependence of E' and E'' of IPN E4 | 66 |
| 12. | Temperature dependence of E' and E'' of IPN P1 | 68 |
| 13. | Temperature dependence of E' and E'' of IPN P3 | 69 |
| 14. | Temperature dependence of E' and E'' of IPN P4 | 70 |

| <u>No.</u> | <u>page</u> |
|--|-------------|
| 15. Temperature dependence of E' and E'' of IPN P5 | 71 |
| 16. Temperature dependence of E' and E'' of 2 IPN's I1 and E1 | 73 |
| 17. Temperature dependence of E' and E'' of 2 IPN's I2, L1 and blend | 74 |
| 18. Temperature dependence of E' and E'' of 2 IPN's I3 and P1 | 75 |
| 19. Temperature dependence of E' and E'' of 2 IPN's I4 and E4 | 76 |
| 20. Temperature dependence of E' and E'' of 2 IPN's I5 and L6 | 77 |
| 21. Temperature dependence of E' and E'' of 2 IPN's I6 and P5 | 78 |
| 22. Electron micrograph of IPN L1 | 80 |
| 23. Electron micrograph of IPN L4 | 82 |
| 24. Electron micrograph of IPN L5 | 83 |
| 25. Electron micrograph of IPN L6 | 84 |
| 26. Electron micrograph of IPN G1 | 85 |
| 27. Electron micrograph of IPN E1 | 87 |
| 28. Electron micrograph of IPN E2 | 88 |
| 29. Electron micrograph of IPN E3 | 89 |
| 30. Electron micrograph of IPN E4 | 90 |
| 31. Electron micrograph of IPN P1 | 92 |
| 32. Electron micrograph of IPN P3 | 93 |
| 33. Electron micrograph of IPN P4 | 94 |

| <u>No.</u> | <u>page</u> |
|---|-------------|
| 34. Electron micrograph of IPN P5 | 95 |
| 35. Electron micrograph of IPN I2 | 97 |
| 36. Electron micrograph of IPN I1 | 98 |
| 37. Electron micrograph of IPN I3 | 99 |
| 38. Electron micrograph of IPN I6 | 100 |
| 39. Mastercurve for IPN G5; (+) single relaxation time assumption (T-A-D theory); (o) equation (VI,4), assuming a random distribution of compositions (from (93)) | 107 |
| 40. Experimental shift factors compared with those predicted by WLF equation (VI,6) for IPN G5 (from (93)) | 108 |
| 41. Slopes of intermediate E'-plateau regions for PEAB/PS IPN's | 130 |
| 42. Slopes of intermediate E'-plateau regions for PEAB/PMMA IPN's | 131 |
| 43. Storage moduli at 25°C for PEAB/PS IPN's | 134 |
| 44. Storage moduli at 25°C for PEAB/PMMA IPN's | 135 |
| 45. Dependency of the PEAB and PS loss peak temperatures on the plastic fraction in the IPN's | 141 |
| 46. Temperature dependence of tan δ of 4 IPN's | 142 |
| 47. Temperature dependence of the PEAB and PX damping maxima on the PS fraction in the IPN's | 144 |
| 48. Compatibility ranges for 3 polyblend systems | 149 |

| <u>No.</u> | | <u>page</u> |
|------------|---|-------------|
| A-1. | Temperature dependence of E' and E'' of PEAB | 157 |
| A-2. | Temperature dependence of E' and E'' of PS | 158 |
| A-3. | Temperature dependence of E' and E'' of PMMA | 159 |

LIST OF TABLES

| <u>No.</u> | | <u>page</u> |
|------------|--|-------------|
| 1. | Compositions of the investigated IPN's | 40 |
| 2. | Rubbery moduli, E_2 , of the employed homopolymers and the ² G-series IPN's | 55 |
| 3. | Rubbery moduli and crosslink densities of PEA and PEAB | 114 |
| 4. | Glass transition temperatures ($^{\circ}\text{C}$) and maximum loss peak temperatures of the employed homopolymers | 138 |

LIST OF ABBREVIATIONS

The following abbreviations are used throughout the thesis:

| | |
|---------|---|
| ABS: | acrylonitrile-butadiene-styrene polymer blend |
| AN: | acrylonitrile |
| AS: | acrylonitrile-styrene copolymer |
| DMF: | N-dimethyl formamide |
| DMGDM: | decamethylene glycol dimethacrylate |
| DVB: | divinyl benzene |
| EA: | ethyl acrylate |
| EGDM: | ethylene glycol dimethacrylate |
| EVA: | ethylene-vinylacetate rubber |
| HIPMMA: | high impact resistant poly(methyl methacrylate) |
| HIPS: | high impact resistant polystyrene |
| IPN: | interpenetrating polymer network |
| IEN: | interpenetrating elastomeric network |
| MBS: | methyl methacrylate-butadiene-styrene polymer blend |
| MEK: | methyl ethyl ketone |
| MMA: | methyl methacrylate |
| NBR: | acrylonitrile-butadiene rubber |
| PB: | polybutadiene |
| PEA: | poly(ethyl acrylate) |

PEAB: butadiene doped poly (ethyl acrylate)
PI: poly(methyl methacrylate)
PS: polystyrene
PU: polyurethane
PVC: poly(vinyl chloride)
S: styrene
SB: styrene-butadiene block copolymer
SBR: styrene-butadiene rubber
SBS: styrene-butadiene-styrene block copolymer
SI: styrene-isoprene block copolymer
SIN: simultaneous interpenetrating networks
SIR: styrene-isoprene rubber
SIS: styrene-isoprene-styrene block copolymer
TEGDM: tetraethylene glycol dimethacrylate
THF: tetrahydrofuran

ABSTRACT

Interpenetrating Polymer Networks (IPN's) have been synthesized by swelling a crosslinked rubbery polymer (I) with a second plastic monomer (II or III or II-co-III) plus initiator and crosslinking agent and polymerizing the second monomer in situ. IPN's have also been produced by inverting the order of preparation. According to the overall compositions IPN's of elastomeric or leathery or plastic behavior have been obtained. Polymers employed were poly(ethyl acrylate) (I), polystyrene (II) and poly(methyl methacrylate) (III).

Electron microscopy revealed a very complex structure exhibiting various degrees of compatibility: cellular phase domains exist simultaneously with a fine structure. Dynamic mechanical properties also indicate the extent of phase separation. Inverting the sequence of preparation showed that the network synthesized first controls the morphology and thus the properties of the IPN's.

I. GENERAL INTRODUCTION

Modification of homopolymers ranks as one of the most important processes in polymer technology.. The general objective for any kind of modification is to make the polymers more suitable for special applications. One way to modify homopolymers is by incorporating a second, different homopolymer, thus yielding two-phase materials. In this fashion rigid polymers have been altered by inclusion of elastomers while rubbery polymers have been modified by the addition of plastics. Improvement in toughness without a significant loss in rigidity serves as an example for the former case and an increase in ultimate tensile strength for the latter. The first commercially important heterophase polymer system was an impact resistant polystyrene introduced in 1948 by Dow Chemical Co. (1).

Most of the two-phase polymers can be denoted as polyblends. They are mixtures of structurally different homo- or copolymers. Graft- and block-copolymers are a special type of polyblends. They are not strictly blends in the physical sense, but they form "solid arrays that physically resemble mixtures" (2). Substantial contributions to the development of commercial polymeric materials are due to graft- and block- copolymers. The most common examples are plastic-rubber blends¹⁾, which can vary from homogeneous and transparent and thus more compatible to heterogeneous and opaque and thus incompatible materials.

The polyblends do not include random copolymers, because the homogeneous copolymers do not have enough long segments in the chain of either monomer to yield characteristic features of either homopolymeric structure (1); i.e. a random copolymer behaves almost like another homopolymer with a transition temperature between the ones of the pure homopolymers (3).

Interpenetrating Polymer Networks (IPN's) are structurally closer related to graft copolymers than to the other types of polyblends. Here two or more polymeric networks are superimposed on each other, as shown in Figure 1 (page 30). According to their preparation and synthesis IPN's are considered to be approximately chemically independent but physically interlocked. They have first been polymerized in 1960 by MILLAR (4). All networks of his IPN's consisted of polystyrene crosslinked with divinylbenzene. When one elastomeric and one plastic component are superimposed to form an IPN, a novel type of polyblend appeared, which has at first been synthesized by SPERLING and FRIEDMAN (6). Thus IPN's consisting of an elastomeric and a plastic network are expected to exhibit interesting properties.

1) Rubber-rubber and plastic-plastic blends are also known. The former ones are employed in the tire industry while the latter ones are used in the fiberglass industry.

This thesis is concerned with the elucidation of such IPN's with respect to the dynamic mechanical behavior, the morphology, the relationship between these two features, and with the degree of compatibility between the elastomeric and the plastic component.

II. BACKGROUND AND REVIEW OF TWO-PHASE POLYMERIC SYSTEMS

Since the IPN's can be considered as a special type of polyblends, this chapter deals with several general aspects of these two-phase polymeric materials. The first section, on general thermodynamic considerations of mixing, is followed by a brief description of the most important methods of preparing such systems. Deliberately this second section does not review the voluminous literature on preparative methods, except for a few examples. However, appropriate references will be cited and briefly discussed in the following sections on dynamic mechanical behavior and on the morphology of two-phase polymers.

A. Thermodynamic Considerations

Preparation of two-phase polymers is thermodynamically considered to be a mixing process of two different polymers. Provided the molecular weights of both polymers are equal, the following relation holds (7):

$$\mu_1 - \mu_1^0 = RT (\ln v_1 + \chi_{12} v_2^2) \quad (II,1)$$

$$\mu_2 - \mu_2^0 = RT (\ln v_2 + \chi_{12} v_1^2)$$

where μ = chemical potential or partial molar free energy

μ^0 = chemical potential in the standard state

v = volume fractions in the homopolymers

χ_{ij} = interaction parameter between components i and j

Equation II,1 represents the chemical potential "for a regular binary solution in which the heat of dilution can be expressed in the VAN LAAR form" (7,8). The parameter χ is proportional to the size of the molecule as given by the number x of segments per molecule. The free energy of interaction is very small when x is very large. That is why the occurring entropy change in a mixing process of high molecular weight polymers is small - "orders of magnitude less than that for mixing equivalent masses of low-molecular weight liquids" (9,10).

The change in GIBBS free energy of interaction, ΔF , for a mixing process is:

$$\Delta F = \Delta H - T\Delta S \quad (\text{II},2)$$

where ΔH and ΔS are the changes in enthalpy and entropy, respectively, and where T is the absolute temperature at which these changes occur. ΔS is small, but positive, since mixing increases the randomness of disorder, and thus favors mutual solubility. The heat of mixing, ΔH , determines the degree of solubility and thus compatibility. The mixing of a pair of polymers is endothermic in most cases. The last is analogous to mixing of low molecular liquids and results from the fact that the free energy of interaction, w_{ij} , associated with the

formation of a contact between a pair of segments of two different molecules usually exceeds the arithmetic mean of w_{ii} and w_{jj} of two identical molecules (7). Because of the small value of $T\Delta S$ for mutual solubility to occur, i.e. for $\Delta F < 0$, the enthalpy of mixing must be very small or negative.

The quantity ΔH expresses the affinity of molecules for their neighboring molecules. The solubility parameter, δ , which describes the cohesive energy density, allows prediction of the affinity of polymer pairs. For endothermic mixing of nonpolar substances the enthalpy change, ΔH is given by (8):

$$\Delta H = v_1 v_2 (\delta_1 - \delta_2)^2 \quad (\text{II},3)$$

It is easily seen that ΔH is always positive. That means that in equation II,2 the term $T\Delta S$ has to be larger than ΔH in order for true solution to occur. This is equivalent with the condition of approximate equality of the two solubility parameters.

The case $\Delta H < 0$ which is possible for polar polymers indicates a decrease in the systems' energy upon mixing, which expresses the extremely rare case that molecules are attracted more by their neighbors than by their own species. These exceptions occur in cases of strong interactions, i.e. "hydrogen bonding between substituent groups on the different molecules" (9) and stereoisomerization. Both processes provide favorable association energies in the mixture, and therefore tend to

produce homogeneous polymers (2,9-11).

SMITH and coworkers investigated the effect of hydrogen bonding on polymer mixtures (12). Many polymer pairs possessing a multiplicity of ether and carboxylic acid functions exhibit this phenomenon. Upon mixing aqueous solutions of poly(acrylic acid) and poly(ethylene oxide) a polymeric substance is precipitated whose characteristic properties differ from the ones of the two homopolymers. WATANABE and coworkers (13) - in an example for stereoisomerization - prepared mixtures of isotactic and syndiotactic poly(methyl methacrylate) which melts sharply to clear solution. This mixture is considered a complex of "linearly ordered arrays of isotactic and syndiotactic helical sequences" (13).

Several tables are available listing sequences of compatible polymer pairs (2,12-16). The difference in the solubility parameters, δ , of the two polymers does usually not exceed the value of 0.5. However, in many cases the listed composite polymers do not exhibit mutual solubility and thus compatibility occurs neither over the whole range of composition (14) nor for all different methods of preparation (17). Thus the method by which two-phase polymers are produced influences their properties.

B. Methods of Preparation of Two-Phase Polymers

Today there exists a considerable number of standard techniques of preparing two-phase polymeric materials. Some basic methods will be presented here. However, only the imagination limits the multiplicity of methods.

Generally there are four different classifications (14) for producing those materials which can be considered polyblends:

1. The most direct method is mechanical blending, which is mostly done in the melted state.
2. The second process involves mixing of two polymers in a common solvent where the product is obtained by precipitation or drying.
3. Dissolving a polymer in a second monomer (or dissolving a monomer in an emulsion polymer) and polymerizing the solution in bulk produces graft copolymers: grafted chains of one component on a backbone of the other.
4. Block copolymers are generally prepared in a two-step process. The functional groups at the chain ends of the first polymer allow a second polymer to be polymerized through the activation of the end groups.

1. Melt Blending

Intimate contact and eventually molecular mixing between two amorphous polymers can only be achieved by blending above the glass transition temperature, T_g , because of the otherwise

insufficient mobility of the polymer molecules and in order to minimize the breakage of bonds.

The blending of latexes, which also fits into this category, yields an intimate, uniform dispersion. It enables one to control the particle size of the dispersed phase to a limited extent "without affecting the properties of the individual component phases" (9).

The determining factor for the degree of molecular mixing is the mutual diffusion of the macromolecules (18,19). With limited time of mixing, the degree of mutual solubility obtained depends on the extent of thermodynamic equilibrium reached. If this is not reached then even compatible polymer pairs would exhibit at least partial phase separation. A detailed concept of the term "compatibility" in relation to phase separation will be developed in section VI, E, 1.

2. Solution Mixing

The restricting factor of not reaching equilibrium as with melt mixing can be overcome by dissolving both polymers, if possible, in a common solvent. A compatible polymer pair at sufficient dilution is capable of forming a homogeneous solution. Evaporation, drying and precipitation methods are applied for gaining the polymeric substance in solid form (14). However, the removal of the diluent often changes the domain sizes of the blend and may even cause complete phase separation. Since in

most cases the affinity of both polymers for the diluent is not equal, the one with the lesser affinity will selectively precipitate. Thus even macroheterogeneous systems might result by this method (2).

The conditions favorable to solution mixing of polyblends for the preparation of microheterogeneous or homogeneous one-phase materials are "obviously more stringent than those necessary from the thermodynamic analysis" (2).

3. Graft Copolymers

Conceptually and mechanistically, graft and block polymerization reactions can generally be treated as one. Both involve initiation of the polymerization reactions with functional groups bound to polymer molecules. With graft copolymers, however, the activation is restricted to internal repeating units of the backbone and the polymerization reaction is directly initiated by the polymer chain radical. There exist three general methods for the synthesis of graft copolymers, namely: (a) the chain-transfer mechanism mentioned above, (b) a radiation or photochemical activation of polymer molecules, which provide the active sites for grafting, and (c) "either the use of polymer molecules with labile functional groups or the chemical modification of polymers to create active sites for grafting" (20). In all cases only a small percentage of the molecules in a graft-copolymer are actually grafted. High impact resistant polystyrene (HIPS) and the acrylonitrile-butadiene-styrene plastics

(ABS) are the most common commercial examples. The former one is prepared by dissolving polybutadiene (PB) in styrene (S) monomer and subsequent polymerization. The latter one is often produced by emulsion polymerization, in which PB rubber latex is used as starting material and monomers acrylonitrile (AN) and S are added as glassy components. "The key reaction in this process lies in the graft reaction of AS copolymer onto rubber polymer molecules" (21).

4. Block Copolymers

Materials of homopolymeric segments of considerable size which are chemically linked end to end in a polymeric chain are termed block copolymers (14, 22,128). As mentioned above they are produced in a multiple-step process. The number of steps depends on the number of segments in the polymeric chain. The first homopolymer or chain segment is synthesized under conditions, such that the chain ends contain functional groups. These can be either alcohols, amines, halides, or radicals, cations and anions (2). The second monomer is then polymerized through the activation of the end groups. Commercially the most frequently applied technique is anionic polymerization. S-B and S-B-S block copolymers are the most common examples produced in this way (22-24).

C. Dynamic Mechanical Behavior of Two-Phase Polymers

Dynamic mechanical tests measure the response or deformation of a material to periodic or varying forces. Those tests provide simultaneous information about an elastic modulus, mostly the shear modulus, and a mechanical damping, which corresponds to the fraction of thermal energy dissipated during the deformation of the sample.

Out of the large number of different instruments, frequently designed privately, only very few are commercially available. The commercial unit employed in this laboratory is the direct reading viscoelastometer, Rheovibron, Model DDV-II. Besides the torsional pendulum this is the most often used commercial equipment. Since 1967 most of the dynamic mechanical data reported in the literature have been obtained with the Rheovibron (see section IV,C,2).

Several investigations of commercially important two-phase polymeric systems of general novelty are presented and summarized below.

HUGHES and BROWN (26,27) investigated several heterogeneous polymer systems by conducting torsional modulus studies measuring shear moduli. Among these systems was the isomeric combination PEA/PMMA, the IPN of which is investigated by this author. Their samples were prepared (a) by mixing of the two homopolymer emulsions (50 PEA/50 PMMA),

(b) by dissolving the two polymers together in CHCl_3 (21 PEA/79 PMMA), and (c) by polymerization of EA in the presence of the PMMA-backbone containing mercaptan groups which resulted in a graft copolymer (21 PEA/79 PMMA). With samples (a) and (b) a transition was found at -28°C corresponding to the PEA-homopolymer. No attempt has been made to explain why this transition is below the measured T_g for PEA (-22°C), although partial molecular mixing between the two isomeric materials should cause the opposite effect. The corresponding graft copolymer begins to soften slowly above T_g (PEA), however, it does not exhibit any transition corresponding to its PEA-content. Thus it is the most compatible system among these three pairs.

The same system of PEA and PMMA has been investigated by other authors(28). They prepared their two-phase materials by mixing aqueous dispersions of the homopolymers (particle size 1000 \AA). They found between the elevated damping peak temperatures of PEA (3°C) and PMMA (108°C) an intermediate peak (51°C), which they ascribed to interactions of the PEA- and PMMA- segments in the vicinity of the phase boundaries. This peak vanished upon annealing the materials. The dynamic moduli of a series of PEA/PMMA samples, prepared by the same investigators (28) via polymerizing EA in the presence of PMMA, showed in all cases only two clear transition

regions, i.e. incompatibility. Indications of a peak in the middle region could not be observed.

In a classical paper TAKAYANAGI and coworkers (29) developed and investigated a method for the evaluation of the viscoelastic behavior of blends of two amorphous polymers from those of component polymers. They derived equations expressing the behavior of several types of blends. The researchers investigated an ABS polymer and a blend of PVC and NBR prepared by evaporation of the THF-solution of the two components where the former served as an example of two separate phases and the latter as an example of a molecularly mixed system.

Dynamic mechanical experiments employing a Rheovibron, Model DDV-I, at 138 cps confirmed that the behavior of two separate phases could be described by a simple mechanical model. Glass and rubbery plateau moduli of the component polymers as well as their volume fractions and the type of mixing were used for developing this model (29). For the molecularly mixed system the investigators found one broad dispersion at an intermediate temperature between glass transition regions of the two component polymers. The broadening of the dispersion was explained by the existence of a microheterogeneous phase. No mechanical model has been successfully applied in this case.

MANABE and coworkers from TAKAYANAGI's laboratory (30) recently made a new approach of developing a model for a microheterogeneous blend (PVC/NBR blend). They assumed that a blend system is composed of many cells having different values of free volume fraction. An explanation of the viscoelastic behavior of actual polymer blends was presented by using a distribution function of a free volume fraction. This function was obtained from dilatometric experiments. The agreement between the calculated dynamic storage modulus, E' , and the experimental data was fairly good, while the experimental dynamic loss modulus, E'' , deviated considerably from the model values.

MATSUO (31,32) investigated the dynamic mechanical behavior of the same system TAKAYANAGI (29) did. However, he prepared the PVC/NBR materials by mechanical blending of the two polymers. TAKAYANAGI did not specify the AN-content (acrylonitrile content) in the NBR-phase, while MATSUO varied the AN-portion systematically. He found that the compatibility in PVC/NBR blends is controlled by the AN-content of the NBR: an increase in AN-content results in an increase in their compatibility with PVC. A comparison of the two studies by MATSUO (31) and TAKAYANAGI (29) reveals that besides the AN-content also the method of preparation determines the degree of compatibility. This conclusion has been investigated in

detail and confirmed by MANABE and coinvestigators (30). They prepared samples of PVC/NBR containing various small amounts of DMF and chloroform. It should be noted that DMF and chloroform are the solvents for NBR and PVC, respectively. The investigators found that by treatment with chloroform the peak of E'' became broader and its location was shifted to lower temperatures but that this peak did not separate into two peaks. "This means that PVC, which is insoluble in chloroform itself, becomes soluble in chloroform by the existence of NBR" (30), i.e. the free volume of PVC/NBR and the solvent are communized¹⁾ with each other. A similar tendency is found for the system containing DMF as solvent.

Among the commercially widely used block copolymers much attention has been given to ABA type polymers in which the intermediate block is PB and the end blocks are PS (SBS block copolymers). One of the most frequently investigated materials of this type is the elastomeric Kraton 101 (Shell Chemical Co.) (33-37) which contains 30 wt.% of styrene. COOPER and TOBOLSKY (36) showed in modulus-temperature curves that this material exhibits an extended high rubbery "plateau modulus", at intermediate temperatures from which they concluded that physical

¹⁾Free volumes of several components are communized, when all components after mixing behave as one component with a common free volume (30).

interaction reinforces the structure until the T_g of the higher modulus is reached.

BEECHER and coworkers (33) showed that for SBS block copolymers time and temperature can be considered equivalent variables, because the fit of the WLF equation is surprisingly good (below 0°C, the chosen reference temp.). This has been confirmed by SMITH and DICKIE (35). The investigators (33) found in addition to the two distinct transitions of PS and PB an intermediate broad damping peak for Kraton samples cast from CCl_4 . This peak was less marked for samples cast from mixtures of benzene/heptane and THF/MEK (33,37). The intermediate peak was interpreted to be due to a glass transition of PS segments which are not completely separated from the PB phase, thus indicating a certain degree of phase mixing. Since HOLDEN and coworkers (34) did only find two glass transitions for compression molded Kraton samples, however, no intermediate peak, the partial phase mixing (33) must be due to the presence of the solvents.

MATSUO (31) systematically investigated the PS/PB block copolymers. His first series of samples contained various block fractions like SB, BSB, SBS, SBSB of a constant mole ratio of S/B. A similar series was also studied by HARPELL and THRASHER (38). Essentially no differences were found from dynamic mechanical measurements, which showed two E'' -peaks

indicating a heterogeneous, two-phase system. NIELSEN (39) and STAVERMAN (40) have reported these two E'' -peak already several years ago for HiPS, where the two phases of PS and PB are connected by physical blending. The later discovered graft type HiPS shows approximately the same dynamic mechanical behavior (31). The mechanical differences between the block copolymers are evident. The SBS and SBSB samples were demonstrated to be extremely tough while SB and BSB samples are as brittle as pure PS (31,32,34,41). References (31,32,42,43) show that the differences in physical behavior between the various block copolymers and also between the HiPS blend and graft type depend on the morphology (see section II,C). MATSUO's second series of SBS samples with various block B fractions showed variations in heights of the E'' -peaks according to the S/B mole ratio(31).

Dynamic mechanical properties of a model reinforced elastomer, SBR reinforced with PS particles (400 \AA), were studied by KRAUS and coworkers (44,45) and by NIELSEN (46). The rubbery plateau region was raised dramatically by the addition of the PS filler, while the glass plateau region remained almost constant. The height of the loss tangent maximum was unaffected. MORTON and HEALY (47) demonstrated that the PS filler increases tensile strength of the elastomers because of the increased viscoelasticity. All the essential features of the dynamic behavior of SBR reinforced with PS "could be described

in terms of the properties of the component polymers by the phenomenological equivalent mechanical model treatment of TAKAYANAGI" (44). A system similar to the SBR is the SIR(36, 41,48,49). Here the PB has been replaced by PI (polyisoprene); however, this system has not been as successful commercially as the SBR's.

COOPER and TOBOLSKY (36) investigated polyurethanes (PU). Their dynamic mechanical experiments showed that the PU behave like block copolymers, which has been confirmed by ESTES and coworkers (50) and by HARRELL (51). PVC and many of its altered forms is another commercially very important polymer, which in many cases can be considered as a two-phase system (e.g. when plasticized). Their dynamic mechanical properties have been extensively investigated (52-56). Mentioning of similar investigations for blends of poly(2,6-dimethyl-1, 4 phenylene ether) and PS (57) and of epoxy polymers (58) may conclude this list.

D. Morphology of Two-Phase Polymers via Electron Microscopy

KATO's discovery of the OsO_4 -staining (59) of unsaturated polymer particles in 1966 led the research in the field of morphology of two-phase polymeric systems in a completely new direction. Before that many investigators tried various methods of sample preparation such as bromination (59,60), Cr-shadowing (59,61), staining by heavy metal salts (62), phase

contrast microscopy (63) or fracture electron microscopy (28,40).

KATO found that exposure to OsO_4 vapor (59) and soaking in dilute aqueous solution of OsO_4 (64) "produces excellent fixing and staining of polybutadiene and other unsaturated polymer particles, resulting in good electron micrographs"(59). He postulated that unsaturated double bonds are responsible for the OsO_4 reaction and that the extent of staining caused by osmium precipitation is apparently proportional to the content of the unsaturated component involved.

An extensive electron microscopical investigation of various ABS polymers was undertaken by KATO himself (21,64,67). ABS polymers belong to the family of rubber reinforced plastics, such as HiPS, MBS (methacrylate butadiene styrene), HiPMMA (high impact resistant PMMA) and modified PVC. With all of these examples the plastic phase is continuous wherein the rubber is dispersed.

One generally distinguishes two types of ABS plastics. The type G resin is manufactured by an emulsion polymerization process. PB latex is used as starting material (seed latex) and monomers AN and S are added as glassy components to provide polymerization such that grafting of the AS copolymer onto rubber molecules takes place. The electron micrographs for the grafted ABS plastic (type G) show a cellular (salami type) structure: rubber particles up to 1μ in

diameter are finely dispersed in the continuous plastic matrix, however, the rubbery domains contain occluded AS copolymer particles. The type B resin results from latex blending of the two components where AB or SB copolymer can serve as the rubbery material and AS or PS as the plastic component. These materials exhibit also a dispersion of rubber particles in the continuous AS phase, however, the elastomeric particles are coalesced to some extent.

MATSUO and coworkers (31,32) studied the same types of ABS plastics. Their results differ slightly from KATO's, which might depend on the preparation method. They did not detect any essential difference between the blend and the graft type ABS polymers, except good separation of the individual rubber particles with the latter. The G-type, however, showed exceedingly higher impact values than the former. With some commercial ABS polymers these investigators did find the cellular structure mentioned above.

The morphology of PVC/rubber blends, and of SBR-block copolymers has been systematically investigated by the same researchers (31,32). For various compositions of PVC/PB (high in PVC) the investigators found irregularly shaped, well defined rubber particles, several microns in diameter, dispersed in the PVC matrix. These rubber particles decrease in size as increasing amounts of AN are added to the PB, until clear in-

dications of a network formation of the NBR-phase appear. Then "the rubber phase no longer forms particles but a network structure extends throughout the PVC-matrix" (31). At still higher concentrations of AN (40%), a system exhibiting apparent compatibility from dynamic mechanical data, shows that micro-heterogeneous particles of 100 \AA still remain, i.e. that viscoelastic experiments are not as sensitive to the morphology as microscopy.

Compression molded sheets of SBS, SB and BSB block copolymers exhibited interesting features (31,68,69). The SBS materials show an almost spherical agglomeration of the block B phases where the diameter increases with the B content. The block B phases tend to link together with the SB and BSB block copolymers forming irregularly shaped rods. MATSUO also investigated the fine structure of the SBS block copolymers as cast from toluene solutions (31). He found that an increase in the block B fraction in the copolymer changes the structure from spheres to rods of the rubbery phase and finally to alternate layers of both phases, a lamellar structure. These morphological features, however, were found to depend on the type of solvent, which is extensively discussed by MOLAU (70).

Electron microscopy studies on narrow molecular weight distribution SB-block copolymers were done by BRADFORD and VANZO (61). The interior of the samples exhibited regular

alignment, where the spacing of the internal layers corresponds with those at the surface. The widths of the copolymer layer spacings increase with molecular weight and agree well with theoretically calculated values. The observed structures resemble very much the alternate layers MATSUO found (31,68,69). Similar patterns have also been observed by INOUE and coworkers (71) and by ROBINSON and WHITE (48) for SI-block copolymers cast from toluene and MEK solution.

BEECHER and coworkers (33) investigated a SBS block copolymer (Kraton 101, 30 wt.% PS) via electron microscopy as cast from different solutions. In all cases aggregated domains of S blocks could be observed. They consisted of spherical formations, the size of which ($110 \pm 30 \text{ \AA}$) depended on the solvent.

An interesting type of a graft copolymer is the system PVC/EVA (ethyl vinyl acetate) as investigated by MATSUO and SAGAYE (68,69), where the normally unsaturated rubber (PB) has been replaced by the saturated EVA in order to yield better weatherability. Samples with low EVA content (5 and 20%) exhibit a rubbery network formation resembling a cellular structure. The excellent flow properties of these materials are interpreted by a slippage mechanism: "PVC phases separated by the thin EVA network flow as one flow unit" (69).

A system prepared by mixing aqueous dispersions of the isomeric homopolymers PEA and PMMA (particle size $0.1\ \mu$) exhibited an interesting fine structure (28). Already at a content of ca. 15% PMMA the samples showed PMMA as the continuous phase whereas PEA forms discrete almost spherical particles up to $4\ \mu$ in diameter. The border regions between PEA and PMMA indicate a certain degree of network formation. IPN's of the same components will be discussed in section V,C.

E. Domain Formation

In an attempt to develop a better understanding of the domain formation in two phase polymeric materials mechanisms and models have been derived. It is difficult to generalize such findings because the methods of preparation strongly influence the morphology and thus the question whether phase separation occurs on a macroscopic level as with polymer mixtures or on a microscopic scale as e.g. with block copolymers.

MOLAU and KESKKULA (72) presented a mechanism for the formation of rubber particles in the polymerization of solutions in vinyl monomers. While a solution of rubber in styrene-a P00-emulsion¹⁾ (73) - is polymerized, phase separation occurs as soon as a sufficient amount of PS has been formed and the complete "immiscibility approximation" (74) holds at a relative-

¹⁾ P00-emulsions, i.e. polymeric oil in oil emulsions, consist of immiscible polymer solutions which are emulsified with graft copolymers as emulsifying agents.

ly low degree of conversion. This initial PS phase must necessarily be the dispersed phase, because it is much too small to be the continuous phase. As the polymerization process continues a point of conversion is reached at which the polystyrene phase is too large for still being the dispersed phase of the P00-emulsion. At this point, an inversion of the phases occurs, due to employed agitation where the rubber phase becomes the discontinuous phase. The rubber still contains the occluded PS-particles, thus exhibiting the well known structure of grafted HiPS (31,32,72,75). It is believed that the same mechanism produces the cellular structure of the graft-type ABS polymers (21,31,32,65-67).

In their investigation of block-copolymers, a SBS type thermoplastic elastomer (Kraton 101), BEECHER and coworkers (33) arrived at a general conclusion: PS chain ends aggregate forming an almost spherical domain of $120 \pm 20 \text{ \AA}$ in diameter. KRAUSE (76,77) took this as evidence for the existence of microphase separation in block copolymers. Upon ignoring the effect of the boundaries between the microphases she developed reasonable predictions of the circumstances under which microphase separation takes place: it becomes more and more difficult, i.e. separation occurs at higher and higher values of the interaction parameter, χ_{AB} , as the number of blocks increases in block copolymers of equal composition, and molecular

weight of each block. According to MEIER (78) "the critical block molecular weights required for domain formation are many-fold greater than required for phase separation of a simple mixture of the component blocks" (78).

In a subsequent paper MEIER (79) varied his statistical thermodynamic theory in order to make predictions of stable domain shapes (lamellar, cylindrical) other than spherical. He is the first to consider the influence of solvent on domain morphology. It was shown that the domain structure which forms first as solvent evaporates - depending on the two interaction parameters of the two block components with the solvent - will persist as solvent is removed. INOUE and coworkers (71, 80,81) present an alternative treatment from a completely different viewpoint, however, their results are similar to MEIER's.

III. INTERPENETRATING POLYMER NETWORKS

In addition to the variety of two-phase polymeric systems a new composition of polymeric matter, the IPN's, is presented in this endeavor. According to their preparation and synthesis IPN's are considered to be largely chemically independent but physically interlocked. This chapter treats the historical background of the IPN's in the first part, while the second section presents a statement of the problem as derived from the stage of developments of IPN's when the author started this investigation.

A. History of IPN's

IPN's have first been prepared by MILLAR (4) in 1960. Because of the two plastic phases his materials could also be termed interpenetrating plastic networks. He synthesized cross-linked polymers from styrene and divinylbenzene (DVB), which served as crosslinking agent, by a "conventional pearl" polymerization (4), i.e. suspension polymerization technique. These primary products, also called parent or mother polymer, were fully swollen to equilibrium in their appropriate styrene monomer mixtures containing the same amount of DVB. The swollen system was then polymerized again under heat as before. Thus he obtained two interpenetrating networks, each of them having the same crosslinking density. A schematic illustration of molecular and phase domain morphologies in IPN's of

two superimposed networks is given in Figure 1. A repetition of the above process yielded a tertiary intermeshed copolymer, i.e. three interpenetrating networks. The polymerization for the second and third step was carried out after the initial beads had imbibed the added monomer solution and after "the network had reached a state of balanced stress, as indicated by the disappearance of the characteristic strain patterns between crossed polarizing filters" (4).

MILLAR compared physical properties and swelling behavior of his secondary and tertiary networks with conventionally crosslinked polystyrene. He found slight progressive increases in density and decreases in toluene regain. Furthermore, the results reported in his paper emphasize the importance of the entanglement concept for the physical properties of simple crosslinked polymers, and "show how it may be possible to modify physical properties by increasing the entanglement factor without increasing the concentration of covalent crosslinks" (4), i.e. by producing an IPN.

SHIBAYAMA and SUZUKI (5) prepared IPN's of the same polymer and crosslinking agent as MILLAR. The polymerization process was carried out between glass plates by heat (between 90 and 130°C). They polymerized two series of IPN's. The first one had increasing crosslinking density, which was the same for the mother polymer and the superimposed polymer net-

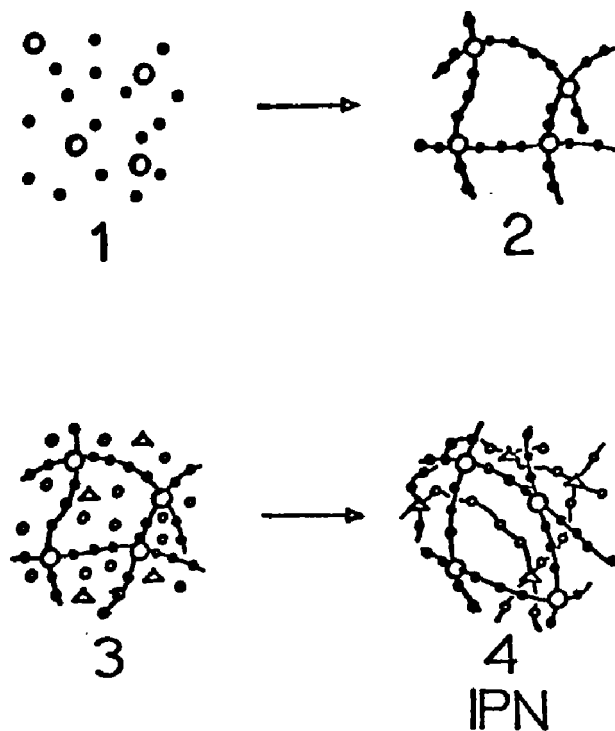


Figure 1. Schematic illustration of an IPN synthesis

work, while the second one consisted of samples which had different crosslink density in the mother and the superimposed polymer. All composite polymers, i.e IPN's were prepared from equilibrium swelling.

The authors (5) investigated the viscoelastic properties using a direct reading apparatus at 138 cps. This equipment was an earlier model of the dynamic viscoelastometer "Rheovibron", Model DDV-II, which has been employed by this author. All of their IPN's exhibited higher rubber modulus values than the mother polymer. Furthermore the rubbery plateau values were increasing with increasing DVB content. The maxima of the loss tangents are shifted towards higher temperatures and are decreased in amplitude with increasing crosslinking density.

SHIBAYAMA and KODAMA (126,127) also synthesized plastic IPN's of PS and PMMA, divinylbenzene (DVB) and ethylene glycol dimethacrylate (EGDM) being the crosslinking agents, respectively. They varied the composition stepwise from pure PS to pure PMMA, where the network with the higher weight fraction was polymerized first. The viscoelastic measurements (relaxation modulus and loss tangent) exhibited in all cases one transition. The maximum loss tangent temperatures increased gradually from $T_g(\text{PS})$ to $T_g(\text{PMMA})$. The occurrence of only one transition was also confirmed by specific volume measurements. The authors (5,126,127) drew the conclusion that their

IPN's have characteristic features of multiple network structures.

FRISCH and coworkers (82-84) prepared a partial interpenetrating elastomeric network (IEN) by mixing equal portions of aqueous emulsions of two different elastomers. They employed a crosslinked polyether-based poly(urethane urea) (U) and a linear poly(butadiene-co-acrylonitrile) (A) together with crosslinking agents and stabilizers. Films were cast, followed by curing at 130°C to form a partial IEN. The authors were able to present partial proof for the structure by separating the poly(butadiene-co-acrylonitrile) from the partial IEN by hydrolysis of the partially interpenetrating poly(urethane urea) network. This demonstrates that there is no chemical interaction between the two polymer phases. A second indication for partial interpenetration is an effective crosslinking density of the IEN's which is greater than the arithmetic mean of the crosslinking densities of the component networks. For a series of IEN's varying in the polymer composition, the authors found that both tensile strength and crosslinking density exhibit a maximum at about 70% poly(butadiene-co-acrylonitrile). Both maximum values are significantly higher than those of the highest component polymers.

MATSUO and KWEI (85) investigated the materials prepared by FRISCH et al. (82-84) for structure-property relationships,

via electron microscopy, dynamic viscoelasticity and tensile measurements. They successfully fitted the results to one of the theoretical models of polyblends proposed by TAKAYANAGI (29). A further discussion of their dynamic mechanical data will be presented in connection with the corresponding results of this author in section IV, 2. The electron microscope study confirms the structures predicted from the dynamic viscoelastic data, including a phase inversion which occurs at a composition of $A/U = 30/70$. They drew the conclusion that "the original particles of the urethane-urea prepolymer latex ($1-5\mu$) are preserved in the mixture even after cure, whereas those of the polyacrylate latex cover the poly-U particles and fuse together to form a continuous phase" (85). Thus interpenetration of the two networks apparently has occurred only partially near the interface.

A novel type of IPN's has been prepared by SPERLING and ARNTS (86). Herewith, a simultaneous synthesis of two polymer networks in the same batch requires two independent, noninterferring reactions (87,88). These materials have been termed Simultaneous Interpenetrating Networks (SIN's) in order to distinguish them from IPN's which are sequentially polymerized. The authors (86) employed an epoxy resin formulation cured by a tertiary amine and an ethyl acrylate formulation. Thus minimal interference occurs between the condensation and the

addition polymerization. Their method of preparation employed a polymerization cell which contained the two appropriate components. The cell was simultaneously subjected to heat and ultraviolet light. An investigation of the properties of the SIN's is currently being undertaken.

The type of IPN's this thesis is concerned with has been polymerized by SPERLING and FRIEDMAN (6) predating the IEN's by FRISCH and coworkers (82). Following the swelling technique which had been applied earlier by other investigators (4,5,89), they synthesized IPN's of poly(ethyl acrylate) (PEA) and polystyrene (PS). They were first to combine an elastomeric and a plastic material to form an IPN, in order to take advantage of the favorable properties of both components.

Their method of polymerization was identical with the one used by this investigator. Therefore it will be discussed in detail in section IV,B. SPERLING and FRIEDMAN employed a GEHMAN-torsion apparatus to measure the shear modulus at 10 sec. They determined the modulus as a function of composition at 22°C and for a midrange composition as a function of temperature. They found two distinct glass transitions, which was interpreted to be indicative of the presence of two distinct polymer phases. The IPN exhibited a relatively flat modulus plateau between the two glass transitions, similar to polyblends. The lower glass temperature was raised somewhat while

the higher one was lowered, which suggests that molecular mixing does occur to a very limited extent. Chains of "visiting" polymer change the glass transition similar to the way observed in copolymers (90). The modulus was found to undergo a sharp transition at a midrange composition. The authors suggest that a phase inversion occurs at this composition range.

In a later publication SPERLING and coworkers (91) report on the glass-rubber transition behavior and the compatibility of an IPN consisting of PEA and PMMA. This isomeric polymer pair has a heat of mixing almost equal to zero, thus allowing mutual solubility or chemical compatibility (14). This IPN-series exhibits one broadened glass transition for all compositions. This might indicate a single phase or a series of two phase regions varying in composition.

Two further contributions, to which this investigator is a coauthor, have been published (92,93). The results presented in these were to a major extent obtained during the early stages of this investigation. Therefore they will be discussed in detail in section VI.

B. Statement of the Problem

The preliminary experiments carried out with IPN's as developed by SPERLING and coworkers (6,91) showed interesting results with respect to their glass-rubber transition behavior, which was also indicative of a change in compatibility. A detailed investigation of the IPN's is highly desirable in order to compare these materials with common polyblends. It should be noted, however, that it will not be tried to optimize the IPN's with respect to physical properties.

The component polymers have been chosen such, and the concentrations will be altered such that the IPN's will express different degrees of compatibility.

The three major questions which will be emphasized are:

- a. How are the glass-rubber transitions and the shape of dispersion regions affected by increased molecular mixing?
- b. What is the detailed morphology of the IPN's and how does it express variations in compatibility?
- c. How does the inversion of the preparative sequence of the IPN's affect the morphology and thus the dynamic mechanical behavior?

Based on the answers to the previous questions a qualitative concept for compatibility of polyblends will be developed phenomenologically.

IV. EXPERIMENTAL

The experimental work involved in the elucidation of the IPN's was exclusively carried out by the author in this laboratory. The only exception was the elemental analysis of the polymerized samples which was done by an outside laboratory (see section IV,B). The materials and the equipment items as well as the associated experimental procedures used in this research investigation are discussed in detail below.

A. Materials

PEA has been selected as the elastomeric polymer, while PMMA or PS or random copolymers of the latter two served as the plastic component. The corresponding three monomers were supplied by the Borden Chemical Co., Philadelphia, Pa.

In order to make the rubbery phase susceptible to staining by OsO_4 (Fisher Scientific Co., New York, N. Y.) traces of butadiene were added to the ethyl acrylate monomer. Butadiene gas was supplied by Air Products and Chemicals, Inc., Trexlertown, Pa. It was liquified in a solution of dry ice in acetone and then bottled under pressure. For storage it was kept at -30°C .

The crosslink agent and the activator used for the polymerization process were tetraethylene glycol dimethacrylate (TEGDM) and benzoin, respectively. Both components were supplied by K & K Laboratories, Inc., Plainview, N. Y.

B. Synthesis

All IPN's were synthesized by a photopolymerization technique according to references (6) and (91). The photo-polymerization unit as built in this laboratory consists of an asbestos-lined wooden box containing several common, commercially available ultraviolet sunlamps (General Electric Co., 275 watts). The lamps are placed 30 cm apart from each other. Light is incident through one open side of the box onto the polymerization cells, which are set 15 cm apart from the lamps, such that the center of a lamp faces the center of a cell at the same height. Each cell consists of 2 glass plates ($10 \times 10 \times 0.3 \text{ cm}^3$) separated by a Teflon gasket (0.3 or 0.7 mm thick). The "sandwich" is kept together by two steel frames attached on both sides of the glass plates and by four C-clamps.

The monomer solutions were injected into the cells through a hole in the Teflon gaskets, using a hypodermic syringe (Propper Mfg. Co. Inc.) and a hypodermic needle (Huber point with bevel, Yale, 27G, 3/8", Becton, Dickinson and Co., Rutherford, N. J.). Upon injection of the monomer solution the hole in the gasket was closed with adhesive tape in order to minimize evaporation. The polymerization cells were exposed to the sunlamps for 24 hours, each side facing the light sources for 12 hours, in order to ensure equal exposure time on both sides of the polymer sample. Overheating was eliminated

by placing one fan each on both sides of the polymerization units.

Monomer solutions were made according to the following recipe: 0.3 g benzoin (as activator or initiator) and 0.5 ml TEGDM (as crosslinking agent) per 100 ml monomer. (2 ml TEGDM have been used with samples for GEHMAN-experiments, series G; see Table I) The homopolymer was kept at 90°C in a vacuum oven between 12 and 60 hours and dried to constant weight. The polymer was cut into strips and a certain weight of the second monomer or comonomer solution was swollen into it at ambient temperature. The duration of imbibing depends on the desired overall composition of the IPN. In order to reach internal swelling equilibrium, i.e. a state of balanced stress,¹⁾ the swollen polymers were stored (except for series I; see Table I) for 12 hours in an airtight container. The sample was then subjected to a second photopolymerization in situ, again for 12 hours per side upon which the drying to constant weight was repeated.

Five series of IPN's have been polymerized, the compositions of which are given in Table I. The underlined polymer

1) A state of balanced stress is identical with a molecularly uniform distribution of the second monomer solution provided the molecular weight of the chain segments between the chemical crosslinks is constant.

| Series | ml TEGDM | wt. % | 1 | 2 | 3 | 4 | 5 | 6 |
|--------|----------|-------------|------|------|------|------|------|------|
| G | 2 | <u>PEA</u> | 50.5 | 50.4 | 50.0 | 50.0 | 49.4 | |
| | | PMMA | 0 | 10.6 | 19.6 | 34.5 | 50.6 | |
| | | PS | 49.5 | 39.0 | 30.4 | 15.5 | 0 | |
| L | 0.5 | <u>PEAB</u> | 48.8 | 48.7 | 49.8 | 51.2 | 48.4 | 47.1 |
| | | PMMA | 0 | 12.9 | 17.9 | 25.4 | 38.0 | 52.9 |
| | | PS | 51.2 | 38.4 | 32.3 | 23.4 | 13.6 | 0 |
| E | 0.5 | <u>PEAB</u> | 74.4 | 75.9 | 75.5 | 72.2 | | |
| | | PMMA | 0 | 8.4 | 14.6 | 27.8 | | |
| | | PS | 25.6 | 15.7 | 9.9 | 0 | | |
| P | 0.5 | <u>PEAB</u> | 23.9 | 26.7 | 24.7 | 25.4 | 23.3 | |
| | | PMMA | 0 | 20.9 | 34.4 | 49.7 | 76.7 | |
| | | PS | 76.1 | 52.4 | 40.9 | 24.9 | 0 | |
| I | 0.5 | <u>PS</u> | 24.6 | 50.7 | 71.4 | 0 | 0 | 0 |
| | | <u>PMMA</u> | 0 | 0 | 0 | 27.0 | 53.7 | 77.5 |
| | | PEAB | 75.4 | 49.3 | 28.6 | 73.0 | 46.3 | 22.5 |

Table 1. Compositions of the investigated IPN's

has been polymerized first. This was always PEA, except for series I (inverse series), where the plastic homopolymer PS or PMMA was polymerized first. The samples of series G (GEHMAN series) were only tested for their shear moduli in a GEHMAN torsion stiffness tester. The amount of crosslinking agent in the G series was 2 ml of TEGDM.

Two changes were made with the preparation of the samples of the four remaining series. Firstly, the amount of crosslinking agent was lowered to 0.5 ml TEGDM for the following reason. Swelling experiments of PS indicated that the initial crosslinking density of 2 ml TEGDM was very high. PS samples (0.7 mm thick) fell apart into little pieces when they were swollen for 1000 to 1500 seconds with styrene- or MMA- or EA-monomer solution. The same phenomenon occurred upon swelling with common solvents like benzene, acetone or tetrahydrofuran. PS-samples containing 0.5 or 0.2 ml TEGDM per 100 ml monomer did not fall apart after swelling them for one week. These samples did probably not break up because the ultimate strain of the internal chains between two crosslinks is much bigger at these lower crosslink densities than the strain with the high crosslink density. Since a PEA sample with 0.2 ml TEGDM per 100 ml monomer was very sticky and could not be completely separated from the sandwich type polymerization cells it was decided to prepare the remaining four series with a crosslinking density corresponding to 0.5 ml of TEGDM per 100 ml

monomer. It may be noted that pure PEA samples containing 0.5 ml TEGDM are considerably stronger than the others when compared qualitatively.

Secondly, traces of butadiene (1-2%) were added to the EA-monomer solution, in order to make the rubbery phase susceptible to OsO_4 staining (59,64), which enables one to distinguish between the rubbery and the plastic phase under the electron microscope. The poly(ethyl acrylate) prepared from a butadiene doped monomer will be denoted as PEAB and treated like a homopolymer.

Series L (leathery series) contains approximately 50 wt.% of PEAB, which provides leathery materials, while series E (elastomeric series), which contains ca 75 wt.% of PEAB, yields self reinforcing elastomeric materials. Series P (plastic series) contains approximately 25 wt.% PEAB and thus exhibits properties of toughened plastics. With these three series of IPN's (L,E and P) the second component again is either PS or PMMA or a random copolymer of the latter two.

In an IPN the component polymerized first is always strained due to the diffusional swelling forces of the second monomer solution. Therefore it was of particular interest to prepare an inverse series of IPN's (series I) where the plastic component has been polymerized first. Since the compositions of this series are almost identical with some samples of the series L, E and P, they may be effectively compared

with those. The following samples match (see Table I): I1/E1, I2/L1, I3/P1, I4/E4, I5/L6, and I6/P5. The samples of series G,L,E and P will hereafter be referred to as normal samples whereas those of series I will be denoted as inverse samples.

The exact compositions of the IPN's as given in Table I were determined in the following way. When the samples were made up only from two homopolymers the weight difference before and after the second polymerization step provided the necessary information. That was the case with all border compositions of the series G,L,E, and P as well as with all IPN's of series I. The remaining samples contained a random copolymer of PS and PMMA as the plastic phase. Since the rate of diffusion of MMA into PEA was smaller than the one of S, the MMA fraction of the plastic IPN phase was smaller than its part in the monomer solution, i.e. only the overall composition of the elastomeric and the plastic phase could be determined via weight difference. The samples were analyzed due to its C- and H-content by Robertson Laboratory, George I. Robertson Jr., Florham Park, N. J. The C- and H-contents allowed the calculation of the actual S/MMA ratio. For comparison the samples containing two homopolymers were also analyzed in this way. In all cases the compositions calculated from the C- and H-content were in exact agreement with the ones obtained via weight difference. In all calculations the traces of butadiene in the

elastomeric phase were disregarded.

The thickness of the Teflon gaskets used inside the polymerization cells and thus the thickness of the samples was 0.7 mm for series G, and 0.3 mm for the other series L,E,P, and I (see IV, C,2).

A conventional polyblend of 50% PEA and 50% PS has been prepared for the sake of comparison. Uncrosslinked PEA and PS were polymerized according to the following recipe: 0.3 g benzoin (as activator or initiator) and 1 ml 1-dodecanethiol (as chain transfer agent) per 100 ml monomer (EA and S). The monomer solutions were polymerized by UV-radiation from commercial "black lights" in the freezing compartment of a refrigerator (-30°C). After evaporation of the unreacted monomer, the polymers were dissolved in a 50/50 mixture of methyl ethylketone and toluene. The polyblend was obtained by coprecipitation of equal amounts of the two solutions in methanol. Samples for Rheovibron experiments were compression molded from the resulting white precipitate.

Unfortunately this type of polyblend could not be prepared with a butadiene doped PEAB-phase and thus no electronmicrograph could be obtained. The reason is, that PEAB containing ca. 1% butadiene could not be dissolved, even when a higher amount of chain transfer agent was employed than the above. The double bond of the butadiene caused a certain degree of grafting, which prevented the PEAB from being dissolved.

C. Mechanical Experiments

Two types of mechanical experiments were carried out with the IPN's: 1. shear moduli were measured using a torsional wire apparatus (GEHMAN), and 2. dynamic mechanical behavior was investigated with a direct reading viscoelastometer (Rheovibron). Both of these experimental tests are described below.

1. GEHMAN Torsion Stiffness Tester

The torsional modulus was measured with a modified GEHMAN torsion stiffness tester. The experimental procedure consisted in connecting a sample in series with a calibrated torsional wire, twisting the top of the wire 180° and recording the corresponding angle of twist at the bottom of the wire after 10 seconds or as a function of time. The upper portion of the wire is attached to a spring allowing the separation between the jaws of the instrument to become larger as the temperature is raised thus compensating for thermal expansion of the sample.

An assortment of wires of various diameters was calibrated using a calibration bar with a known moment of inertia (130). An appropriate wire was used for a given sample in order to maintain the angle of twist in the preferred range of approximately 30° to 150° .

Samples for this experiment were carefully cut with a special blade into rectangular strips approximately $40 \times 6 \times 0.8 \text{ mm}^3$ in dimensions. These dimensions were measured at

various positions and the values averaged.

YOUNGS's modulus, E, is calculated from the following expression:

$$E = \frac{3 G (t)}{a b^3 \mu} = \frac{2.694 \cdot 10^9 K L}{a b^3 \mu} \left(\frac{180 - \theta}{\theta} \right) \text{ (dynes/cm}^2\text{)} \text{ (IV,I)}$$

where

K = torsional constant of the wire (g cm/degree of twist)

L = length of the test specimen (mm)

a = width of the test specimen (mm)

b = thickness of the test specimen (mm)

$\mu = f(a/b)$, read from Table IV, ASTM D 1053 - 61

θ = angle of twist (degrees)

A DEWAR flask containing 20 cst silicone oil was used as a temperature bath. The apparatus was lowered into the bath until the specimen was covered. The temperature was kept constant within 0.02°C for modulus-time experiments and it was raised at a rate of 1°C per minute for modulus-temperature experiments.

2. Viscoelastometer (Rheovibron)

The measurement of the complex modulus, E^* , and of the damping, $\tan \delta$, are two of the basic methods of examining the physical properties of polymeric materials.¹⁾ For these measurements this investigator used a direct reading dynamic viscoelastometer (model DDV - II), manufactured by Toyo

Measuring Instruments Co., Ltd., Tokyo, Japan, developed by TAKAYANAGI (29,94). In this apparatus a sinusoidal tensile strain is applied at one end of the test specimen. This strain is transformed into an electrical output through an unbonded type strain gauge specified for strain detection. The sinusoidal stress generated at the other end of the specimen is transformed into an electrical output by another strain gauge specified for stress detection. Thus $\tan \delta$ values are read off directly from the meter. The storage modulus, E' , and the loss modulus, E'' , are calculated from the amplitudes of stress and strain and the δ value. Since the specimen between the strain and the stress chucks is situated in a heating chamber, dispersion curves can be prepared over a wide range of temperatures above ambient temperature (94). This heating chamber was modified by providing the upper and the lower insulation compartment with one hole each, which enabled one to pour liquid nitrogen into the chamber, thus allowing measurements below ambient temperature.

Measurements were conducted at a definite frequency, 110 cps, from -50°C to 175°C . The rate of heating was 1°C per minute. The temperature was measured by a thermocouple

1) definition of the complex modulus: $E^* = E' + i E''$, where E' is the dynamic storage modulus and E'' is the dynamic loss modulus; definition of damping: $\tan \delta = E''/E'$

set with its tip close to the specimen. The environmental chamber is equipped with a window on its top for observation of the sample. The test specimen was clamped between the two chucks before the cooling process was started. Proceeding in this sequence keeps the amount of frosting negligible. The sample was held under slight tension in order to keep it straight as it cools. However, as the sample shrinks on cooling, the tension screw at the apparatus had to be partially released so as to keep the slight tension approximately constant.

Preliminary experiments with the Rheovibron showed that the specimen dimensions (< 0.1 mm thick) as proposed by the producer (94) were firstly very hard to prepare, although several different methods were used, and secondly could not be used for temperatures above approximately 60°C , for the dynamic force range of the instrument was insufficient at higher temperatures for samples of that particular cross section. On the other hand specimens of bigger dimensions (1 mm thick) (58) provided very unstable results at temperatures below -10°C . In both cases those difficulties could apparently have been overcome by using two samples of different cross sections for one run throughout the whole temperature range. However, the disadvantage in this case was that the overlapping temperature regions of the two branches of the modulus-

temperature plots did not always exactly coincide. Thus a particular thickness of the specimens was searched for, which allowed the viscoelastic behavior to be investigated over the whole temperature range without exchanging the sample. Sizes of the specimens used for all Rheovibron experiments were approximately 0.3 mm thick, 2.5 mm wide and 4 cm long. In order to extend the temperature range (by ca. 20°C) to even higher temperatures than the dynamic force range allowed at this particular cross section and length, these samples were shortened to 1.5 cm without being forced to exchange them with a completely new sample. Dynamic mechanical data were easily reproduced except for $\tan \delta$ values below -35°C.

D. Electron Microscopy

The technique used here is partially based on KATO's OsO_4 staining technique (59,64) and on MATSUO's two step sectioning method (85). Three pieces per sheet of a polymerized IPN of approximately $0.3 \times 0.5 \times 10 \text{ mm}^3$ were exposed to OsO_4 -vapor for a period of two weeks in order to selectively stain the butadiene portion of the PEAB-phase completely to the center of the pieces. Sections of these stained pieces of about $0.1 \times 0.1 \times 2 \text{ mm}^3$ were imbedded in an epoxy resin, such that the long dimension of the section was perpendicular to the cutting direction of the microtome. A Porter-Blum MT-2 ultramicrotome equipped with a diamond knife was used for ultrathin sectioning

at room temperature. A thickness of approximately 400 Å yielded satisfactory results. Transparency electron micrographs were taken by direct observation of the ultrathin sections employing a RCA, EMU-3G electron microscope.

V. EXPERIMENTAL RESULTS

The results of the endeavor to elucidate the IPN's will be presented in this chapter. Creep data and dynamic mechanical results are presented in sections A and B, respectively, while the electron micrographs revealing the morphology are displayed in section C.

The polymerized samples of the leathery series exhibited a whitish color and opaqueness for the PEA/PS border composition G1. As the S mers were gradually replaced by MMA mers this appearance vanished and a whitish blue haze could be observed. The PEA/PMMA samples were completely clear and transparent. Preliminary turbidity measurements (121) via light scattering showed in spite of broad scattering the following trend for leathery IPN's: the turbidity, τ , decreases with a definite slope from a value of ca. 45 cm^{-1} for a PEA/PS sample and has almost a horizontal slope at ca. 2 cm^{-1} for a PEA/PMMA sample. A similar trend of the optical appearance could be noticed also with the other IPN-series, however, the indications were strongest for the 50/50 overall composition of series G and L.

A. Creep Data

Two types of experiments were carried out with the GEHMAN torsion stiffness tester, as reported in chapter IV, C, 1. Three times the shear modulus at 10 seconds, $3G(10)$, as a function of temperature were recorded for the samples of series G and the shear modulus as a function of time was measured for sample G5. The compositions of these samples are given in Table 1. The terms YOUNG's modulus, E , and three times the shear modulus, $3G$, will be used interchangeably, since POISSON's ratio, ν , can be assumed to almost equal 0.5 (96):

$$E = 2 G (1 + \nu) \quad (V,1)$$

Figure 2 shows modulus-temperature relationships, $3G(10)$ vs. T for three different compositions of the G-series (93): G1, G3 and G5. Sample G1, consisting of 50.5 PEA/49.5 PS, shows two distinct transition regions due to the glass transition temperatures of both component polymers. The lower glass transition of PEA has been raised while the upper one of PS has been lowered somewhat. It is difficult to express this in terms of temperatures, since a generally accepted definition of the glass transition temperature in two phase polyblends does not exist for shear modulus-temperature curves.

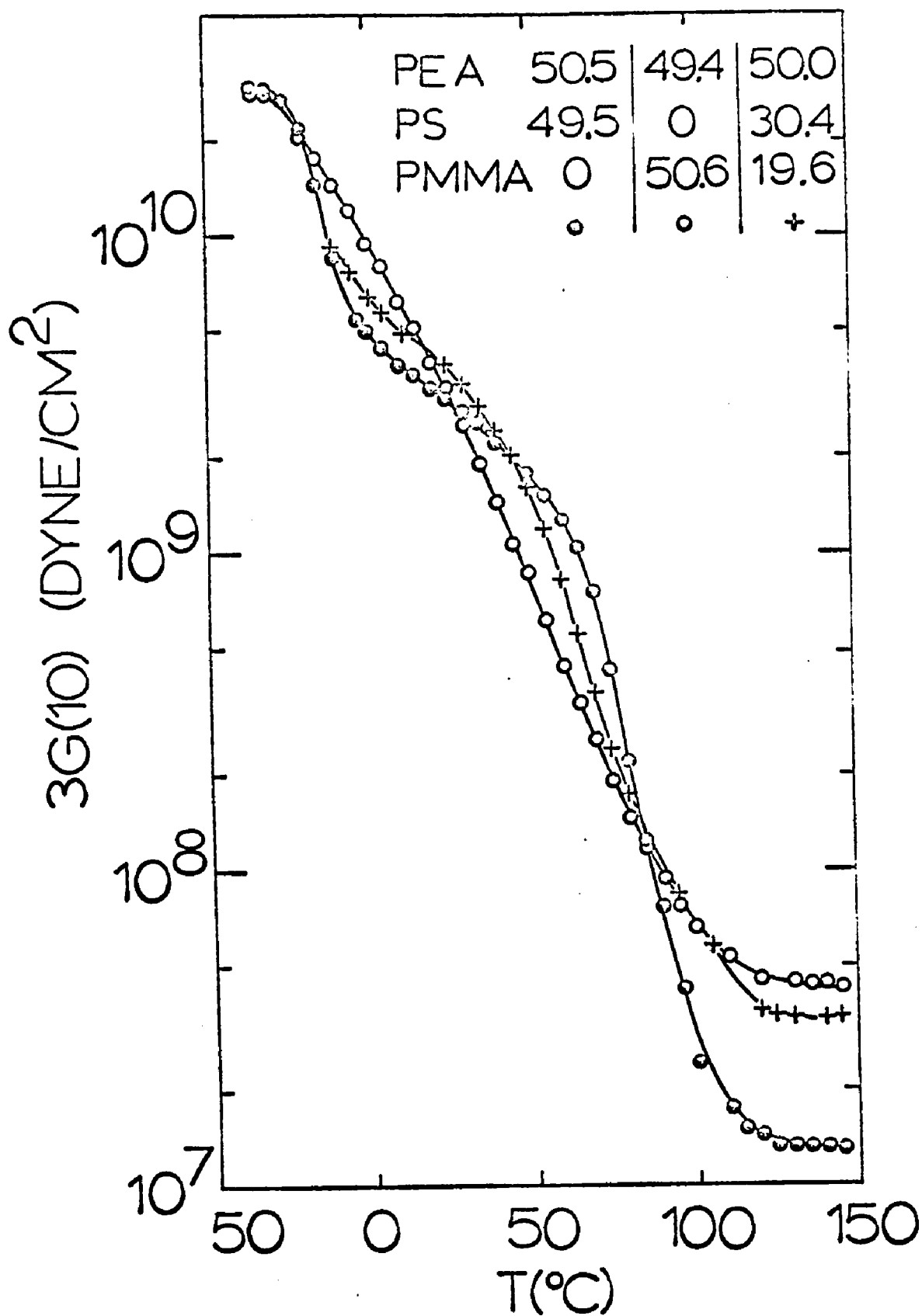


Figure 2. 3 * shear modulus vs. temperature for 3 IPN's
G1 (●), G3 (+), G5 (○) (data from (92))

The indications of two transitions are still noticeable with sample G3 containing 50% PEA and a random copolymer plastic phase of 19.6% PMMA and 30.4% PS.

With sample G5 where all PS has been replaced by PMMA only one broad transition region remains covering a temperature range of approximately 120°C as compared to 40°C with homopolymers and random copolymers.

The different values for the rubbery plateau values, E_2 , as given in Table 2 are worthwhile mentioning. The rubbery modulus of PEA was measured at room temperature while the corresponding moduli for the two plastic homopolymers were measured at 135°C. Figure 2 shows that the GEHMAN-experiments, $G(T)$, for the G-series were carried up to 130°C. The E_2 -values for the IPN's increase from 1.3 to 4.3×10^7 dyne/cm² as the S mers are replaced by MMA mers.

The second type of experiments carried out with the GEHMAN torsion stiffness tester recorded $3G(t)$ at various temperatures for sample G5 (49.4% PEA/50.6 PMMA). A plot of the time dependent YOUNG's modulus is presented in Figure 3 (92).

| Rubbery modulus, $E_2 \times 10^{-7}$ (dyne/cm ²) | | | | | | | | |
|---|--------------|-----|--------------------|------|------|------|------|------|
| | homopolymers | | IPN's (2 ml TEGDM) | | | | | |
| | | | G1 | G2 | G3 | G4 | G5 | |
| PEA | 100 | 0 | 0 | 50.5 | 50.4 | 50.0 | 50.0 | 49.4 |
| PMMA | 0 | 100 | 0 | 0 | 10.6 | 19.6 | 34.5 | 50.6 |
| PS | 0 | 0 | 100 | 49.5 | 39.0 | 30.4 | 15.5 | 0 |
| $E_2 \times 10^{-7}$ | 4.0 | 5.2 | 1.9 | 1.3 | 1.8 | 3.3 | 2.3 | 4.3 |

Table 2. Rubbery moduli, E_2 , of the employed homopolymers and the G-series IPN's

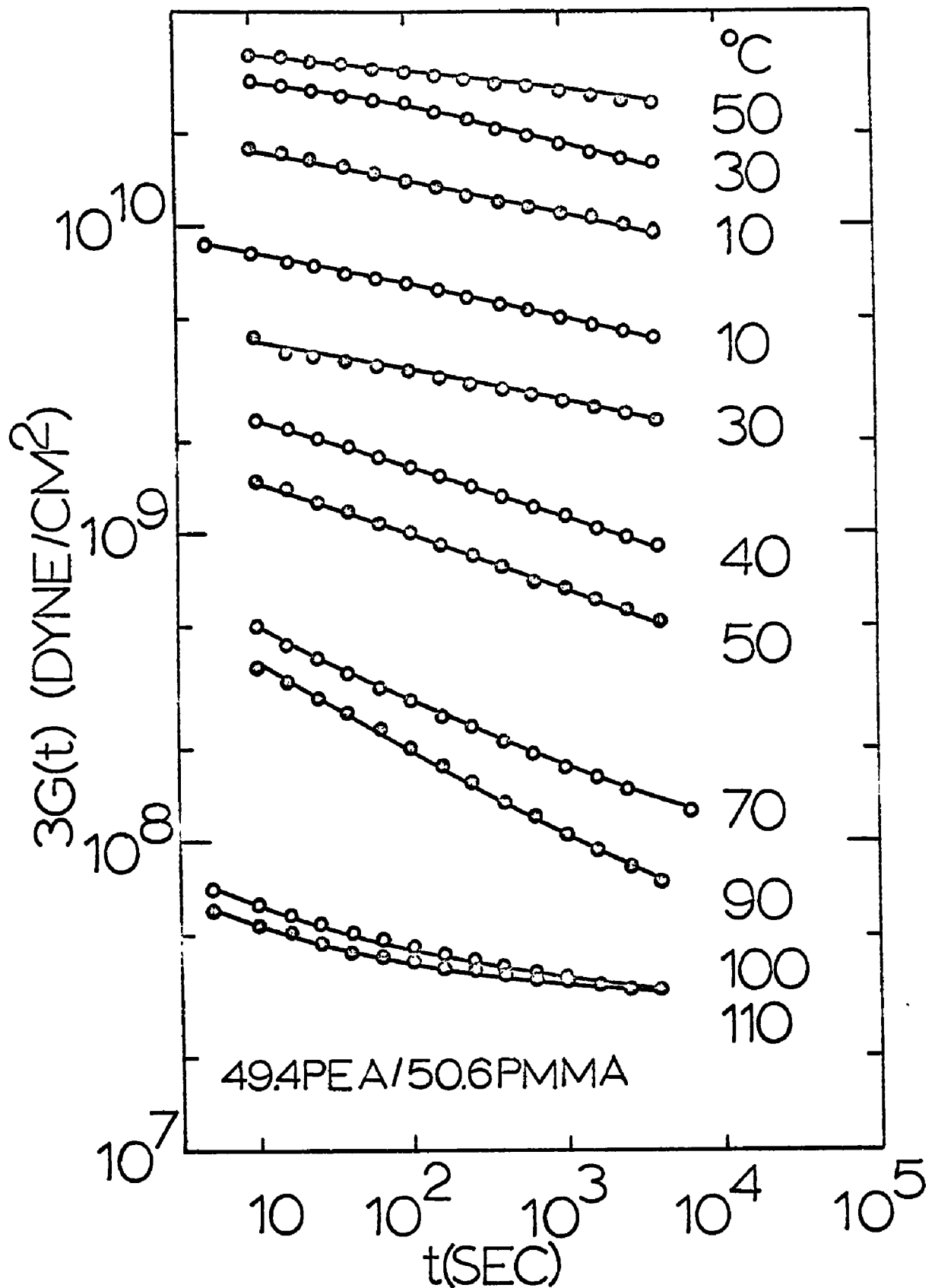


Figure 3. 3 * shear modulus vs. time for IPN G5 (from (92))

B. Dynamic Mechanical Behavior

Rheovibron data for a selection of the IPN's (see Table 1) are presented for samples of the leathery, elastomeric, plastic and inveree series. The IPN's within a series have been chosen such that changes can easily be observed from one composition to another.

1. Leathery Series

Figures 4 through 7 show the temperature dependence of the dynamic storage modulus, E' , and the dynamic loss modulus, E'' , for four IPN's of the leathery series, L1, L4, L5 and L6. The storage modulus, $E'(T)$ for sample L1 (Figure 4) shows two distinct transitions which correspond to the transitions of the two homopolymers, PEAB and PS. The loss modulus curve, $E''(T)$, exhibits two loss peaks at considerably different magnitudes: 2×10^9 dynes/cm² for the PEAB-peak as compared to 1.9×10^8 dynes/cm² for the PS-peak. The temperatures of the loss peak maxima are at -2°C and at 115°C for the PEAB and PS transition, respectively.

As S mers are gradually replaced by MMA mers the two transitions start to merge. The E' -slope of the intermediate portion between the two transitions gets steeper whereas the corresponding region of the loss modulus curve is raised. When the plastic phase of the IPN is pure PMMA (Figure 7, sample L6)

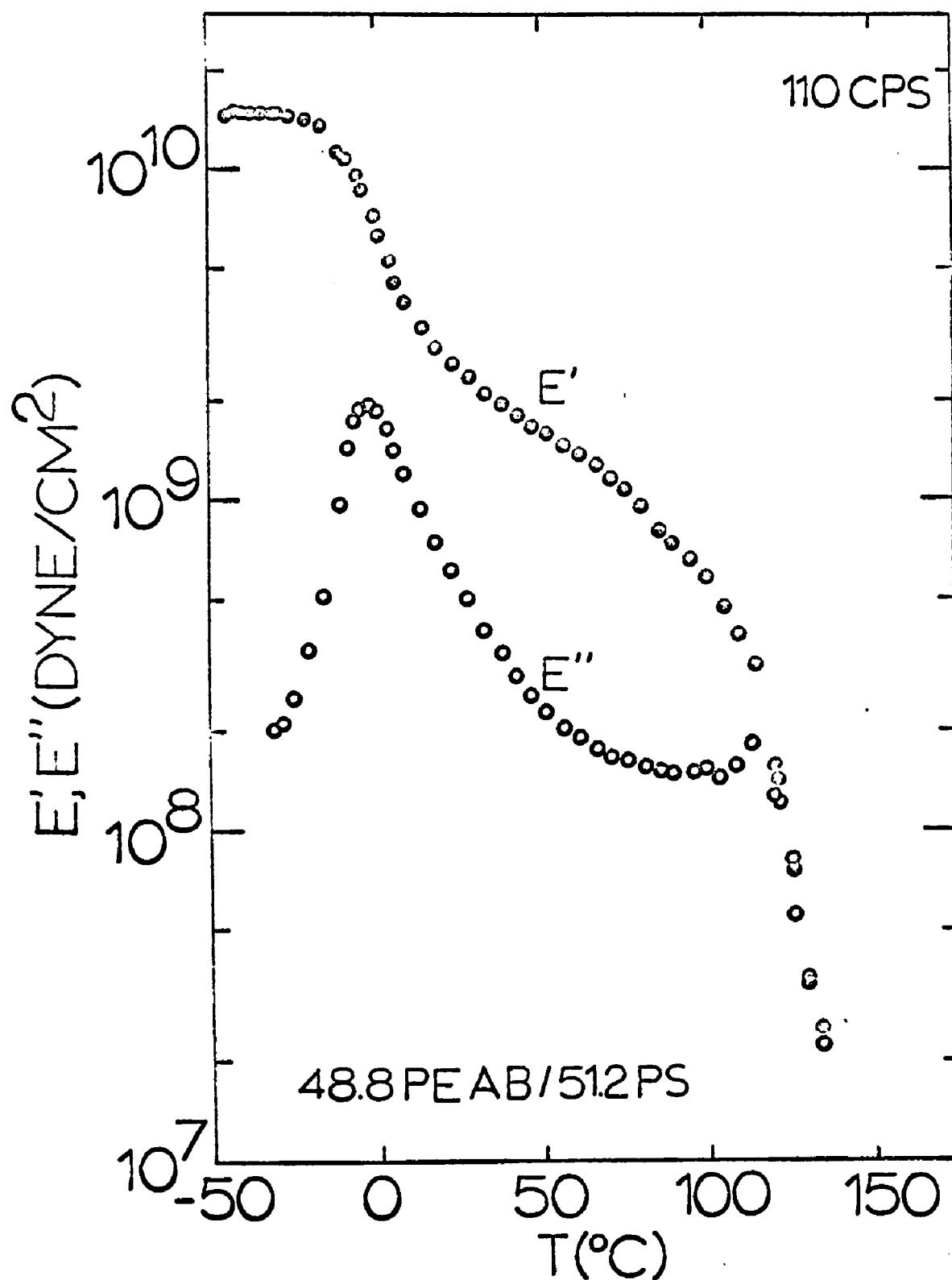


Figure 4. Temperature dependence of E' and E'' of IPN L1

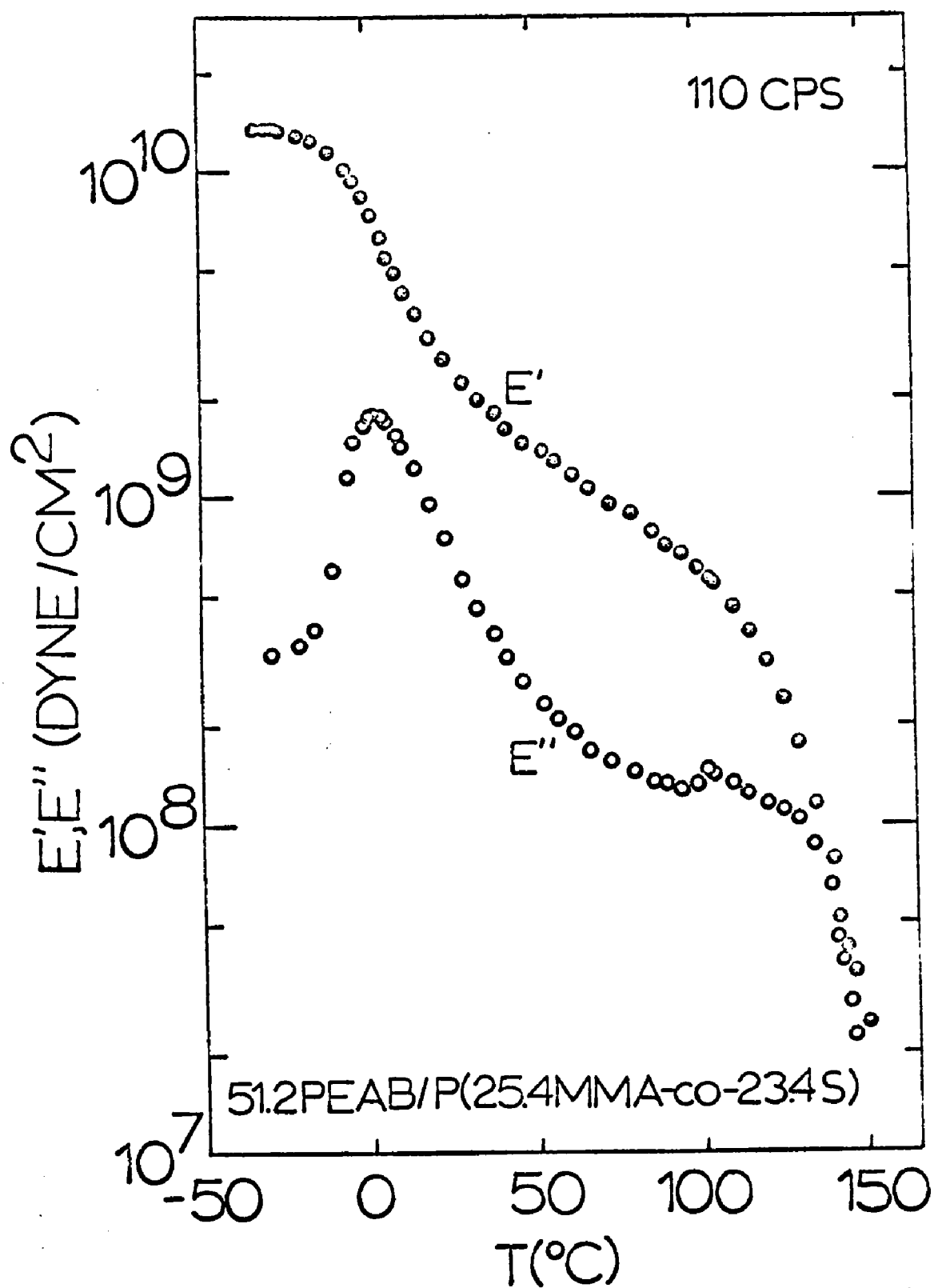


Figure 5. Temperature dependence of E' and E'' of IPN L4

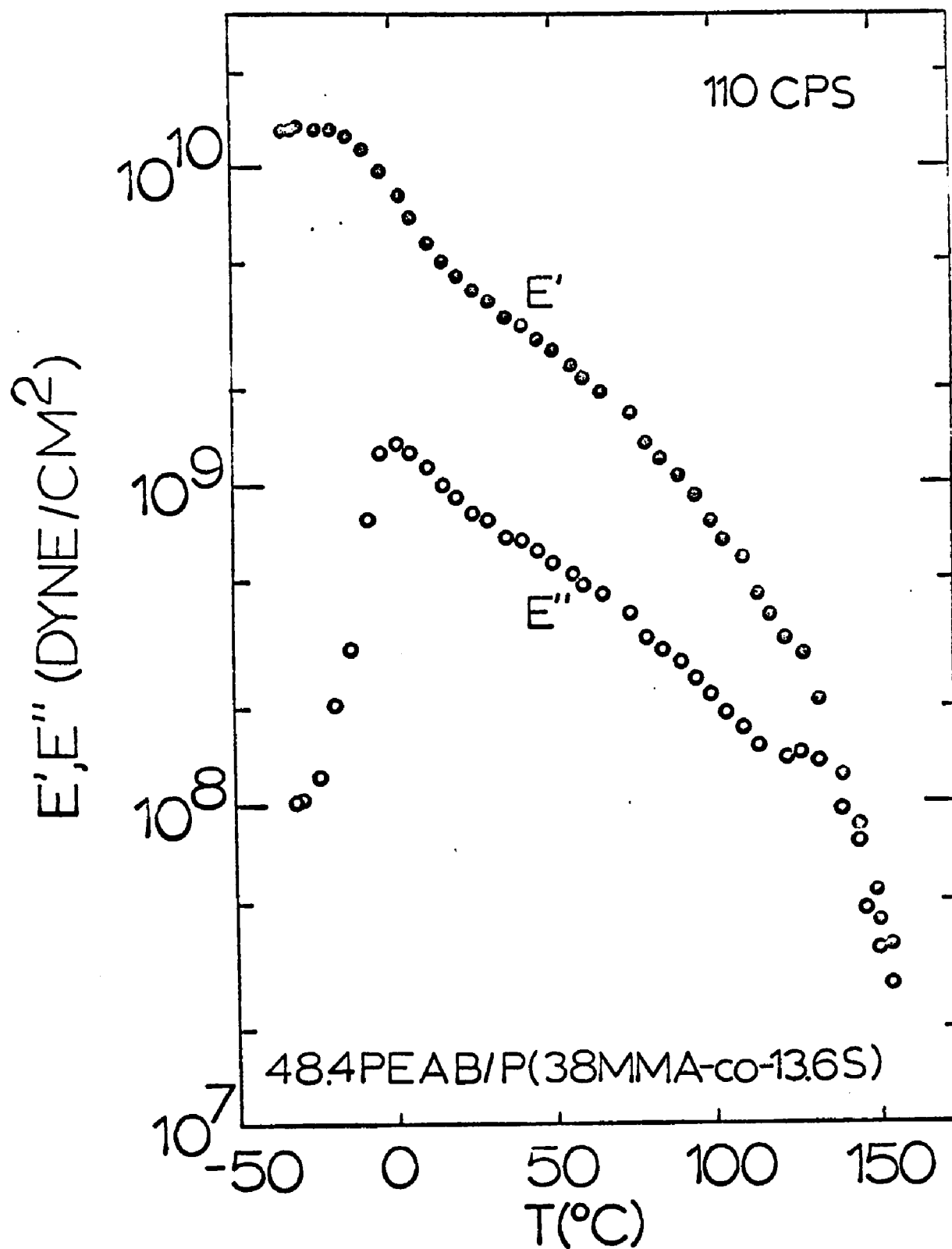


Figure 6. Temperature dependence of E' and E'' of IPN L5

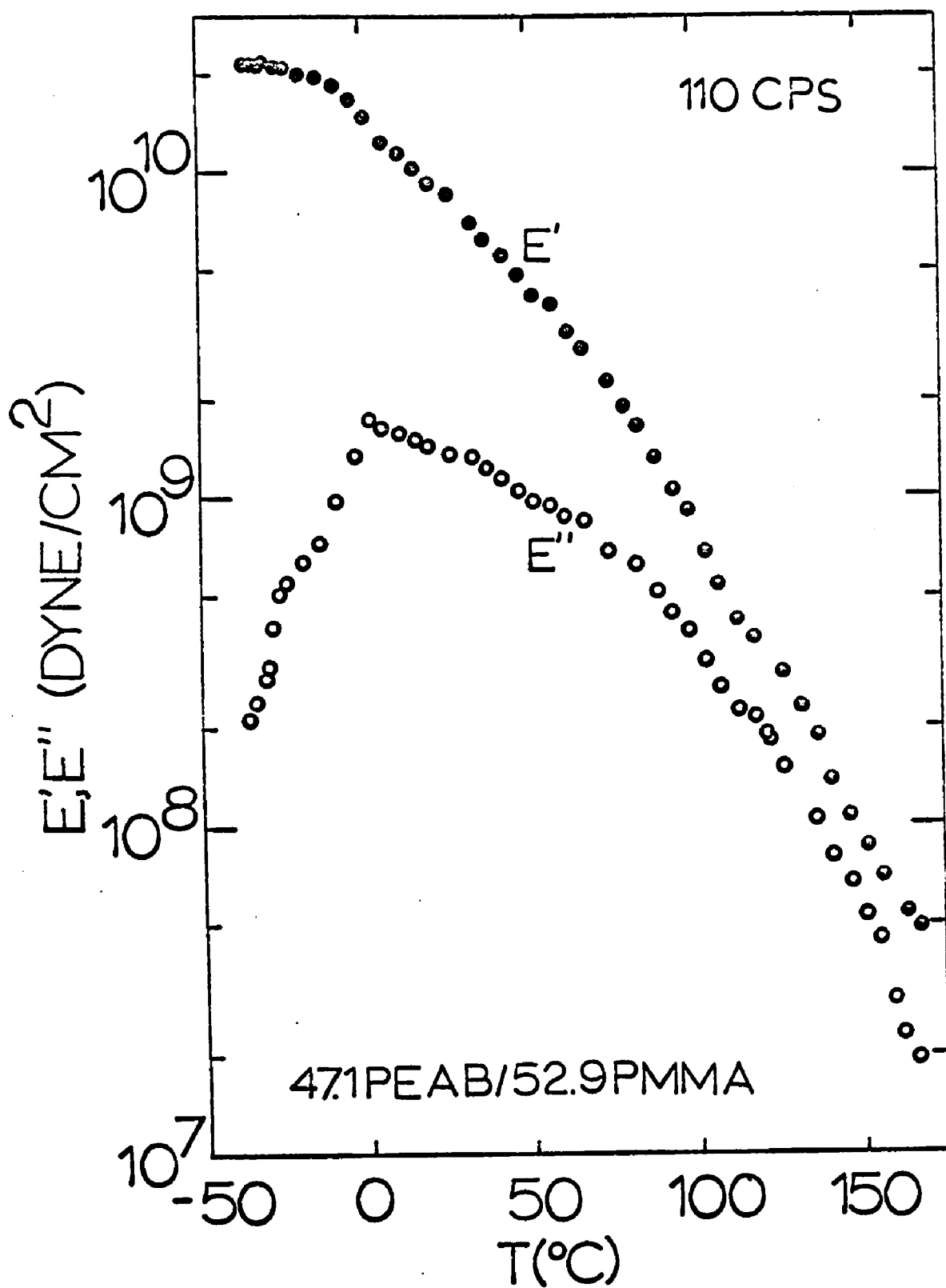


Figure 7. Temperature dependence of E' and E'' of IPN L6

one no longer observes two transitions. The storage modulus exhibits one broad transition whereas the loss modulus shows a broad peak at the PEAB transition which slowly decreases with temperature. No peak is observed due to the PMMA phase, however the decrease of E' with temperature becomes more rapid as 125°C is exceeded, which is indicative of a small shoulder.

The temperatures of the maximum rubbery loss moduli, $T(E''_{\text{max}})$ gradually increase with the PMMA content from -2°C for sample L1 to $+2^{\circ}\text{C}$ for sample L6. The shift of 4°C from the PEAB/PS IPN to the PEAB/PMMA IPN is small but real. The E'' -values of the PEAB-peak fluctuate randomly between 1.3 and 2×10^9 dyne/cm²; i.e. the damping of these materials at approximately 0°C is fairly constant.

2. Elastomeric Series

Figures 8 through 11 present the Rheovibron results for the IPN's of the elastomeric series, E (ca. 75 PEAB/25 P(MMA-co-S). With all samples the E'' -peak corresponding to PEAB was observed at temperatures between -1 and $+1^{\circ}\text{C}$. The intensity of these peaks was fairly constant, the maximum being between 2.5 and 3.2×10^9 dyne/cm².

A peak for the transition of the plastic component could not be observed with any sample. A damping plot, $\tan \delta$ vs. T , did not reveal these peaks either. It is noticed, however,

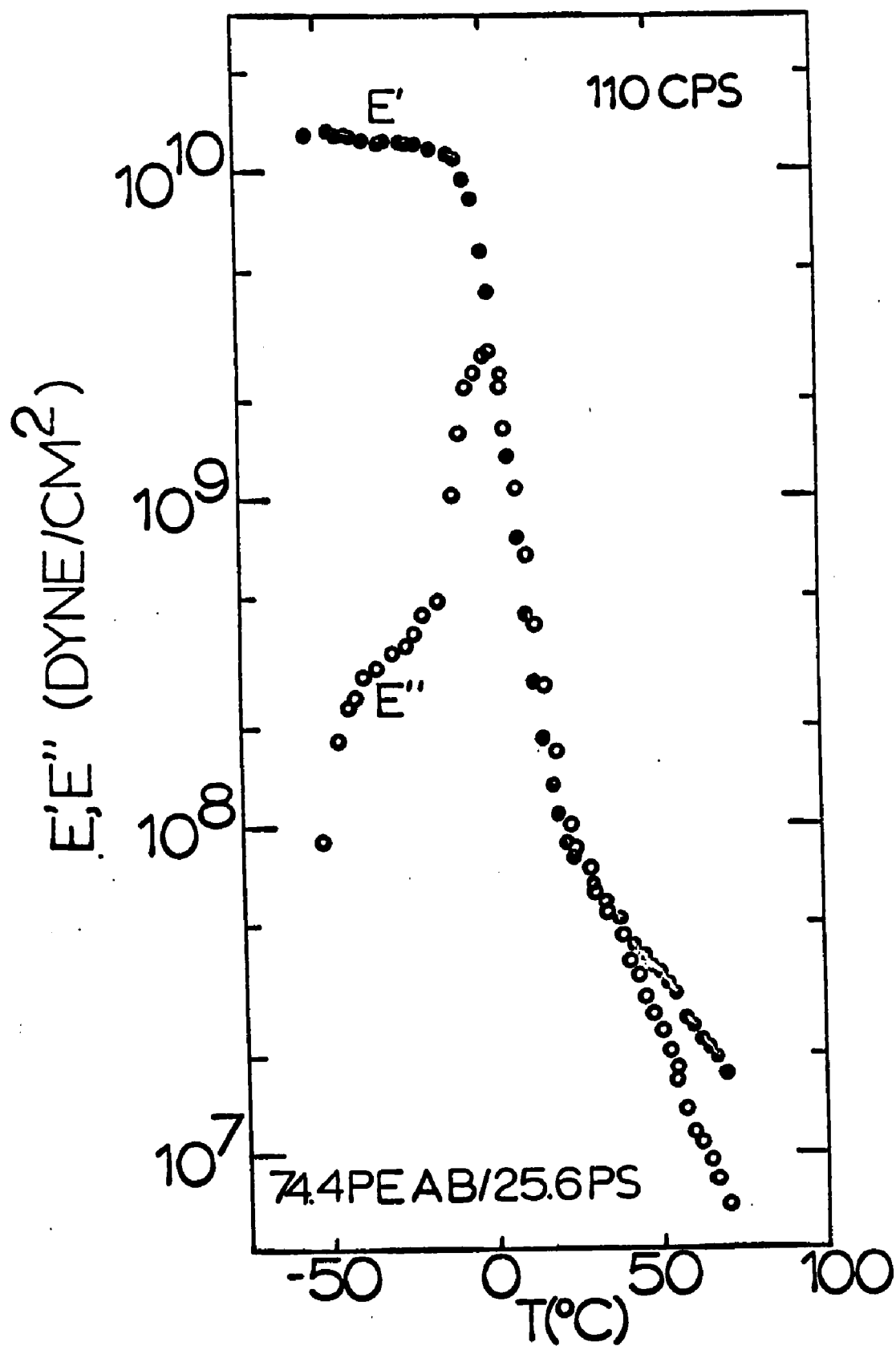


Figure 8. Temperature dependence of E' and E'' of IPN E1

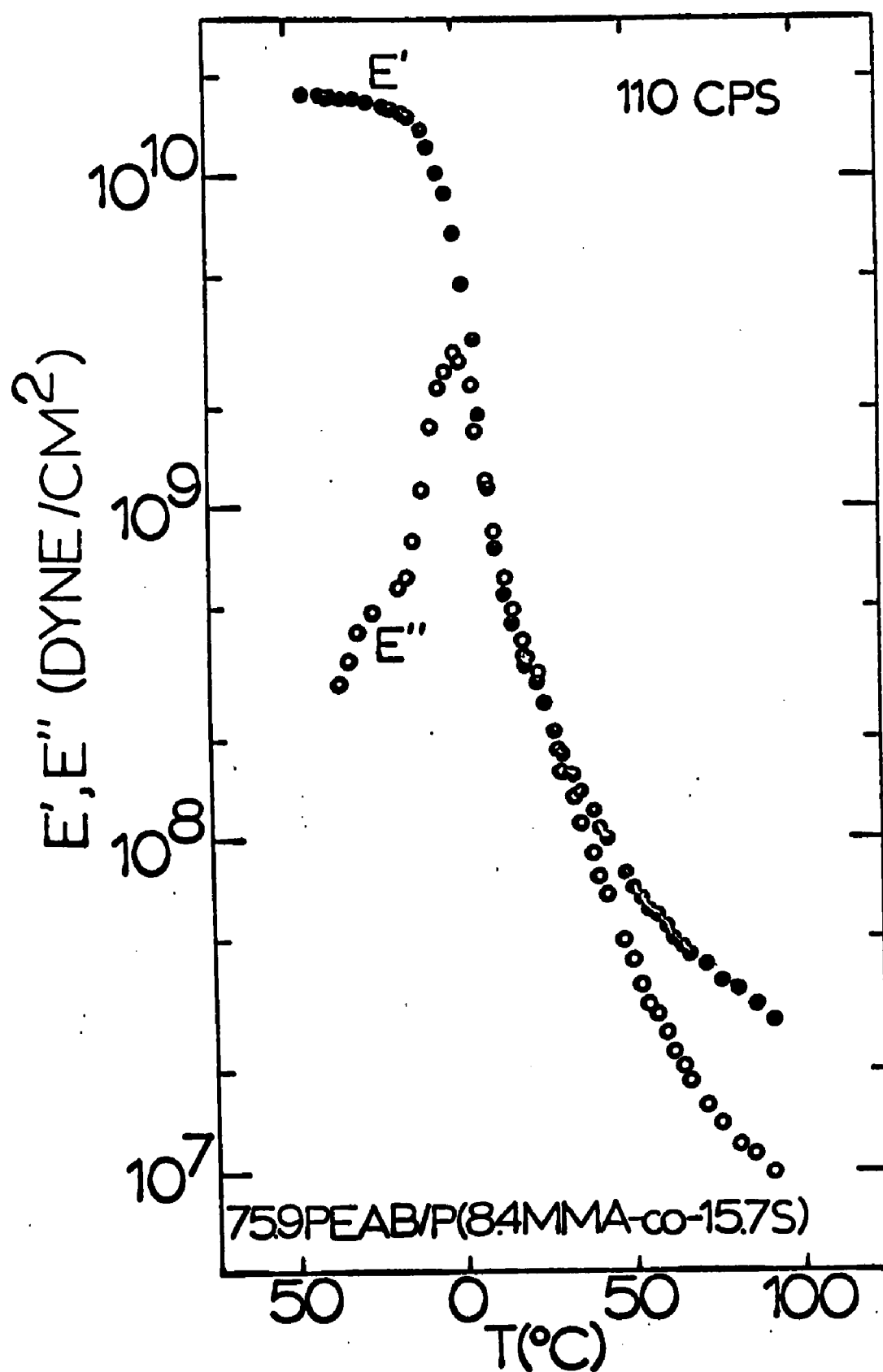


Figure 9. Temperature dependence of E' and E'' of IPN E2

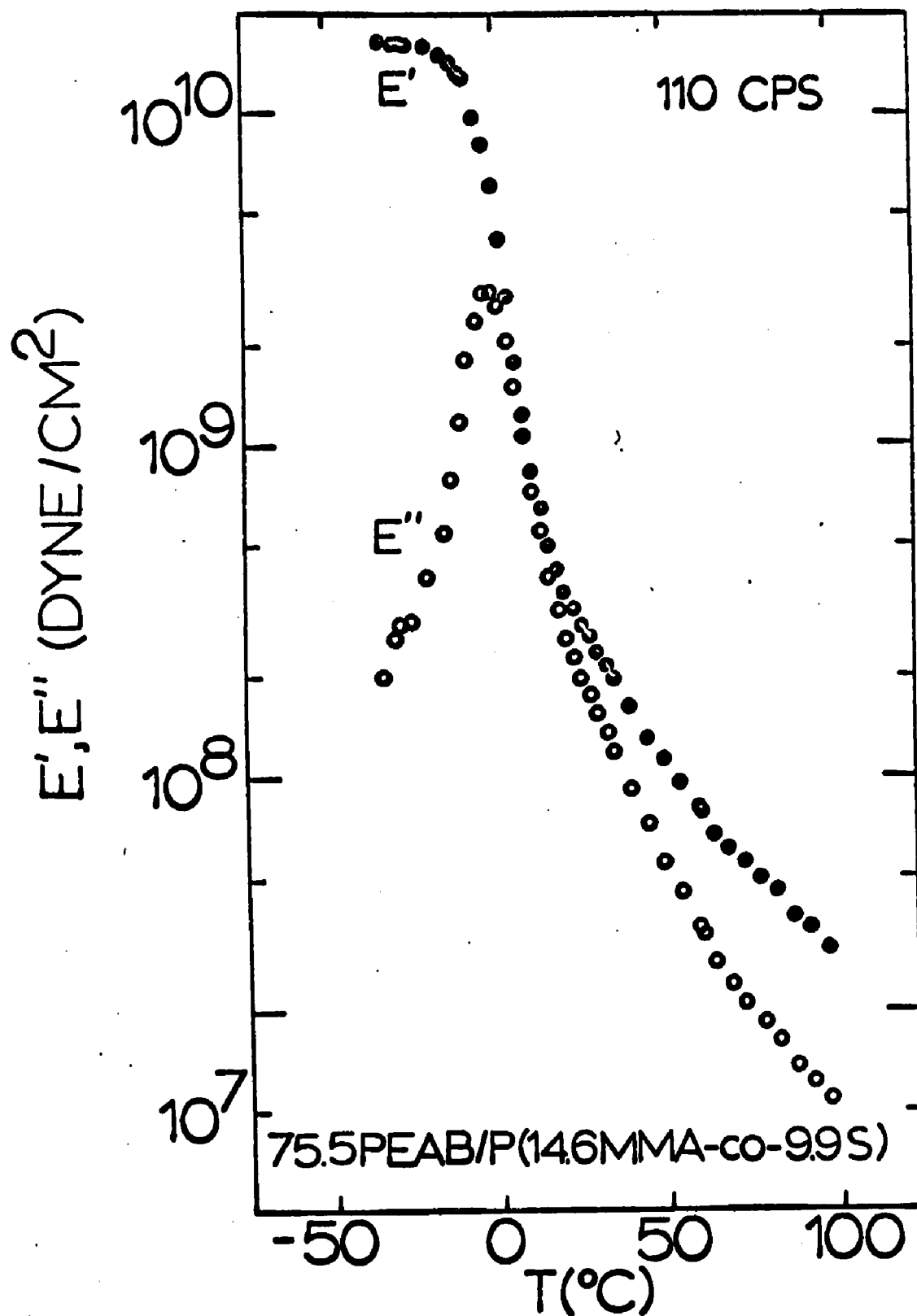


Figure 10. Temperature dependence of E' and E'' of IPN E3

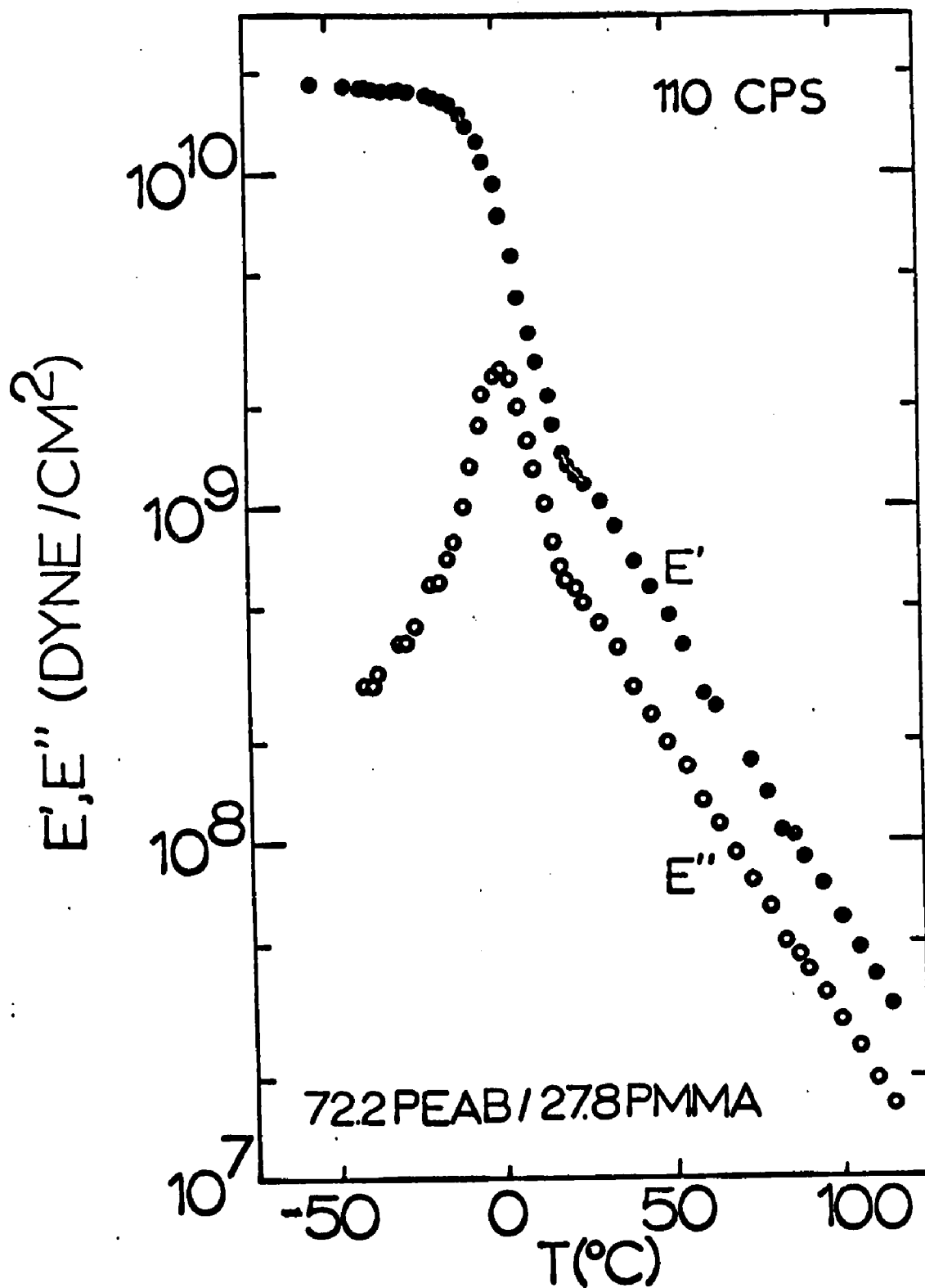


Figure 11. Temperature dependence of E' and E'' of IPN E4

that the experiments might not have been conducted to high enough temperatures. Unfortunately the investigator was restricted here due to the limited dynamic force range of the Rheovibron.

3. Plastic Series

Storage and loss modulus of the plastic IPN's are given in Figures 12 through 15 (samples P1, P3, P4 and P5). Two transitions are observed, as expected, for $E'(T)$ and $E''(T)$ of sample P1. The transition which corresponds to PEAB is very weak in the storage modulus, but quite distinct in the loss modulus. With this IPN the intensity of the PS-peak (1.2×10^9 dyne/cm² at 112°C) is considerably higher than the one of the PEAB-peak (5.6×10^8 dyne/cm² at -5°C). The intermediate plateau of the loss modulus curve exhibits a broad minimum with a relatively high modulus value of 3.2×10^8 dyne/cm². The intensity of this plateau modulus increases as MMA mers gradually replace S mers. With sample P4 (Figure 14) one does not observe a PEAB-peak any more since the loss modulus of the plateau at this composition is higher than the initial PEAB-peak. The plastic peak at this composition has been transformed into a shoulder. With sample P5 (Figure 15) a very broad intermediate plateau maximum is observed between 60 and 85°C with two shoulders at 15°C and at 135°C.

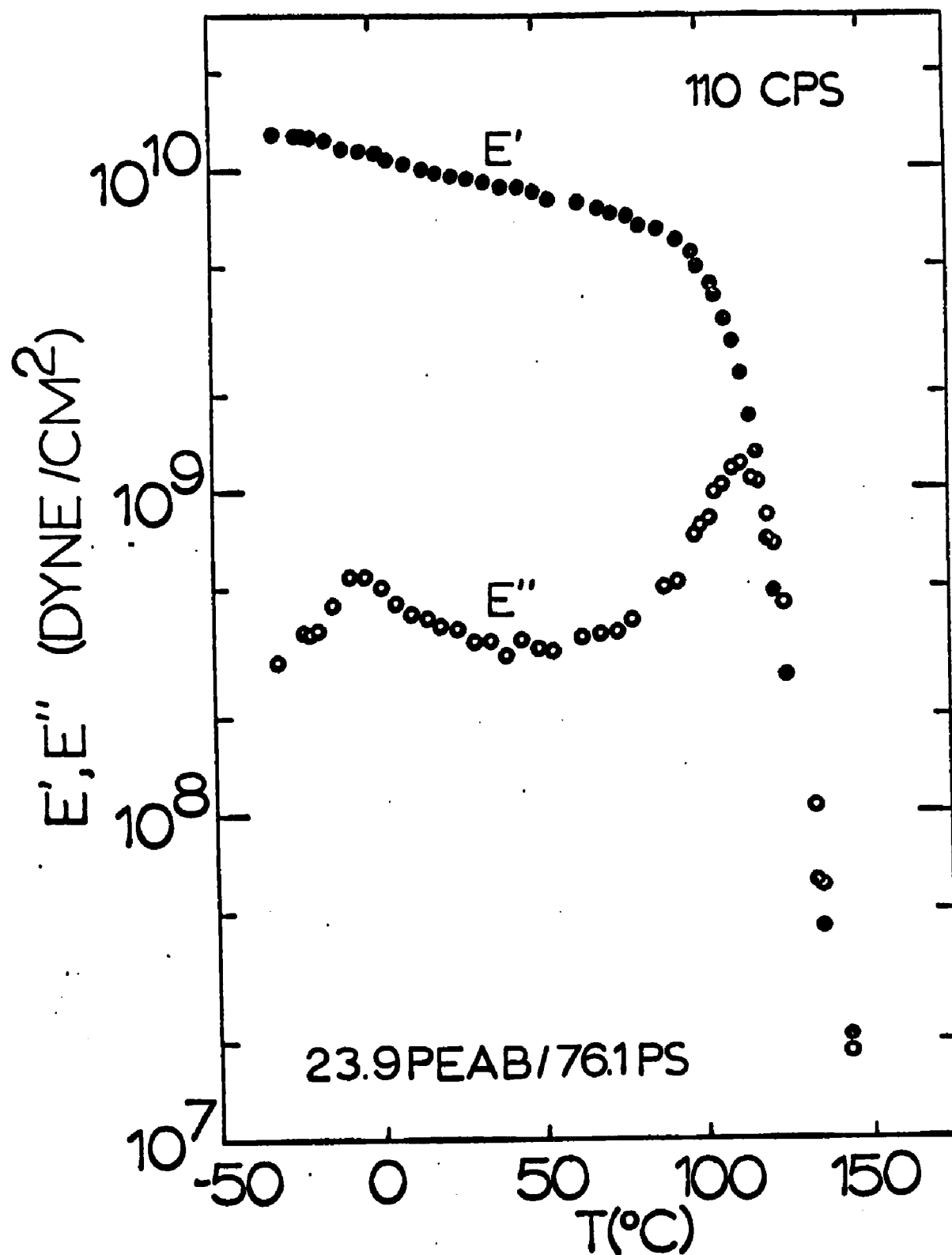


Figure 12. Temperature dependence of E' and E'' of IPN P1

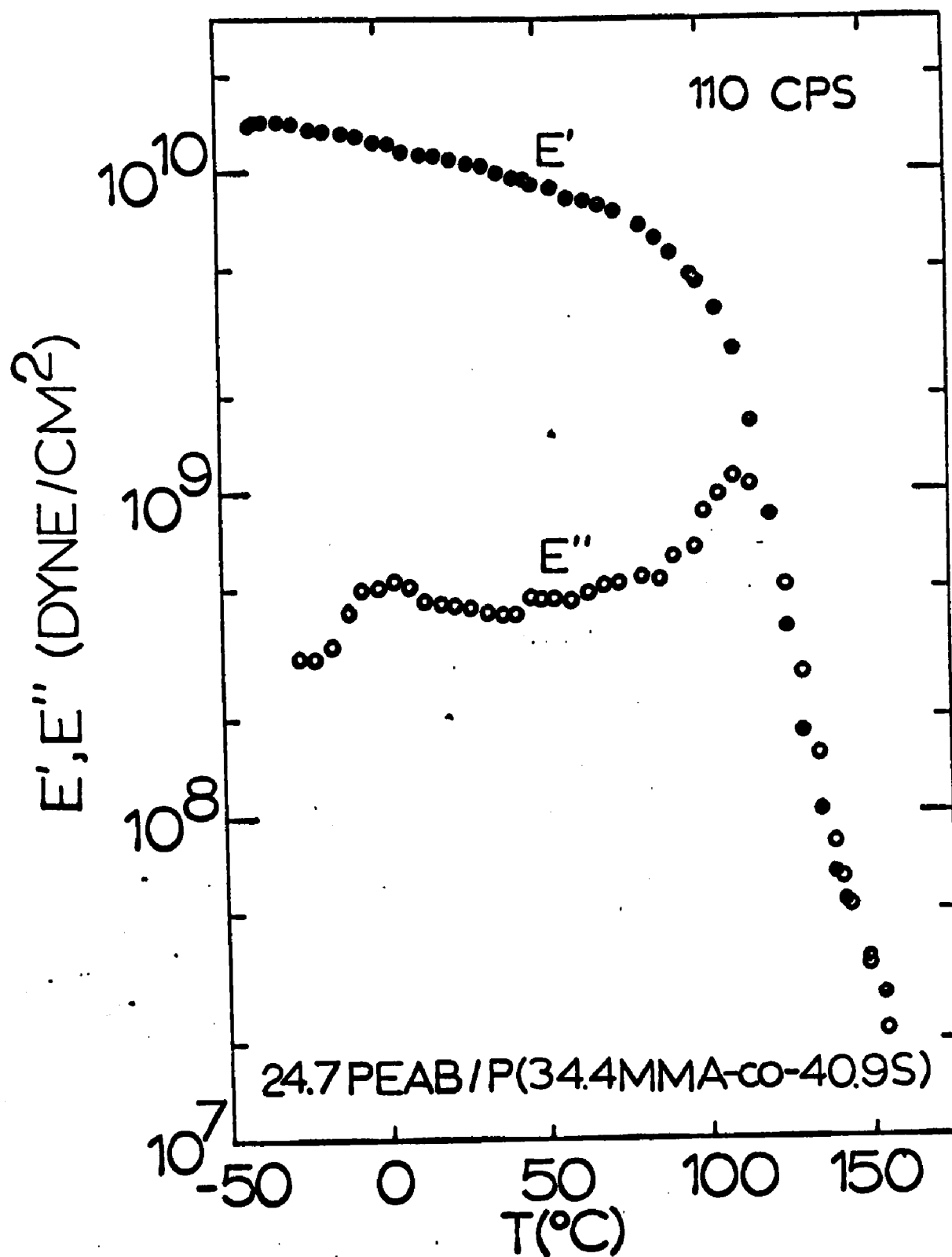


Figure 13. Temperature dependence of E' and E'' of IPN P3

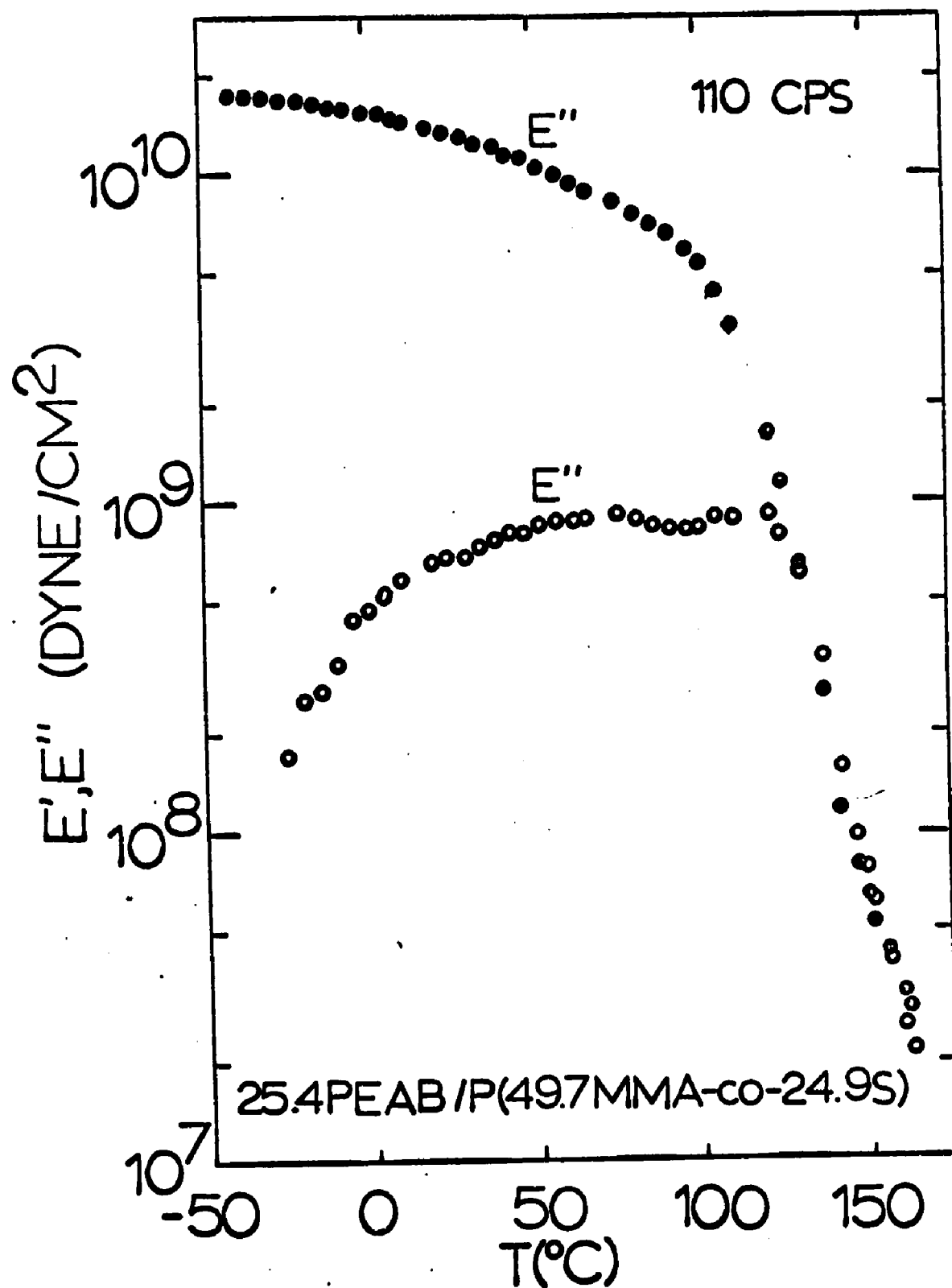


Figure 14. Temperature dependence of E' and E'' of IPN P4

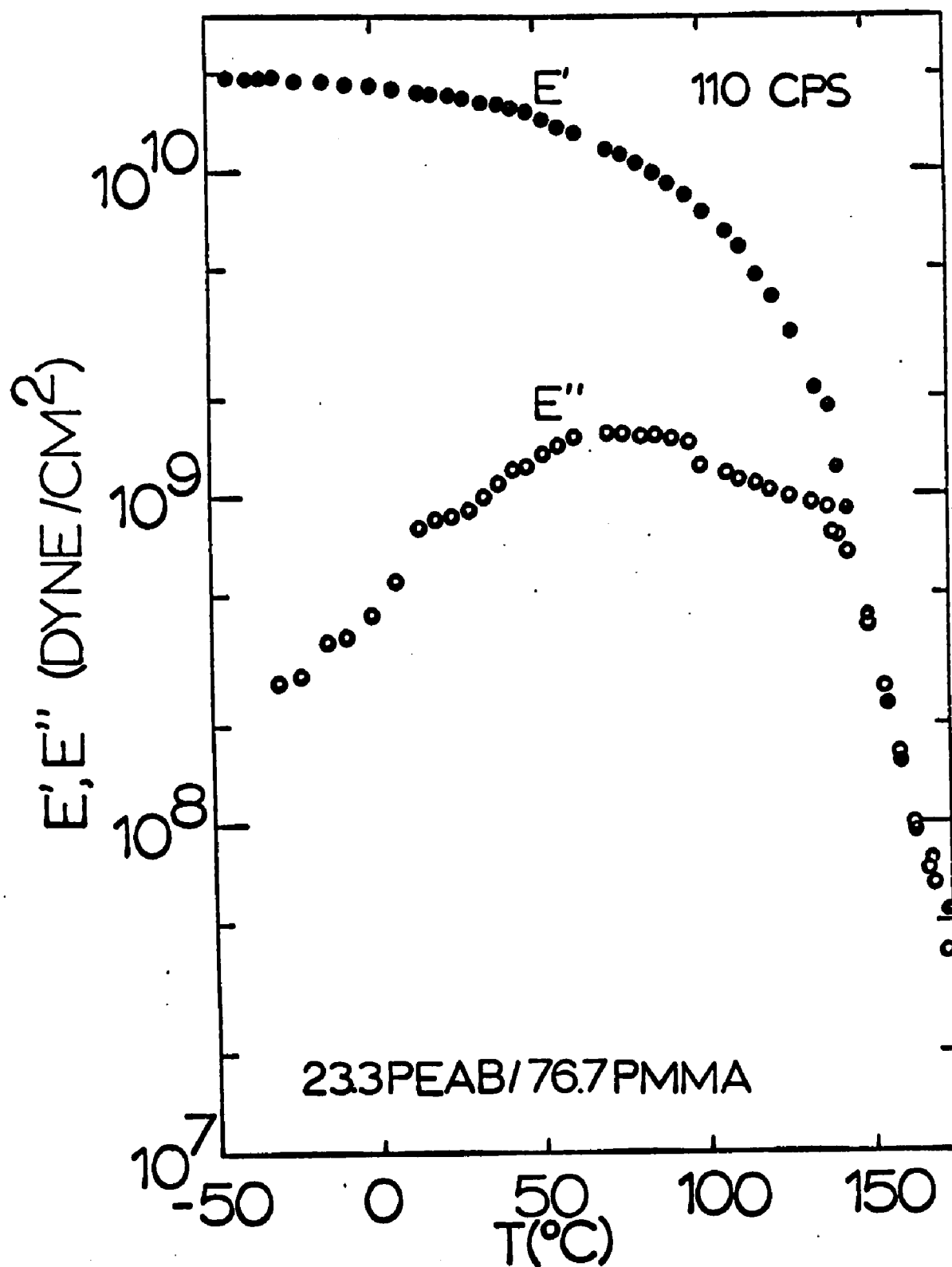


Figure 15. Temperature dependence of E' and E'' of IPN P5

A third shoulder is found in Figure 17 at 95°C. It is considered to correspond to the β -transition of PMMA which will be discussed later.

4. Inverse IPN's

The plots in Figures 16 through 21 show the storage and the loss moduli of the inverse IPN's. The border IPN's¹⁾ of the normal series L, E and P, shown for comparison, have approximately the same composition as the corresponding inverse IPN's, the difference being the sequence of preparation (see section IV, B). The inverse compositions of series L match with the border compositions of the series L, E or P (see Table 1): I1/E1, I2/L1, I3/P1, I4/E4, I5/L6 and I6/P5. The two IPN's I2 and L1 in Figure 17 are compared with a conventional polyblend of the same composition, which has been prepared by coprecipitation of the two homopolymer solutions in a common solvent.

¹⁾ The IPN's of series L, E and P having a pure plastic phase (either PS or PMMA but not P(S-co-MMA)) are denoted border IPN's.

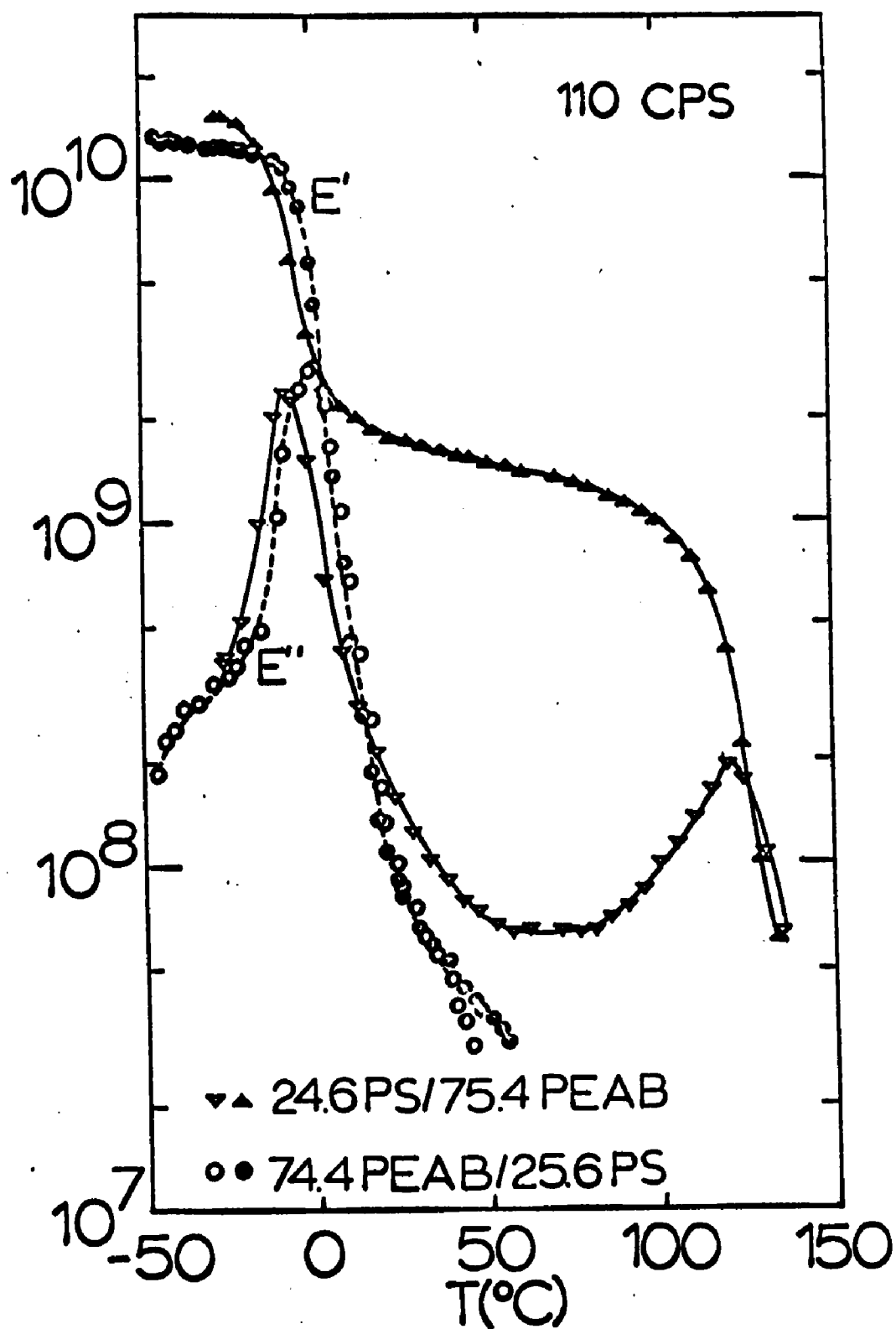


Figure 16. Temperature dependence of E' and E'' of two IPN's, I1 and E1

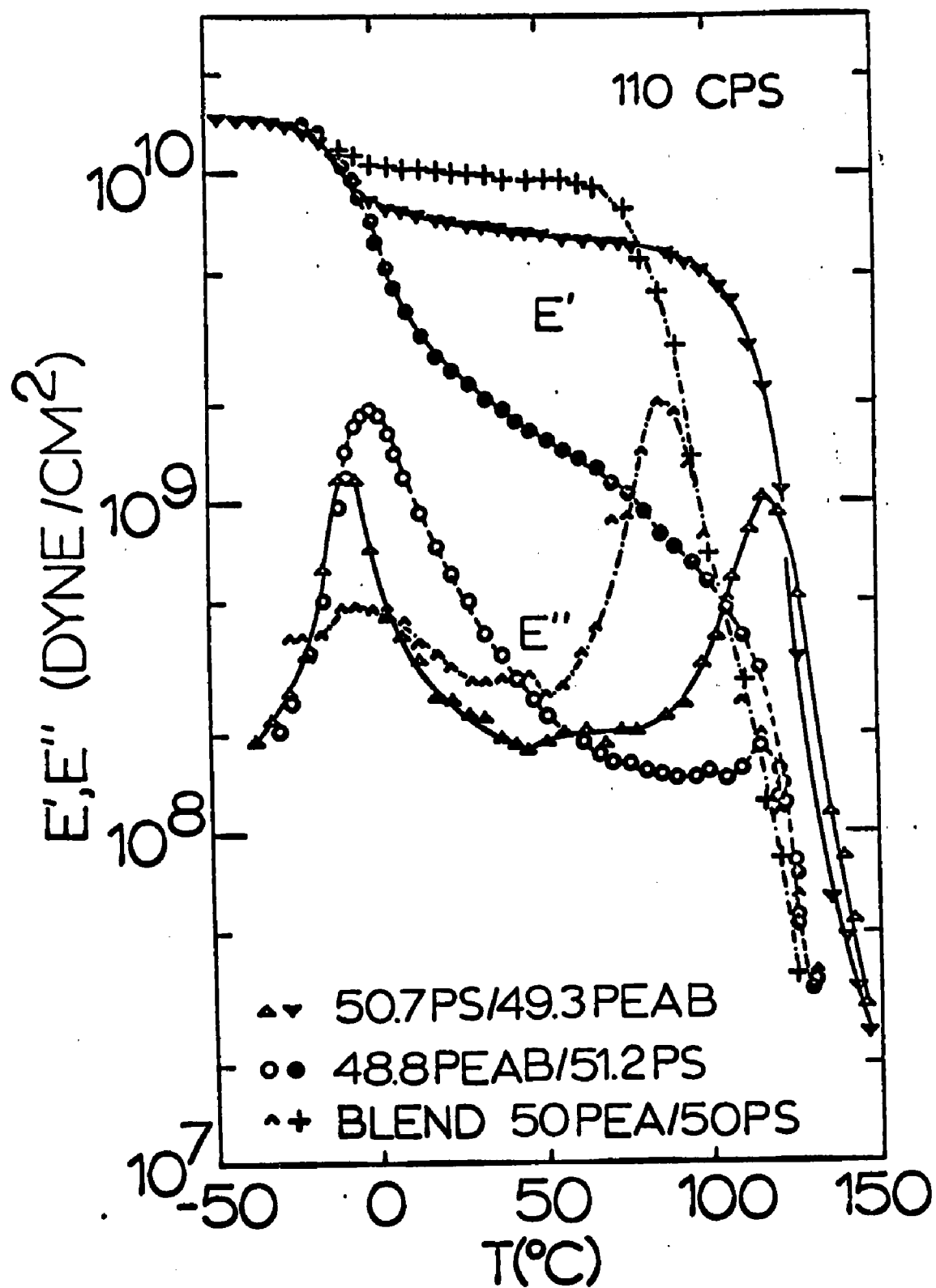


Figure 17. Temperature dependence of E' and E'' of two IPN's, I2, L1 and blend

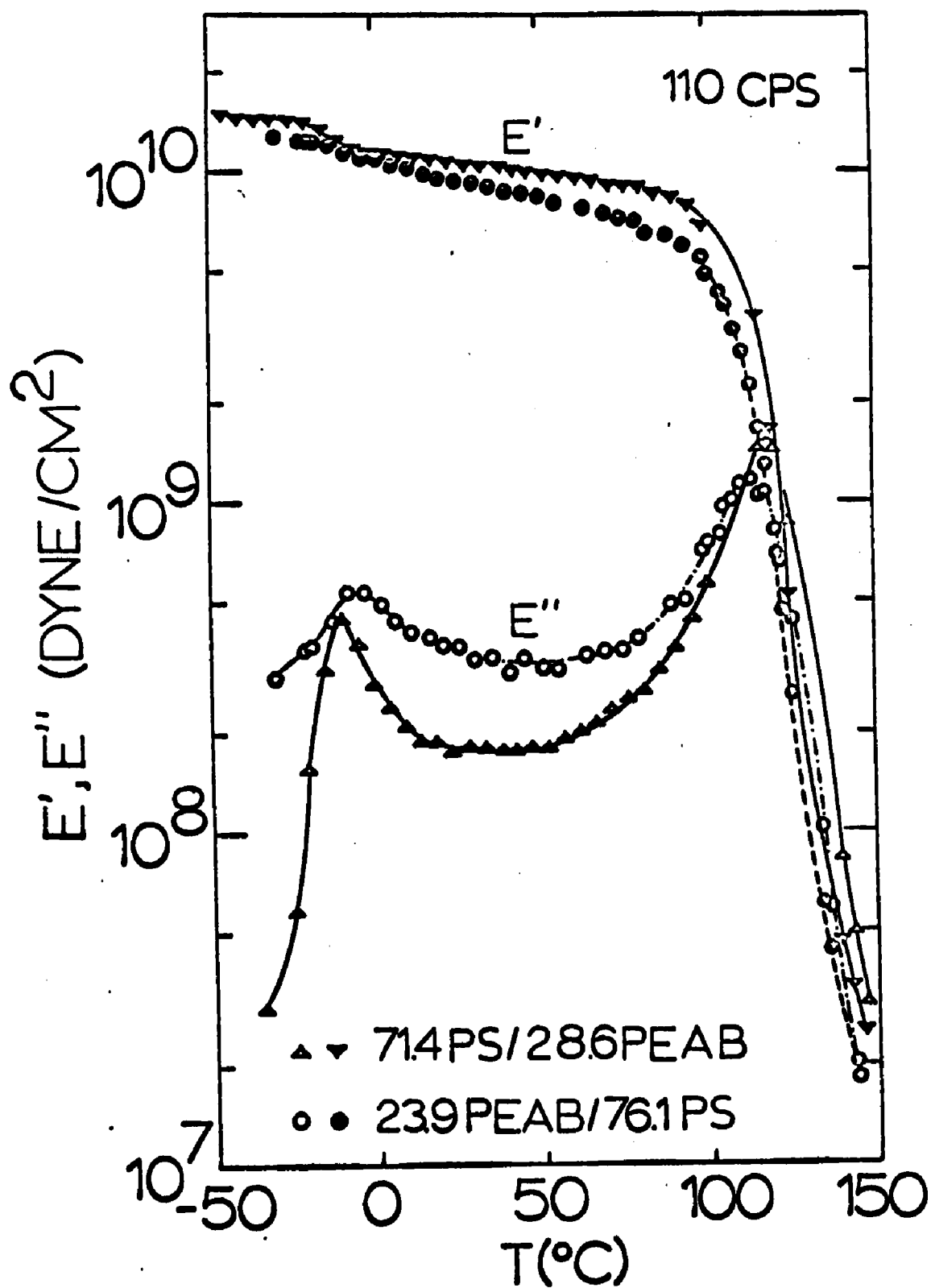


Figure 18. Temperature dependence of E' and E'' of two IPN's, I3 and P1

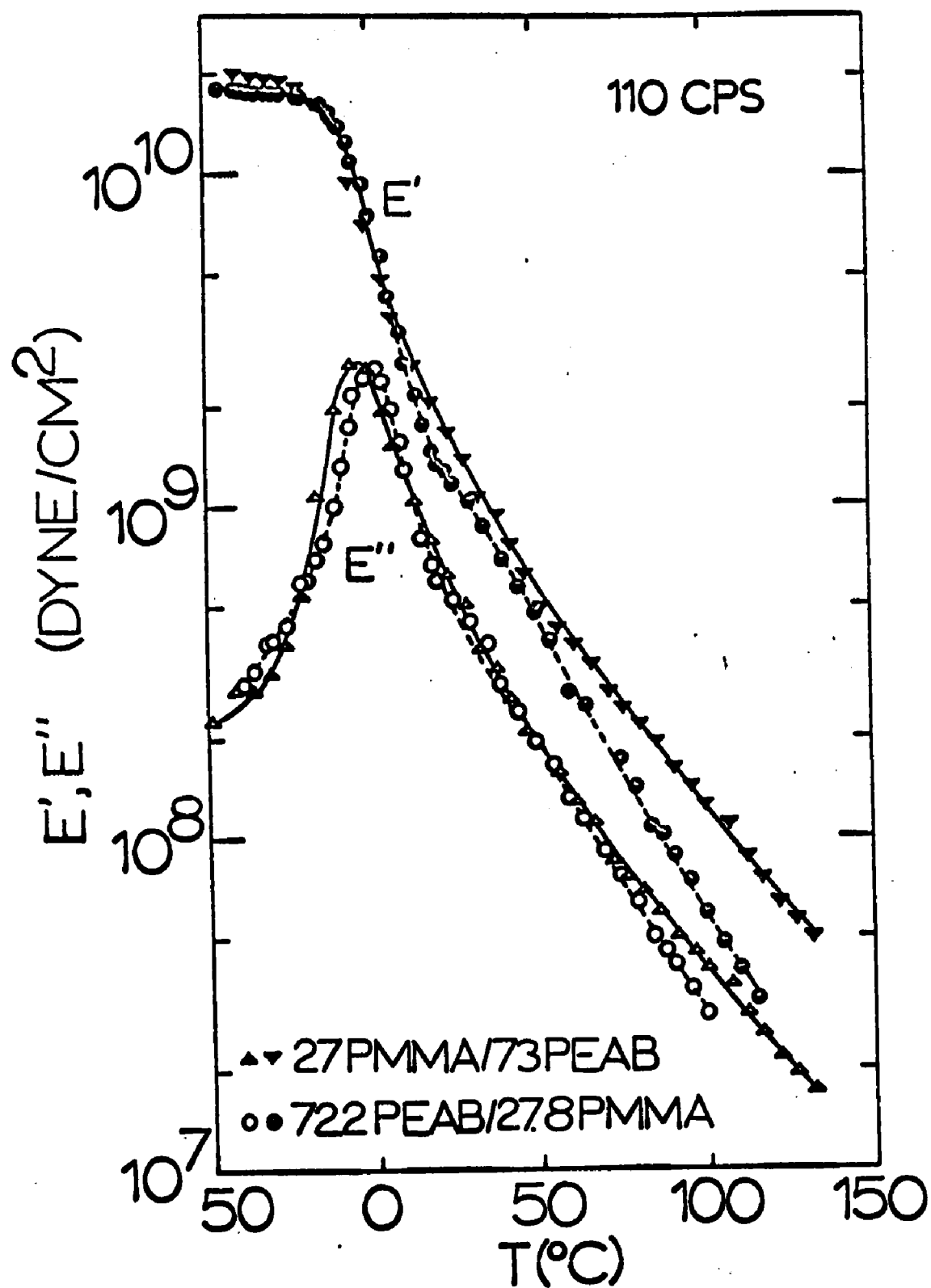


Figure 19. Temperature dependence of E' and E'' of two IPN's, I4 and E4

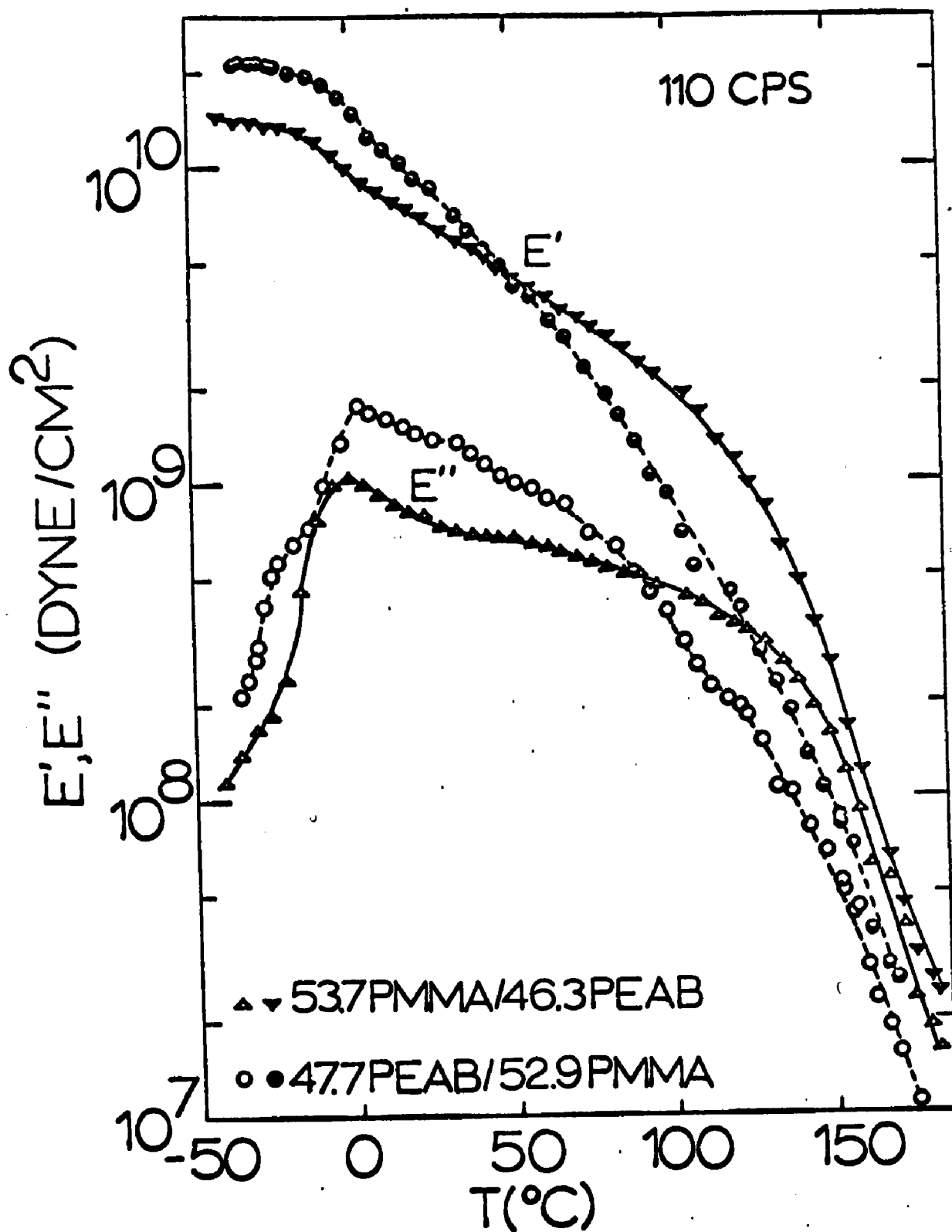


Figure 20. Temperature dependence of E' and E'' of two IPN's, I5 and L6

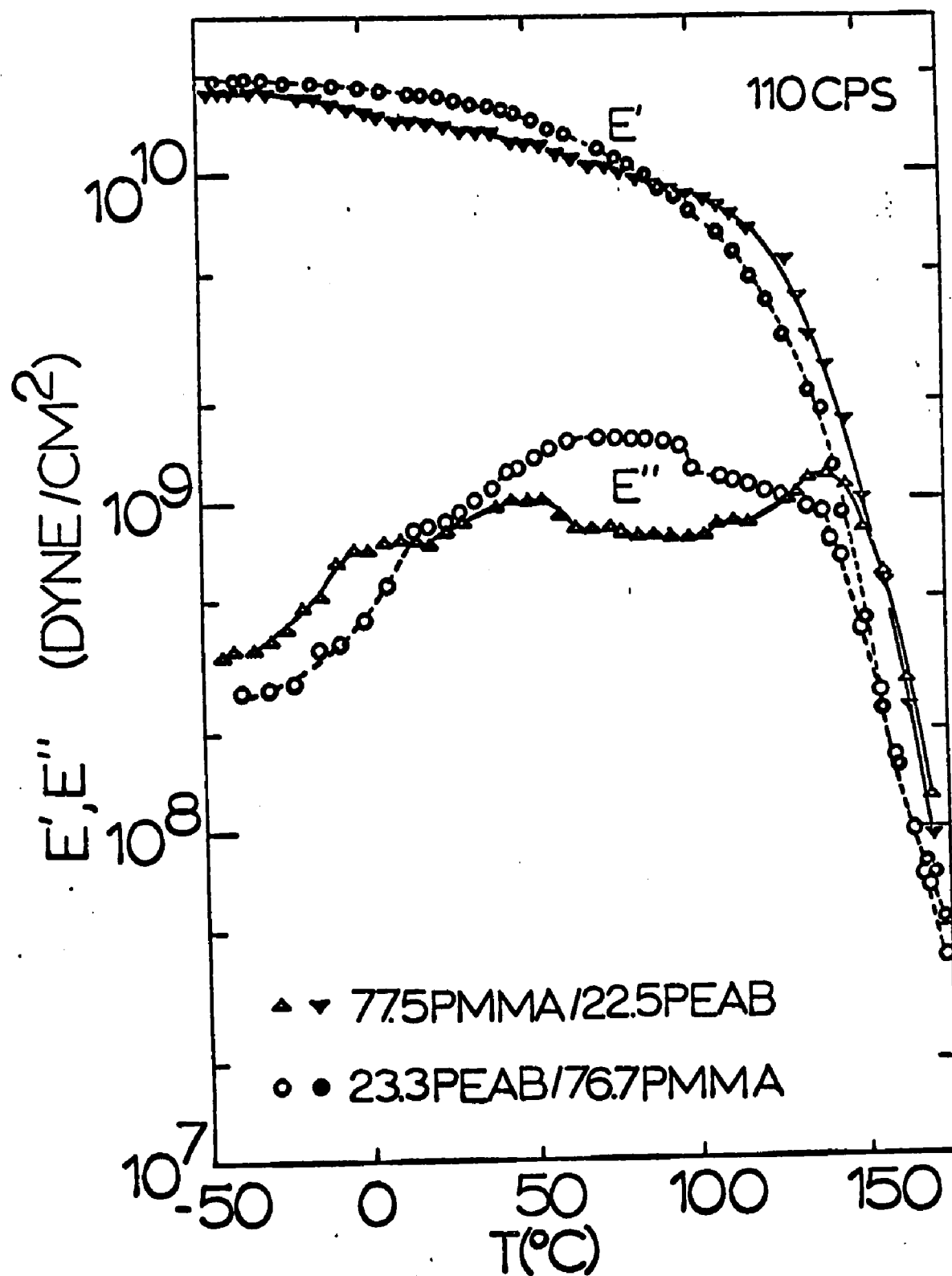


Figure 21. Temperature dependence of E' and E'' of two IPN's, I6 and P5

C. Electron Micrographs

Electron micrographs have been obtained for representative samples of the L, E, P and I series. In general all electron micrographs revealed a very complex structure, which was made visible by the incorporation of butadiene as a comonomer in the PEA component. Subsequent OsO_4 exposure resulted in selective staining of the rubbery phase. Therefore the PEAB domains appear black or dark grey while the unstained plastic regions are whitish or light grey.

1. Leathery Series

The greatest heterogeneity is exhibited by the electron micrographs of the leathery 50/50 composition. Figures 22 through 25 show photo micrographs of series L (nos. L1, L4, L5 and L6). Sample L1 (48.8 PEAB/51.2 PB) exhibits a complex cellular morphology (Figure 22). The cell walls are largely PEAB. The inner cell domains are mainly PS. A fine structure is observed mainly within the cell walls but also - however weaker and not as frequently - inside the cells. In the first case PS domains are pervading the PEAB walls whereas in the latter PEAB particles are pervading the cellular envelopes. The size of the cells are approximately 1000 \AA . The PEAB and the PS microstructure particles are of the order of 100 \AA .

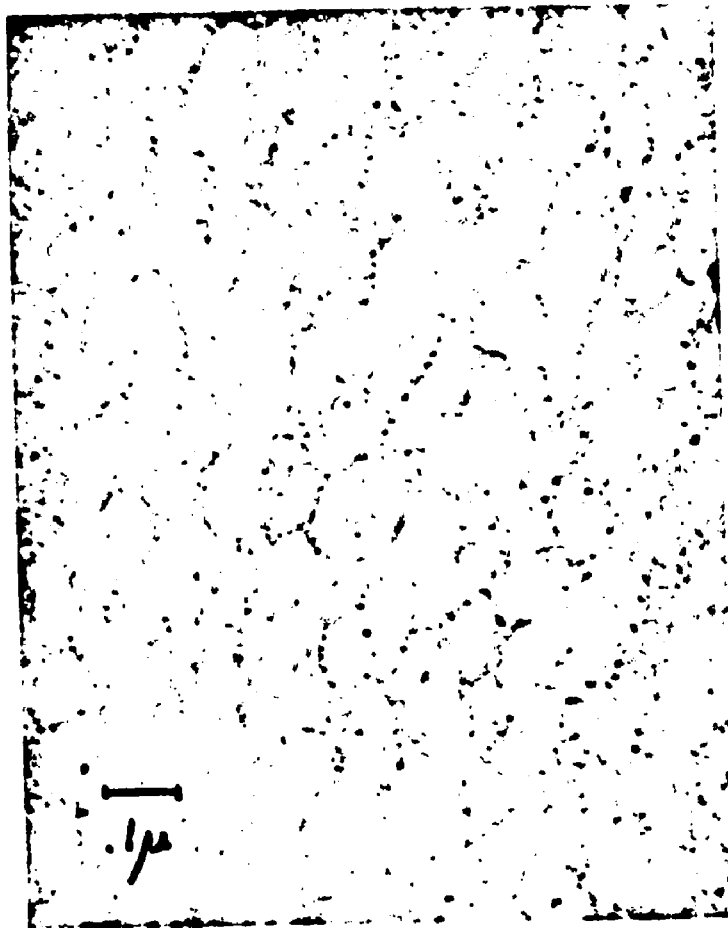


Figure 22. Electron micrograph of IPN L1:
48.8 PEAB/51.2 PS

Although the cells are irregularly shaped, they exhibit a certain orientation which coincides with the radiation direction of the polymerization. Large darker areas often arranged in forms of streaks are not a morphological feature. They result from the microtoming process and coincide with the cutting direction.

Figures 23 and 24 show electron micrographs for IPN compositions of 51.2 PEAB/P (25.4 MMA-co-23.4 S) and 48.4 PEAB/P (38.0 MMA-co-13.6 S), respectively. It can be seen how the cell walls become less distinct as S mers are gradually replaced by MMA mers. Furthermore the areas of fine dispersion increase. One notices a decrease in the rubber particle size to the order below 100 \AA as well as a decrease in the cell size down to about 500 to 600 \AA . It seems like the plastic rich cells are increasingly pervaded by PEAB starting from the walls.

Sample L6 in Figure 25 shows a more compatible structure than the previous ones. The cell walls are completely disintegrated although PMMA phase domains remain without marked boundaries. They are between 300 and 500 \AA in diameter whereas the distinct PEAB particles are below 100 \AA in diameter.

Figure 26 shows an electron micrograph of sample G1 (50.5 PEA/49.5 PS), which has the same composition as sample L1 (Figure 22) except for a higher crosslink density and no butadiene. The dispersed stained portions of 50 to 200 \AA in

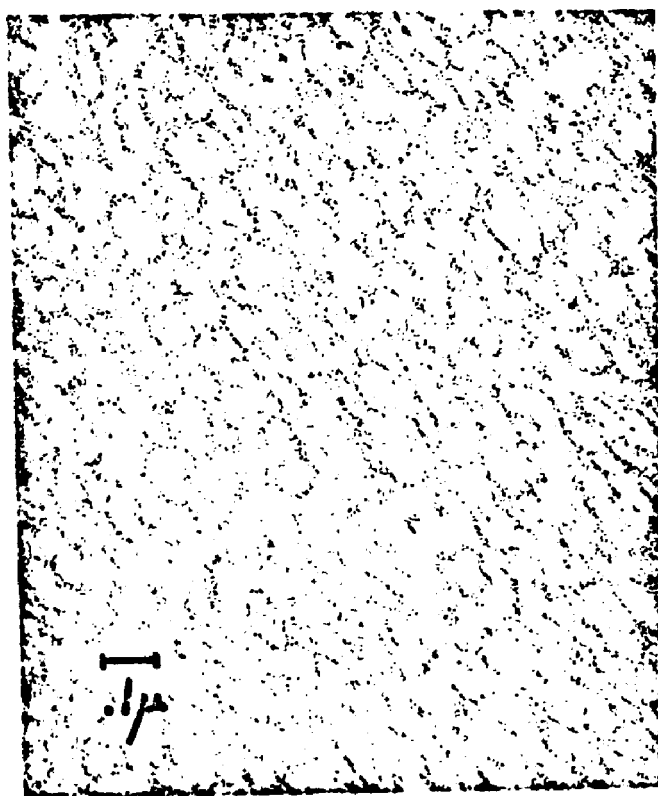


Figure 23. Electron micrograph of IPN L4:
51.2 PEAB/P(25.4 MMA-co-23.4 S)

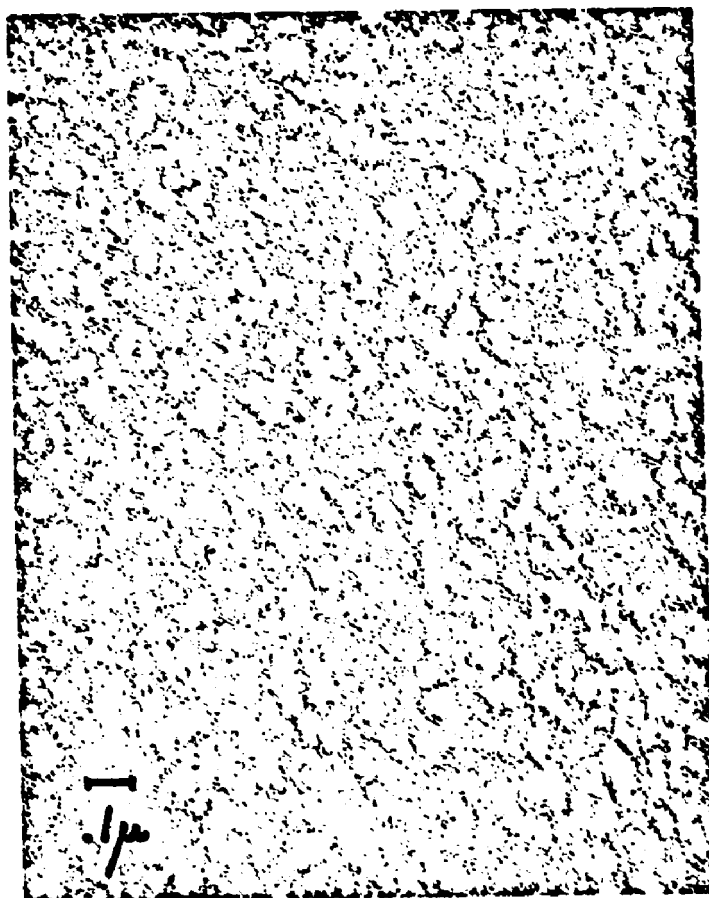


Figure 24. Electron micrograph of IPN L5:
48.8 PEAB/P(38.0 MMA-co-13.6 S)

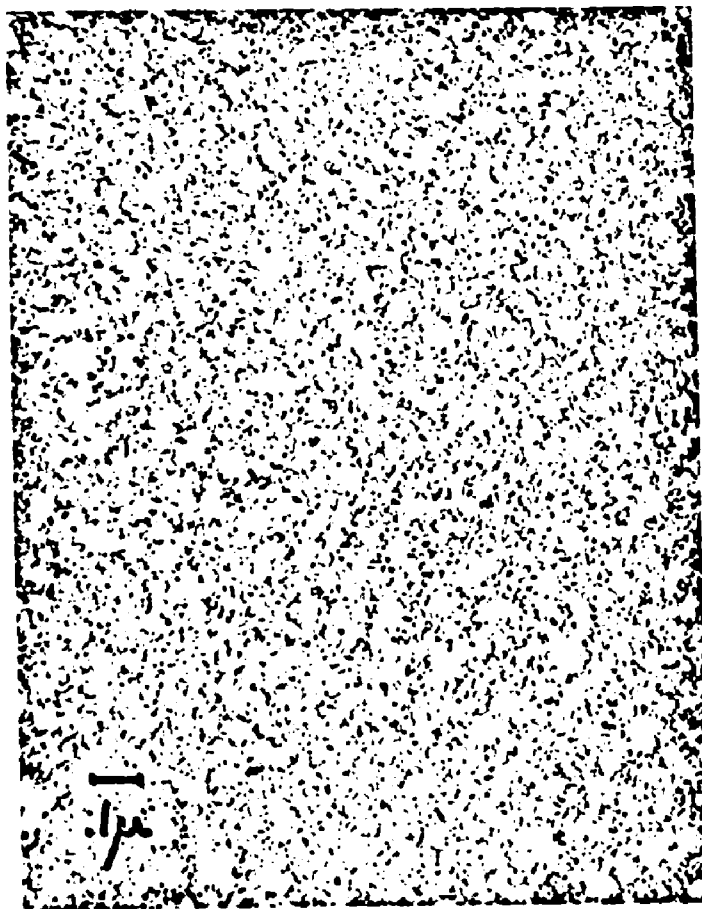


Figure 25. Electron micrograph of IPN L6:
47.1 PEAB/52.9 PMMA

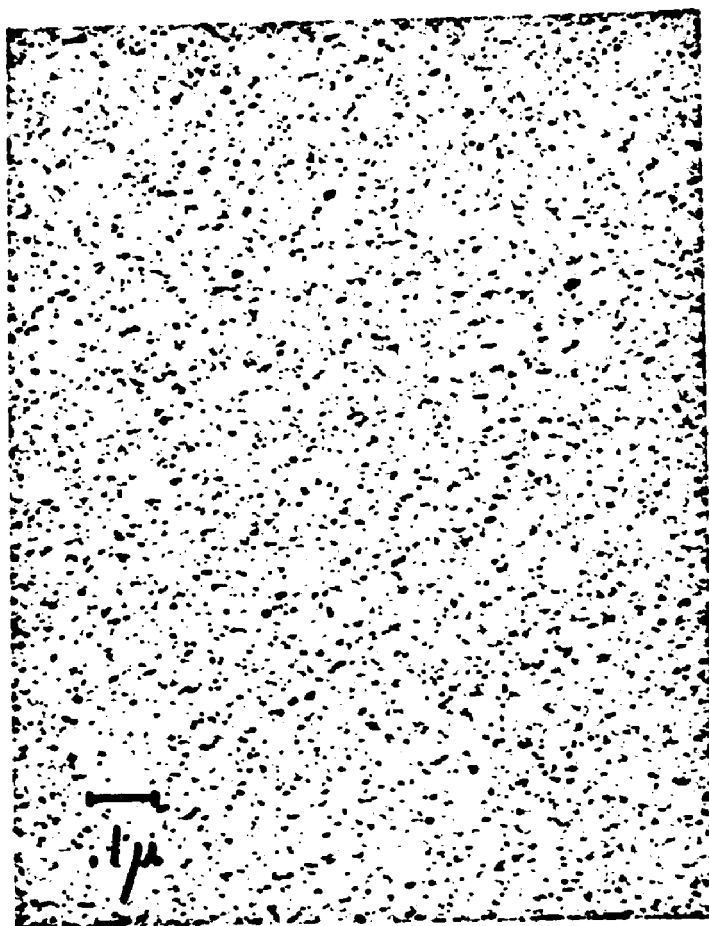


Figure 26. Electron micrograph of IPN G1:
50.5 PEA/49.5 PS

diameter have to represent a precipitate formed by the reaction of OsO_4 with PEA. Figures 22 and 26 do hardly resemble each other.

2. Elastomeric Series

An interesting sequence of structures is exhibited by the IPN's of the elastomeric series given in Figures 27 through 30. Figure 27 shows the microstructure of sample E1 consisting of 74.4 PEAB/25.6 PS. The basic matrix shows two continuous phases, where PS appears to be the more continuous one. The larger oriented white areas are part of the PS matrix which do not contain any rubbery material. They vary considerably in size, the longer dimension being between 800 and 1500 Å. The PEAB particles are again approximately 100 Å in diameter, however, in many cases a few of these PEAB particles form agglomerates.

Figure 28 of sample E2 (75.9 PEAB/P (8.4 MMA-co-15.7 S)) reveals the influence of MMA in the plastic phase. The pure plastic areas are more numerous than in Figure 27, and cover a wider region in domain size (from 200 to 750 Å); their shape is more spherical as compared to the oriented stretched PS domain structure in Figure 27. Sample E3 with the morphology as shown in Figure 29 (75.5 PEAB/P (14.6 MMA-co-9.9 S)) shows a similar structure as sample E2. The number of pure plastic domains has increased again whereas the average size is somewhat smaller.



Figure 27. Electron micrograph of IPN E1:
74.4 PEAB/25.6 Ps



Figure 28. Electron micrograph of IPN E2:
75.9 PEAB/P(8.4 MMA-co-15.7 S)

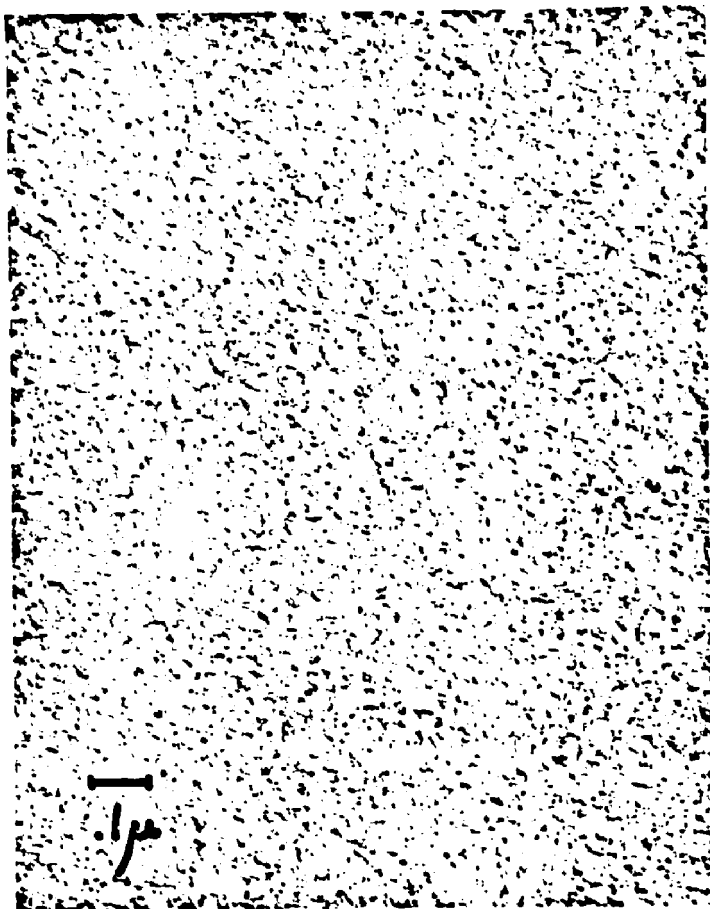


Figure 29. Electron micrograph of IPN E3:
75.5 PEAB/P(14.6 MMA-co-9.9 S)

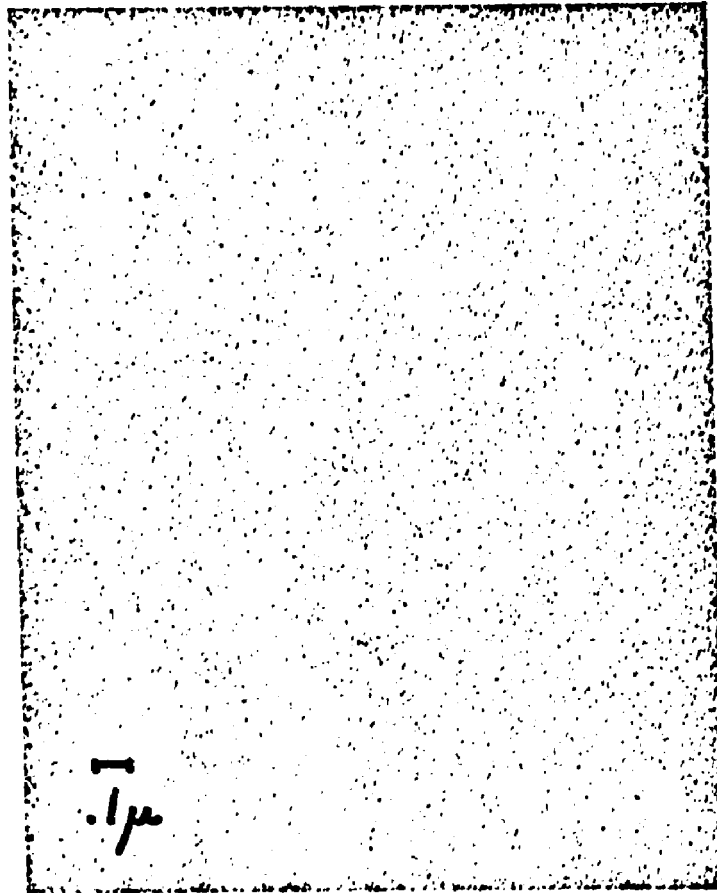


Figure 30. Electron micrograph of IPN E4:
72.2 PEAB/27.8 PMMA

The final figure in this series, Figure 30, corresponds to sample E4 (72.2 PEAB/27.8 PMMA) which does not contain any S mers. It shows a very fine dispersion of PEAB particles in PMMA and vice versa.

3. Plastic Series

The morphology of the plastic IPN's is shown in Figures 31 through 34. The plastic matrix is the more continuous phase in all cases. As long as the samples contain a certain amount of S (samples P1, P3 and P4) traces of a cellular structure are revealed. However, the interconnected spheroids of PEAB do not form long enough particulate chains in order to surround the plastic cell core completely; i.e. the vast majority of the cells are not closed. The differences between samples P1 (23.9 PEAB/76.1 PS), P3 (24.7 PEAB/34.4 MMA-co-40.9 S)) and P4 (25.4 PEAB/49.7 MMA-co-24.9 S)) as observed on the electron micrographs are small. The sizes of the cellular traces are approximately 1000 \AA , their shape is irregular, although a stretched orientation is noticable. Sample P5 (23.3 PEAB/76.7 PMMA) in Figure 34 shows small remainders of a cellular structure with weakly marked walls.

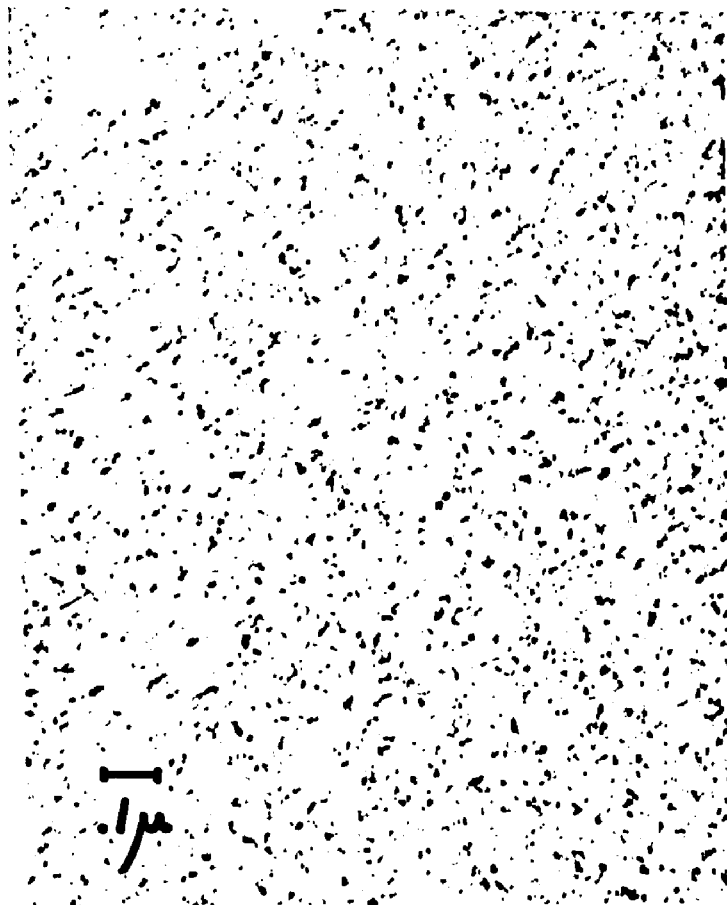


Figure 31. Electron micrograph of IPN P1:
23.9 PEAB/76.1 PS

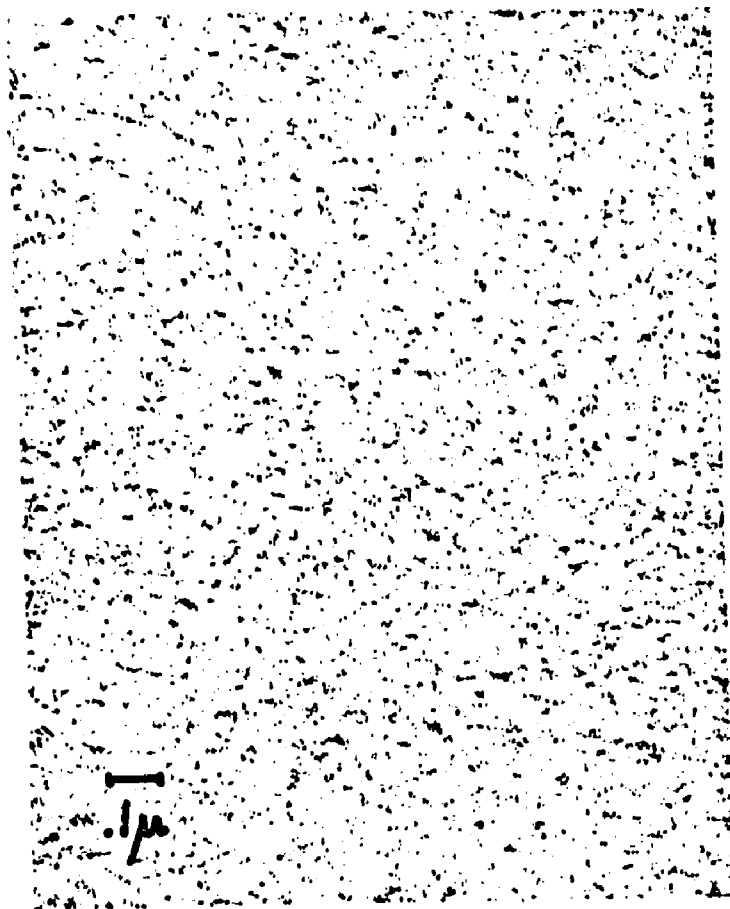


Figure 32. Electron micrograph of IPN P3:
24.7 PEAB/P(34.4 MMA-co-40.9 S)

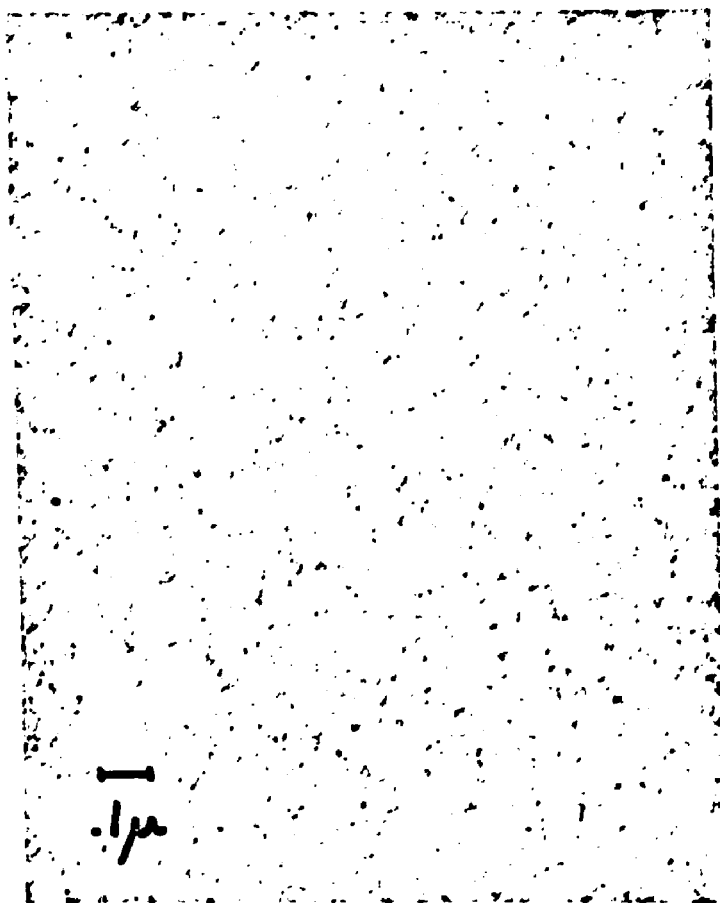


Figure 33. Electron micrograph of IPN P4:
25.4 PEAB/P(49.7 MMA-co-24.9 S)

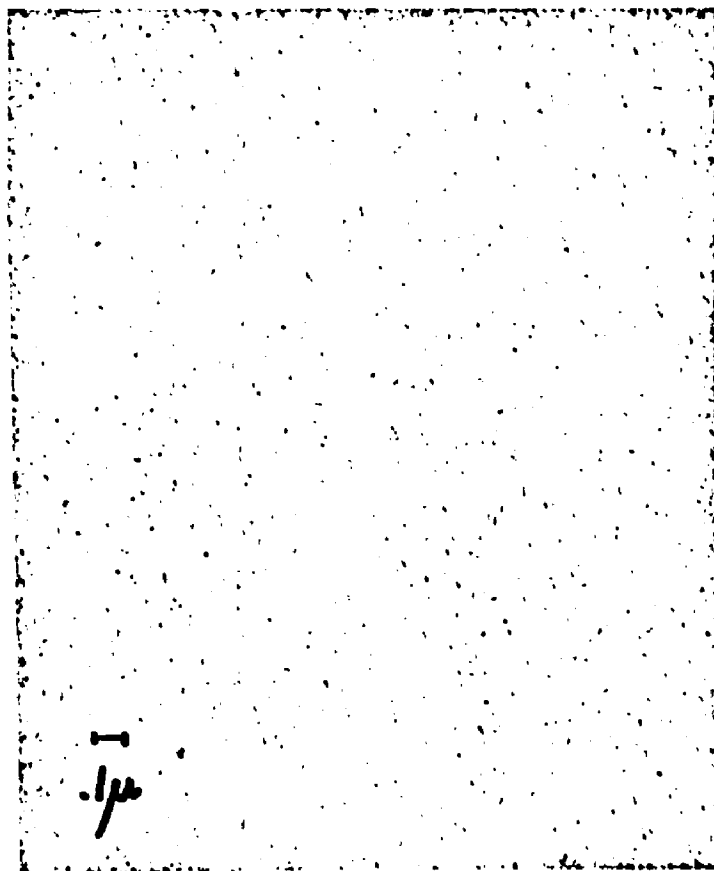


Figure 34. Electron micrograph of IPN P5:
23.3 PEAB/76.7 PMMA

4. Inverse IPN's

Only one inverse IPN containing PMMA has been successfully investigated microscopically (sample I6), whereas photomicrographs for all PS containing IPN's have been obtained.

Figure 35 shows the morphology of sample I2 (50.7 PS/49.3 PEAB). Like its counter composition (sample L1 in Figure 22) it exhibits a complex cellular structure. A PS rich matrix contains PEAB rich cellular inclusions. The cellular domains cover a wide size range; the longer dimension of the stretched cells is between 400 and 2000 Å and the smaller one is between 150 and 1000 Å. It is hard to measure individual particle sizes of the fine structure accurately from the electron micrographs. However they are obviously smaller than 100 Å. The quality of the electron micrograph for sample I1 (24.6 PS/75.4 PEAB, Figure 36) is unfortunately inferior if compared to the other photomicrographs. It reveals, nevertheless, clear indications of a cellular structure. PS or a PS rich phase is the more continuous matrix which contains PEAB rich cells.

The morphology for the inverse plastic IPN of sample I3 (71.4 PS/28.6 PEAB) is revealed in Figure 37. PEAB particles or agglomerates of a few particles up to 150 Å are regularly dispersed in a PS matrix. In many cases they started to form loosely connected cell boundaries which are incomplete and never closed due to lack in PEAB.

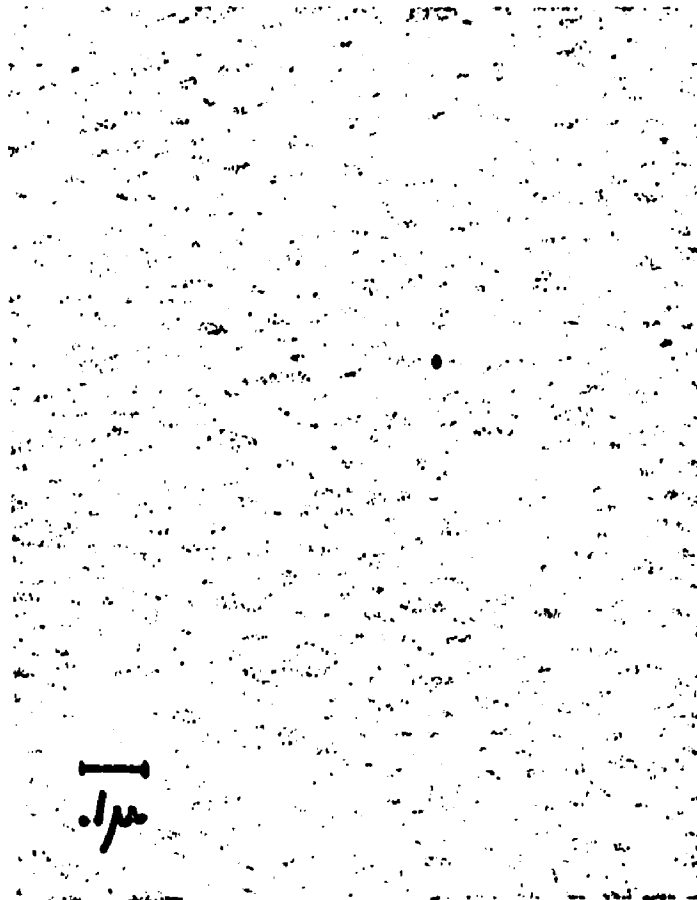


Figure 35. Electron micrograph of IPN I2:
50.7 PS/49.3 PEAB

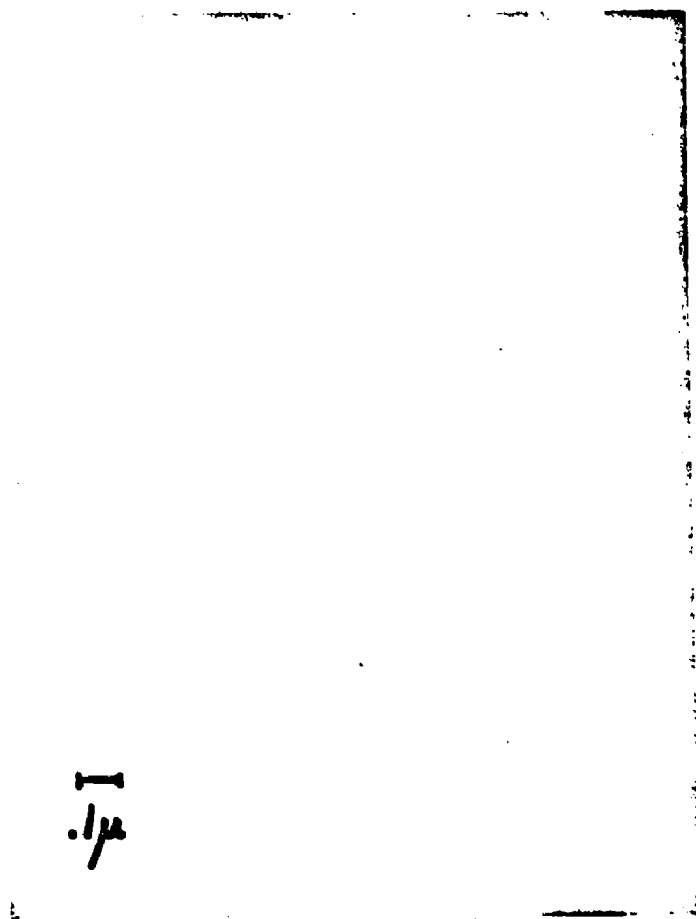


Figure 36. Electron micrograph of IPN 11:
24.6 PS/75.5 PEAB

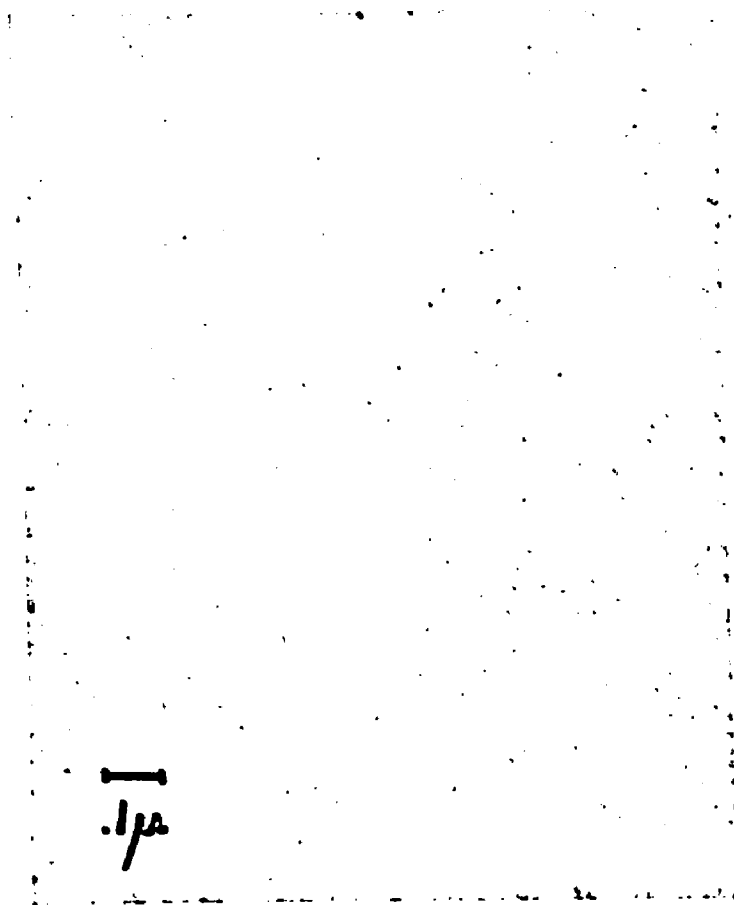


Figure 37. Electron micrograph of IPN I3:
71.4 PS/28.6 PEAB

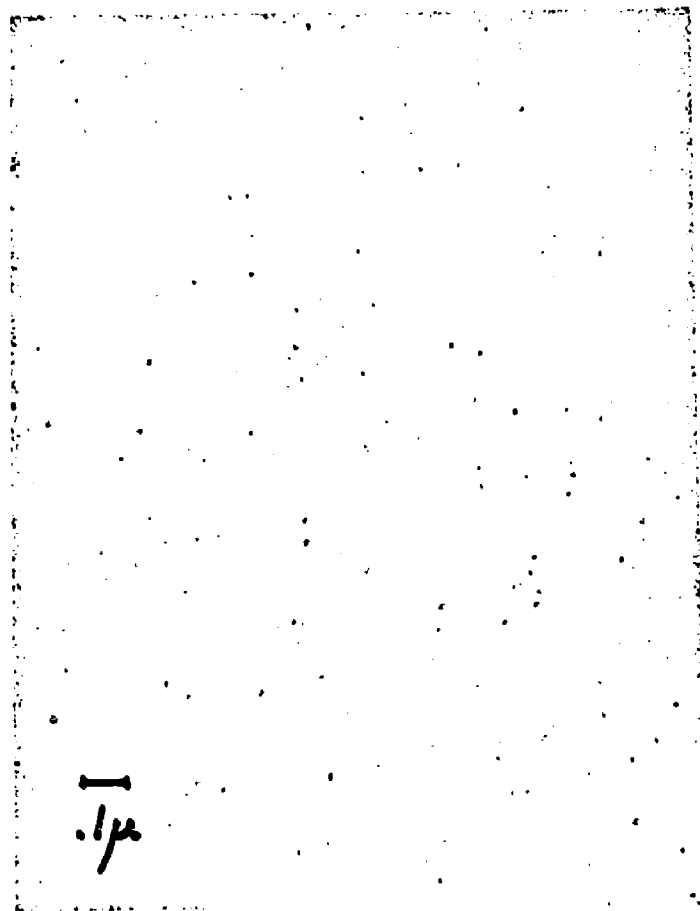


Figure 38. Electron micrograph of IPN I6:
77.5 PMMA/22.5 PEAB

The micrograph for the plastic inverse IPN I6 (77.5 PMMA/22.5 PEAB) exhibits an uniform fine structure which is very similar to its normal counter composition P5 (Figure 38,34) PMMA is probably the more continuous phase with both samples. However, this is difficult to determine. The areas of micro-morphology show finely dispersed particles which are clearly below 100 \AA in diameter. Sample I6 shows besides the interpenetrating structure randomly dispersed dark spots of ca. 150 \AA , in diameter, which might be agglomerates of PEAB particles.

VI. DISCUSSION

In this chapter the results of the research on IPN's presented in chapter V, will be discussed and compared with other two-phase polymeric materials. The research on the viscoelasticity and the morphology will indicate that IPN's are a special type of polyblend. However, it will be clear that no attempts were made to optimize the investigated IPN's for commercial applicability with respect to such properties as impact strength or maximum elongation at break or with respect to the polymeric components used.

A. Creep Behavior

1. Glass Transition Behavior

The GEHMAN data for the three selected samples G1, G3 and G5 (Figure 2) showed interesting changes as S mers were replaced by MMA mers. The intermediate plateau with sample G1, i.e. the slope of the modulus between the two sharply inclined transition regions, is relatively flat. This indicates a high degree of phase separation. However, a certain very limited degree of molecular mixing between the PEA and the PS phases can be read from the fact that the intermediate slope is far from being horizontal. In support of this explanation is the fact that the two glass transitions have been shifted towards each other.

The indications of two glass transitions are less distinct with sample G3 than with G1. These mitigating effects are due to the amount of added MMA, which partially replaced S in the plastic component. Thus it is clearly understood that PMMA, which is isomeric to PEA, increases the compatibility and molecular mixing ensues. This trend is continued with sample G5, where only one broad transition remains. The breadth of the temperature range this transition covers depends of course on the T_g 's of the two homopolymers. This effect had been found for the same system by SPERLING and coworkers (91). The morphological reasons for this change from two transitions to one broad transition become clear from observation of the corresponding electron micrographs (Figures 22 through 25), which exhibit a gradual disintegration of the cellular structure as MMA replaces S in the plastic network.

2. Rubbery Plateau Considerations

Two types of errors are generally involved in the GEHMAN experiments: a) a rapid decrease in the accuracy of the apparatus as the angle of twist exceeds 165° , and b) a certain amount of friction in the mechanics of the equipment. The difference between $E_2(\text{PS})$ and $E_2(\text{G1})$ (see Table 2 and Figure 2) might be within the range of these errors. However, the differences between the E_2 -values for the samples G1 and G5 cannot be explained by the inaccuracies. Thus the indicated trend

must be real.

The same amount of crosslinking agent was employed for all samples in Table 2: 2 ml TEGDM per 100 ml monomer. The effectiveness of the crosslinking agent must differ with each sample in order to explain the differences in the rubbery moduli. It might depend on the affinity of the TEGDM molecule to the monomer molecule or on the diffusion rate into the primary network or on the reaction kinetics. The first reason would explain the considerable smaller difference between the E_2 -values of PEA and PMMA, the monomers of which are isomeric, and the bigger differences between the E_2 -values of PS and PEA or PMMA, respectively.

One has to keep in mind at this point that the polymerized networks are a kind of copolymers, because of the dissimilarities between the monomer molecules and the TEGDM molecule. Thus it might have been more appropriate to use divinylbenzene (DVB) and ethylene glycol dimethacrylate (EGDM) for crosslinking pure PS and PMMA, respectively. In this case the crosslinking of the comonomer solution of S and MMA would have created a problem.

KLEMPNER and coworkers (83) report for their partial IPN's an effective crosslink density greater than the arithmetic mean of the crosslink densities of the component networks. Their preparation method - film deposition from aqueous emulsions

of both components - is quite distinct from the preparation of the IPN's. However, SHIBAYAMA's and SUZUKI's materials (5,126,127) are truly IPN's in the sense employed by this author. Their PS/PS IPN's (5) were in all cases prepared by maximum volume swelling techniques. This difference might explain an increase in rubbery modulus with each additional superimposed network. MILLAR's investigations (4) show clearly that the subsequent swelling is controlled by the network with the highest crosslink density. This means qualitatively that the overall rubbery modulus of an IPN is controlled by the higher modulus of the two independent networks, assuming two continuous phases. These considerations are valid for two superimposed interpenetrating networks of the same homopolymer and for maximum swelling.

The PS/PMMA IPN's by SHIBAYAMA and KODAMA (125) of various composition not obtained by maximum swelling do not show a certain trend in the rubber modulus values. Thus these IPN's correspond closest to this author's materials. So do their findings for the E_2 -values.

3. Relaxation Behavior (92,93,97)

The creep data presented in Figure 3 were converted to relaxation data by using the semiempirical treatment of FERRY (98).

Although it is well known that the standard time-temperature superposition principle (99) and the WLF equation do not strictly apply to broadened transitions, it is still instructive to construct master curves, as has been done by TAKAYANAGY (30).

Figure 39 (92) shows the master curve for sample G5 at a reference temperature of 30°C. The broad transition appearing with this IPN is analogous to the corresponding curve in Figure 2 and to the modulus temperature data reported by SPERLING and coworkers (91).

The empirical shift factors for this IPN are compared to the theoretical WLF values in Figure 40, 20°C being chosen as close to the classical glass transition temperature (based on ref. 92; Fig. 39). For a classical homopolymer, the shift factor covers about 8 decades of time in a temperature interval of approximately 40°C. This corresponds to the central portion (25° to 65°C) of Figure 40 (92). The WLF equation fits the center and the lower portions of the data quite well. The reason lies in the value of the derivative, $d \log(t/t_0)/dT$,

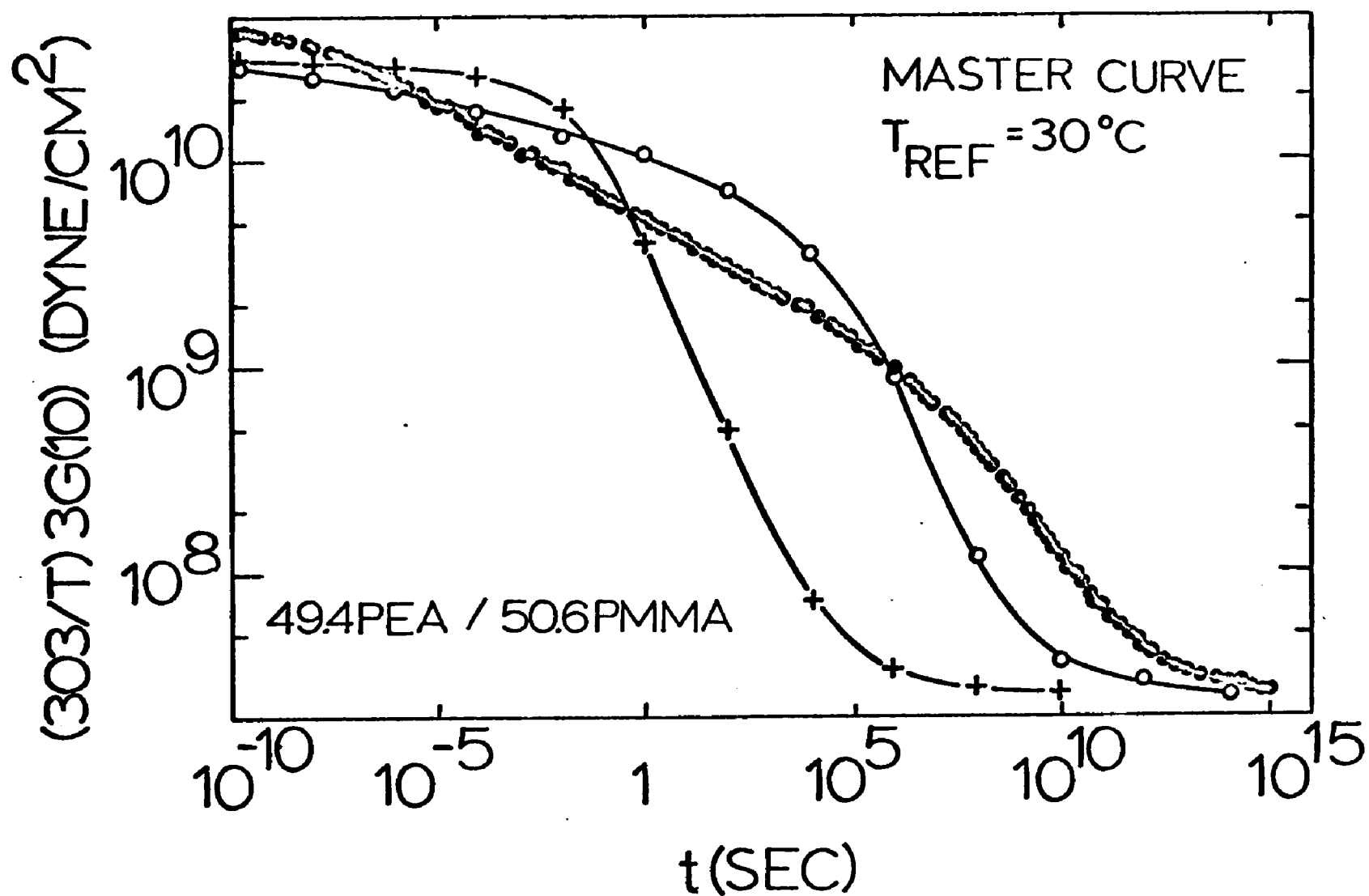


Figure 39. Mastercurve for IPN G5; (+) single relaxation time assumption (T-A-D theory); (o) equation (VI,4), assuming a random distribution of compositions (from (93)).

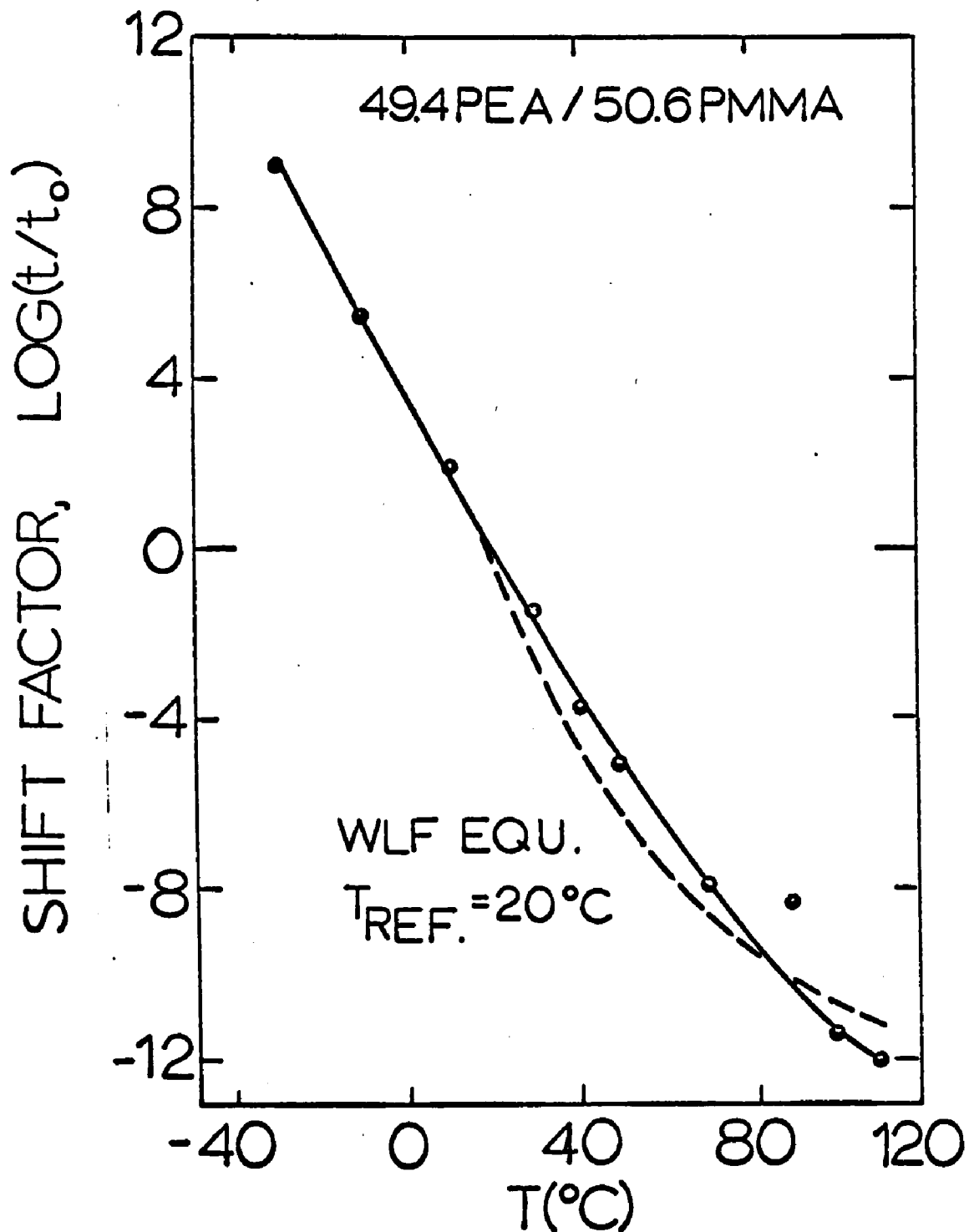


Figure 4o. Experimental shift factors compared with those predicted by WLF equation (VI,6) for IPN G5 (from (93))

which is nearly equal for the WLF equation and the experimental points. This is not surprising since the IPN transition covers both a broader time scale and temperature range as compared to homopolymers. This increased breadth of the IPN transition becomes apparent on observing the upper portion of Figure 40, which does not have an analog in the WLF formulation.

In 1964, the time-dependent relaxation modulus $E_r(t)$ was interpreted by TOBOLSKY and AKLONIS as the sum of two Rouse functions (100). One, R_1 , is associated with torsional vibrations and internal rotations. The other, R_2 , is associated with an entangled network of Gaussian segments. The R_1 function was derived to be

$$R_1 = \frac{E_1 \tau_{\min}^{\frac{1}{2}}}{2} t^{-\frac{1}{2}} \left(\Gamma_{t/\tau_1}(\frac{1}{2}) - \Gamma_{t/\tau_1 Z_1^2}(\frac{1}{2}) \right) \quad (\text{VI},1)$$

where E_1 = the tensile modulus (3×10^{10} dynes/cm²) in the glassy state

min = the minimum relaxation time

$\Gamma(\frac{1}{2})$ = the tabulated incomplete gamma function of argument $\frac{1}{2}$

τ_1 = the first normal mode relaxation time

t = the time

Z = the number of Gaussian segments in a polymer molecule

In a later paper, TOBOLSKY (101) approximated this function with

$$R_1 = \frac{E_1 \tau_{\min}^{\frac{1}{2}}}{\tau_{\min}^{\frac{1}{2}} + t^{\frac{1}{2}}} \quad (\text{VI},2)$$

For the PEA and PMMA homopolymers, a modified form of the double Rouse function will be employed:

$$E_r(t) = \frac{E_1 \tau_{\min}^{\frac{1}{2}}}{\tau_{\min}^{\frac{1}{2}} + t^{\frac{1}{2}}} + R_2 \quad (\text{VI},3)$$

Because of the unusual breadth of the transition with this IPN (sample G5), it will be assumed that the sample does not consist of a single composition but of a continuous range of compositions. Each composition region will be assumed to have its own characteristic relaxation time. The average composition, of course, will be equal to the overall composition. A number of simple distributions were analyzed by use of the formula

$$E_r(t) = 3G(t) = E_1 \cdot \sum_{i=1}^n \frac{w_i \tau_{\min i}^{\frac{1}{2}}}{\tau_{\min i}^{\frac{1}{2}} + t^{\frac{1}{2}}} + R_2 \quad (\text{VI},4)$$

where w_i is the frequency for composition i , normalized to satisfy

$$\sum_{i=1}^n w_i = 1 \quad (\text{VI},5)$$

The values of τ_i appearing in eq.(VI,4) were evaluated as follows. For homopolymers, the single value of τ_{\min} was obtained (100) by use of a plot of $\log (R_1(t)/E_1)$ versus $\log (t/\tau_{\min})$. By sliding tabulated values of eq.(VI,2) over a plot of the experimental values of $\log (3G/E_1)$ versus $\log t$ in the transition region, the values of τ_{\min} which gave the best fit were selected.

For pure PMMA τ_{\min} was estimated at $+30^\circ\text{C}$ to be 1×10^5 sec. The value of τ_{\min} for pure PEA was estimated at -20°C to be 1×10^{-1} sec. τ_{\min} for pure PEA at $+30^\circ\text{C}$ was calculated by use of the WLF equation

$$\log \frac{\tau_T}{\tau_{T_g}} = \frac{-17.44(T - T_g)}{51.6 + T - T_g} \quad (\text{VI},6)$$

to be 4.46×10^{-9} sec (T_g was assumed equal to -20°C).

The above method for determining τ_{\min} is applicable to homopolymers when a slope of $-\frac{1}{2}$ is obtained in the transition region. This method cannot be used with the intermediate IPN compositions since slopes significantly less than $-\frac{1}{2}$ were found. It was therefore assumed that $\log \tau_{\min}$ varied as a linear function of weight per cent PEA. This assumption is quite arbitrary and was made for the sake of simplicity. Other τ_{\min} distributions, such as $\log \tau_{\min}$ -log composition, gave the same or poorer results, as discussed below.

Of the several phase distributions studied (Gaussian, etc.), the simplest, which assumed all compositions to have equal weight, gave the best fit. A distribution containing nine equally spaced compositions of equal weight covering the entire composition range yielded the (o) line in Figure 39. For comparison, a curve based on eq.(VI,3) is shown as the (+) line.

Only distributions which included the whole range of compositions from 0 to 100% by weight PEA reasonably approximated the form of the master curve. As can be seen from Figure 39 even the last yielded an imperfect fit to the experimental data. However, the assumption of a single relaxation time results in a much poorer fit. This suggests that the actual composition distribution, although it may be quite complex, will have to include the whole continuous range of compositions (32).

The original ROUSE-BUECHE theory (102,103) requires

approximately 50 mers to undergo coordinated motion for the glass transition phenomenon to occur. A volume of about $10,000 \text{ \AA}^3$ is involved. Due to the size of polymer chains, however, only much larger regions, perhaps $100,000 \text{ \AA}^3$, can be expected to have a mean composition. A broadened transition will result if the minimum volume required for independent contribution to the relaxation spectrum is subject to wide composition variation, even in thermodynamically compatible polymer mixes. If this argument is valid, one cannot decide whether any polymer pair is compatible or not by observing the glass transition behavior alone.

4. Grafting Effects

An amount of 0.5 ml TEGDM per 100 ml monomer was employed as crosslinking agent through the series L, E, P and I (see Table 1). The PEA phase for these samples was butadiene doped in order to make it susceptible to OsO_4 -staining. It was of interest to estimate the amount of grafting due to the $\text{C} = \text{C}$ double bond of the unsaturated butadiene by comparing the pure PEA with the doped PEAB.

The rubbery plateau values for a pure and a butadiene doped (ca. 2% butadiene) PEA sample were determined at ambient temperature employing a GEHMAN torsion stiffness tester. Table 3 gives the rubbery moduli, E_2 , and the crosslink densities, g_E , as determined from E_2 values. E_2 is an average value

of three experiments, where the maximum scattering was 5%. They are compared with the crosslink density, d , calculated from the amount of crosslinking agent used.

| 0.5 ml TEGDM/100 ml monomer | PEA | PEAB |
|--|-------|-------|
| $E_2 \times 10^{-7}$ (dyne/cm ²) | 1.70 | 1.86 |
| $g_E \times 10^4$ (mole/g) | 2.065 | 2.260 |
| $d \times 10^4$ (mole/g) | 1.85 | 1.85 |

Table 3. Rubbery moduli and crosslink densities of PEA and PEAB

The crosslink density values, g_E , account for the effective chemical crosslinks plus the trapped physical entanglements. The effective chemical crosslinks allow that not every molecule of TEGDM produces a chemical crosslink and that crosslinks at terminated chain ends are less effective. If physical chain entanglements are trapped by chemical crosslinks they become permanent features of the network (104) and thus contribute to the crosslink density. If it is assumed that the effectiveness of TEGDM is constant for both samples, the difference between $g_E(\text{PEAB})$ and $g_E(\text{PEA})$ accounts

for the amount of grafting. Provided, however, that TEGDM is fully effective, the difference between $g_E(\text{PEA})$ and d could be attributed to trapped entanglements. The data indicate clearly that the amount of grafting due to butadiene doping is negligible.

The amount of grafting between both networks, although quantitatively unknown, may be considerable, since α -hydrogens on the four ether groups of the TEGDM act as strong chain transfer agents in addition to the possibility existing on the first polymer's chain structure. This grafting, which is mainly introduced upon swelling in the second monomer solution, occurs with PMMA and PS as well as with PEA. The effect of these grafts in connecting the two networks is estimated to be somewhat smaller than the effect due to the physical interlocking (95).

B. Dynamic Mechanical Behavior

The Rheovibron data will be treated from two different viewpoints: 1) for each series L, E and P particular features will be followed and discussed as the plastic phase is gradually changed from PS via P(S-co-MMA) to PMMA, and 2) the change in concentration of the normal border compositions will be compared with the corresponding inverse IPN's.

The terms "compatibility" and "semicompatibility" play an important part in these discussions. Since it is very difficult to define them for two phase polymeric materials satisfactorily the author will also use more obvious terms like "more compatible" or "trend towards compatibility". A qualitative concept for compatibility is developed in section VI,E.

1. Change in Compatibility within Series L, E, and P

The change in compatibility becomes almost obvious from the dynamic mechanical data for series L (Figures 4 through 7). The two initially observed peaks of the loss modulus start to gradually merge upon replacing S mers by MMA mers. This is an indication for an increase in molecular mixing of the rubbery and the plastic phase, which is supported by the 4°C shift in $T(E''_{\max})$ of the PEAB peak. This trend would be even more evident if the difference between the PEAB and the plastic peak height would be considerably smaller than one order of magnitude.

This is the case with the IPN's of the P series (Figures 12 through 15). There the two loss peaks of sample P1 start to merge and finally in sample P5 form one broad elevated peak. Its E'' value is above the initial peak heights, thus leaving only two shoulders indicative of the rubbery and the plastic transition.

The Rheovibron results for the elastomeric series (Figures 8 through 11) exhibit only one rubbery peak due to the high PEAB concentration. In this case no relationship between composition and peak temperature was found. Thus the shift in T_g from -12°C (for pure PEAB) to ca. 0°C appears to be independent of the plastic component. This is not in contradiction to the observed trend with series L, since one would expect a smaller influence of the plastic network composition upon T_g because of the overall low plastic content. Also these data show a trend towards higher compatibility as the S mers are gradually replaced by MMA mers. Another indication for a broadened transition region is the gradual increase in temperature at a randomly chosen storage modulus value of $E' = 10^8 \text{ dyne/cm}^2$ with increasing MMA content.

2. Comparison Normal - Inverse IPN's

Sections B, C and D in chapter II contain several examples showing that different methods of synthesis produce different polyblends with respect to morphology and behavior in spite of equal overall compositions. Thus it was expected that the behavior of IPN's depends on the order of preparation. This becomes obvious from Figures 16 through 21 where in each plot the storage and the loss moduli of inverse IPN's are compared with normal ones of approximately the same composition.

The following general differences are observed between the normal border composition samples and their inverses:

1. a) For the inverse samples the slope of the intermediate storage modulus plateau (between the two transitions) is always bigger, i.e more flat, than for the normal ones.
- b) For the inverse samples the intermediate plateau moduli E' , for the IPN's containing PS are considerably higher than for the normal ones.
2. a) The loss modulus peaks corresponding to PEAB are observed at lower temperatures with the inverse IPN's than with the normal ones. Likewise, the PS peaks of the inverse IPN's occur at higher temperatures.
- b) The loss modulus peaks corresponding to PEAB are observed at lower E'' -values with the inverse IPN's than with the normal ones. Likewise, the PS peaks of the inverse IPN's

occur at higher E'' -values.

3. The dynamic mechanical differences between the inverse and the normal IPN's are bigger with the system PEAB/PS than with the system PEAB/PMMA.

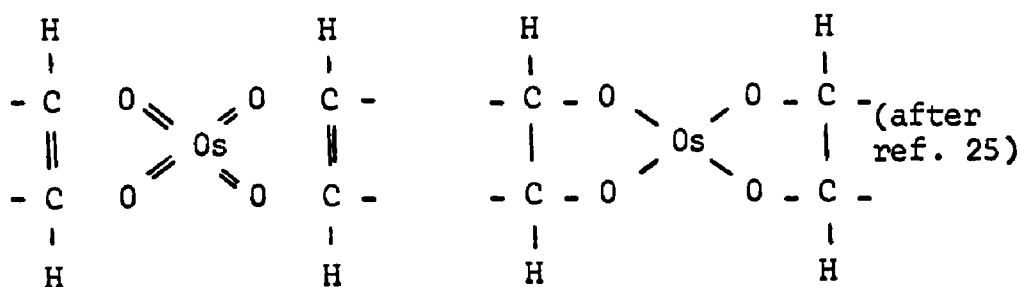
The general observations indicate that the IPN component polymerized first controls the dynamic mechanical properties.

C. Micromorphology

1. OsO₄ Staining Technique

The OsO₄ staining technique has mainly been applied to rubbery phases containing unsaturated PB or PI. A different staining technique employing OsO₄ has been applied by MATSUO (68,69). He treated the PVC/EVA (ethylene vinylacetate) graft copolymers with a saturated solution of NaOH in methanol, thus making the EVA phase near the surface susceptible to OsO₄ incorporation.

KAEMPF and SCHUSTER (122) have shown that an exact representation of the stained phase depends on an adequate OsO₄-fixation, i.e. the proper exposure time. They showed that flattening of spherical rubber particles was caused by a too low fixation, while a too high fixation resulted in swelling of the particles. In both cases excessive particle diameters are obtained. The maximum deviation in diameter of PB latex particles (ca. 600 Å) was 25.6%. The authors found an incorporation of one OsO₄-molecule per eight monomer units of butadiene being appropriate although an incorporation of one OsO₄-molecule per two unsaturated monomer units results in a complete saturation, i.e. split of adjacent C = C double bonds and connection of the two mers by an OsO₄-molecule.



The amount of butadiene employed in the EA monomer solution results actually in a random copolymer of PEA and PB with an approximate concentration of one butadiene mer per 50 or 100 EA mers. Thus a stained particle of 100 \AA in diameter contains approximately 10 OsO_4 -molecules. The photographic contrast is therefore not as good as it would be with an unsaturated rubber phase.

It is unknown how OsO_4 reacts with the $\text{C}=\text{O}$ double bond of the EA molecules. But the black precipitates as shown in Figure 26 clearly indicate that some kind of reaction takes place between OsO_4 and PEA, since OsO_4 does not react with PS. The nature of this reaction is unknown and obviously less than with materials containing butadiene as one phase.

The micrograph in Figure 26 exhibits a random dispersion of stained particles covering a domain size range from 50 to 200 Å. These particles are sometimes loosely arranged so as to form encirclements. Beyond that Figures 22 and 26 do not show any resemblances. CURTIUS et al. (106,124) have shown that for PB/PS IPN's different crosslink densities result basically in the same morphology, however, on a different size scale. It appears that the length of the average chain segment between crosslinks only limits the size of the phase domains that form but does not vary the basic features of the structure. Thus it is believed that the big differences between Figure 22 and 26 are solely due to the butadiene content in the PEA phase of sample L1.

It is clear from these qualitative considerations that the stained portions of the IPN electron micrographs do not exactly represent the complete domain area of the rubber phase even under the assumption of total fixation of the incorporated butadiene mers. Single dark stained PEAB domains are therefore expected to be somewhat smaller than the actual PEAB particles although the measurements are considered to be in the right order of magnitude. However, the arrays of stained PEAB particles (e.g. interconnected spheroids in cellular formations) probably indicate dimensions with fairly good accuracy.

2. Micromorphological Features

Areas of fine dispersion of particles in a matrix - very often to the extent that it is difficult to determine which phase is the continuous one - have been interpreted (31,32,68,69) as being indicative of network formation. If one transfers this interpretation to the IPN's, where those finely dispersed areas are observed on a much finer scale, one can draw the conclusion that those areas are an indication for double network formation and for interpenetration as well.

Almost all electron micrographs contain at least some domains which show this nicely. Excellent examples are given in Figures 23 and 24. They resemble very much - however on a scale of one order of magnitude smaller - those of a graft copolymer of PVC and ethylene vinylacetate rubber (EVA) investigated by MATSUO (68,69). A sample containing 5% EVA exhibits a cellular structure where the EVA phase forms a network which separates the PVC matrix into particles with ca. $0.5\ \mu$ in diameter (68).

The elastomeric series (Figures 27 through 30) reveals interesting features. One observes with sample E1 two continuous networks, where PS appears to be the more continuous one. This is in contradiction to the structure predicted from dynamic mechanical data in Figure 43. This might certainly be caused by the underrepresentation of the rubbery phase as explained

above. The micrograph shows that a little higher concentration of dark particles would easily cause the dark phase to be the more continuous one. It is observed with this series that the plastic domains decrease in size and finally disappear as S mers are replaced by MMA mers. This leads one to the speculation that the plastic domains of samples E_2 and E_3 must be PS rich, while the remaining PEAB rich matrix probably contains mainly PMMA as plastic material since it expresses a higher degree of compatibility and thus real interpenetration and double network formation. The incompatibility between PS and PEAB in Figure 27 might be a reason for the different appearance of the matrix as compared to the ones in Figures 28, 29 and 30.

The variation in size of the cellular domains was observed to be greatest with sample I2 (Figure 35). As reported above the longer dimension of the stretched cells is between 400 and 1000 Å. If the cells are assumed to be spherical, their volume would vary by a factor of up to 200. It is not known why this variation is greatest with this particular IPN, although the biggest heterogeneities have been observed with the leathery series. The border regions of the cellular inclusions appear relatively distinct. This is surprising since the matrix contains PEAB besides PS and since the cells contain PS besides PEAB. There are however indications that the PS rich matrix

is not of constant concentration. It appears that the PS concentration of the matrix is particularly high in the vicinity of the walls, which would cause clear distinctions between the cells and the matrix.

A comparison of this structure with the normal sample L1 (Figure 22) yields big differences in spite of the same overall composition. However, certain features seem to be inverted. The cellular content is PS with the normal and PEAB rich with the inverse sample. The matrix on the other hand is PEAB rich for the normal IPN and PS rich for the inverse IPN. However, the matrix of the normal sample consists mainly of interconnected PEAB spheroids. The partially inverse character of the structures becomes more obvious by comparing sample I2 (Figure 35) with sample L5 (Figure 24). Generally it can be stated that the network synthesized first forms the major content of the more continuous phase.

All the IPN samples exhibiting a complex cellular structure showed an orientation of these cells parallel to the radiation direction. The ratio of the long dimension over the broad one very seldom exceeded a value of 2, which leads one to believe that the cells might approximately describe an ellipsoidal envelope. The electron micrographs show a cross section through the plastic ellipsoids. These cross sections vary considerably in size depending on the thickness of the microtomed slices.

Since the PS domains are unstained and transparent at a thickness below 500 \AA the stained interconnected PEAB spheroids of the cellular envelope are still, however weakly, observable if they are below the cutting surface.

The micrographs of series L and E (Figures 22 through 30) are obvious examples for this presented interpretation of the electron micrographs. This means that the observed cells contain pure PS or P(S-co-MMA). The inverse samples (Figures 35 through 38) apparently cannot be interpreted in this way. They are believed to exhibit clear interpenetration also inside the cells.

It is clearly understood from the "sandwich" polymerization method that all electron micrographs represent a structure of a plane which was normal to the direction of radiation. Thus the question arises whether the morphology in a plane parallel to the radiation would exhibit a different picture. Extreme examples for vast morphological differences in two normal directions have been demonstrated by MATSUO and SAGAYE (69) and have been discussed by MOLAU (70), where cylindrical rods appear like layers in one plane and like spheroids in a normal plane. With IPN's the above interpretation for the cellular structure is evidence for the morphology in two perpendicular planes being the same, provided the differences in the long and broad dimension of the cells are less than a factor of

approximately two.

A general comparison of the morphology of IPN's discussed above with the IEN's prepared by FRISCH and KELMPNER (82-85) shows that heterogeneity takes place on a much bigger scale with the latter. The poly(urethane urea) particles are between 1 and 5 μ in size, which is between 1 and 2 orders of magnitude too large for real network formation and interpenetration to occur. Therefore the investigators drew the conclusion that interpenetration of the two networks could only have occurred near the interfaces. Whether the term interpenetration is properly used here depends on the thickness of the layer within which interpenetration occurs. For interpenetration occurs certainly with all two-phase polymeric materials if the thickness of the layer under consideration does not exceed molecular dimensions. It is certain, however, that bulk interpenetration does not occur with the partial IEN's.

Although electron micrographs of numerous two-phase polymeric systems (see section II,D) have been published there are hardly any examples (see next section) known where the heterogeneity between the two phases is found at a 100 \AA level. This indicates that the technique for preparing IPN's of PEA, PS and PMMA provides extremely fine structures and thus emphasizes the special position of IPN's within polyblends.

The different cellular and fine structures of the IPN's as revealed via electron microscopy require a detailed understanding of molecular interpenetration for proper interpretation. A rough qualitative understanding of the less complex morphology in grafted HiPS has been given by MOLAU and KESKKULA (72). MEIER (78,79) succeeded in developing a quantitative model via statistical thermodynamics for phase separated AB-type block copolymers, which exhibit a dispersion type of morphology.

Several trials of structure predictions for IPN's failed since the problem of simultaneous existence of cells and fine structure within each other as well as separated from each other could not be solved. THOMAS (129) developed a preliminary model for IPN's which is able to account solely for the small size of the domains.

D. General Discussion

1. E' -Morphology Considerations

In Figures 41 and 42 the slopes of the intermediate storage moduli, E' , are plotted versus the compositions of the border IPN's. The Intermediate slopes were taken between 30°C and 70°C, where the storage modulus could easily be approximated by a straight line. The slopes have to be negative, of course. However, the closer they are to zero, i.e. a horizontal intermediate plateau, the less compatible is the particular polyblend and the less molecular mixing takes place between both components.

These slopes are mainly controlled by the choice of the two component homopolymers of a polyblend. The storage modulus value, E' , at the middle of this intermediate plateau region is at midrange compositions (ca. between 20% and 80%) primarily controlled by the overall composition. (The influence of the composition upon the slope is minor). Ample evidence does exist that both, the intermediate slope, $d \log E'/dT$, and the mean modulus value, E' , at this slope are strongly influenced by the method of preparation.

A very illustrating example for the controlling influence of the preparative method is given in Figure 17, which shows three almost extreme cases of dynamic mechanical behavior for approximately equal compositions. The supporting micromorpholo-

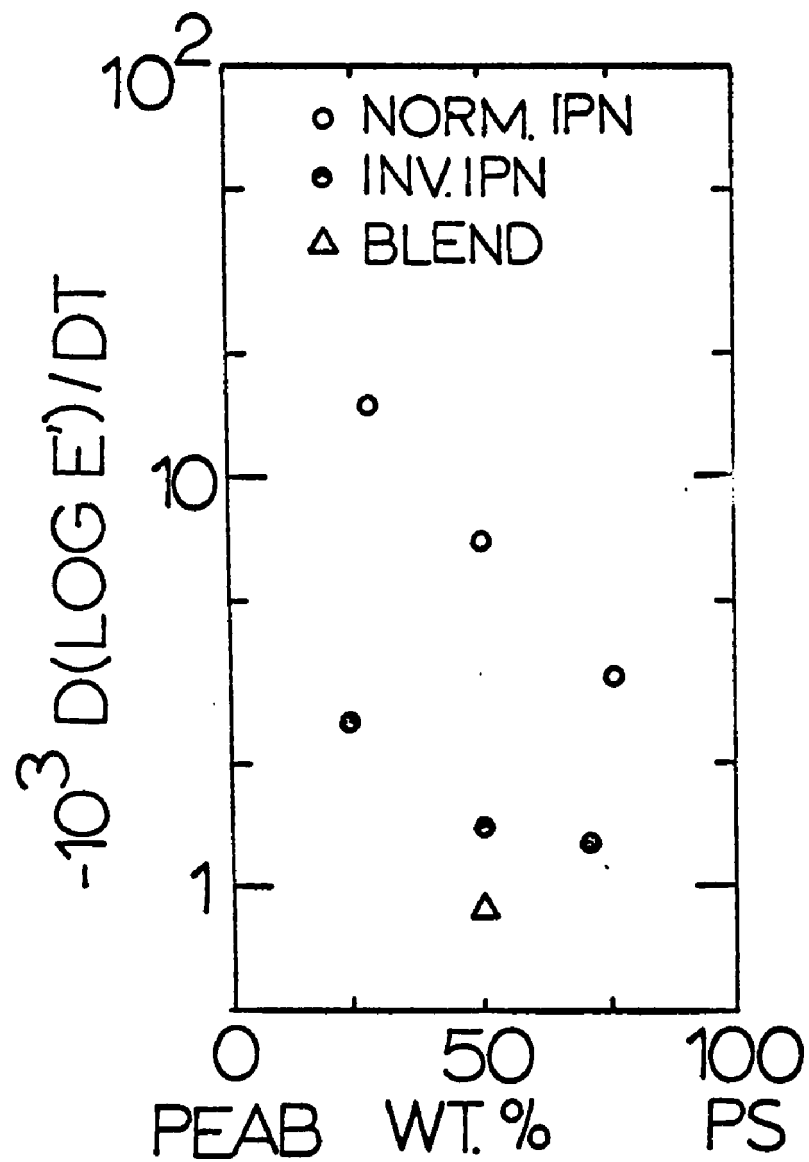


Figure 41. Slopes of intermediate E' -plateau regions for PEAB/PS IPN's

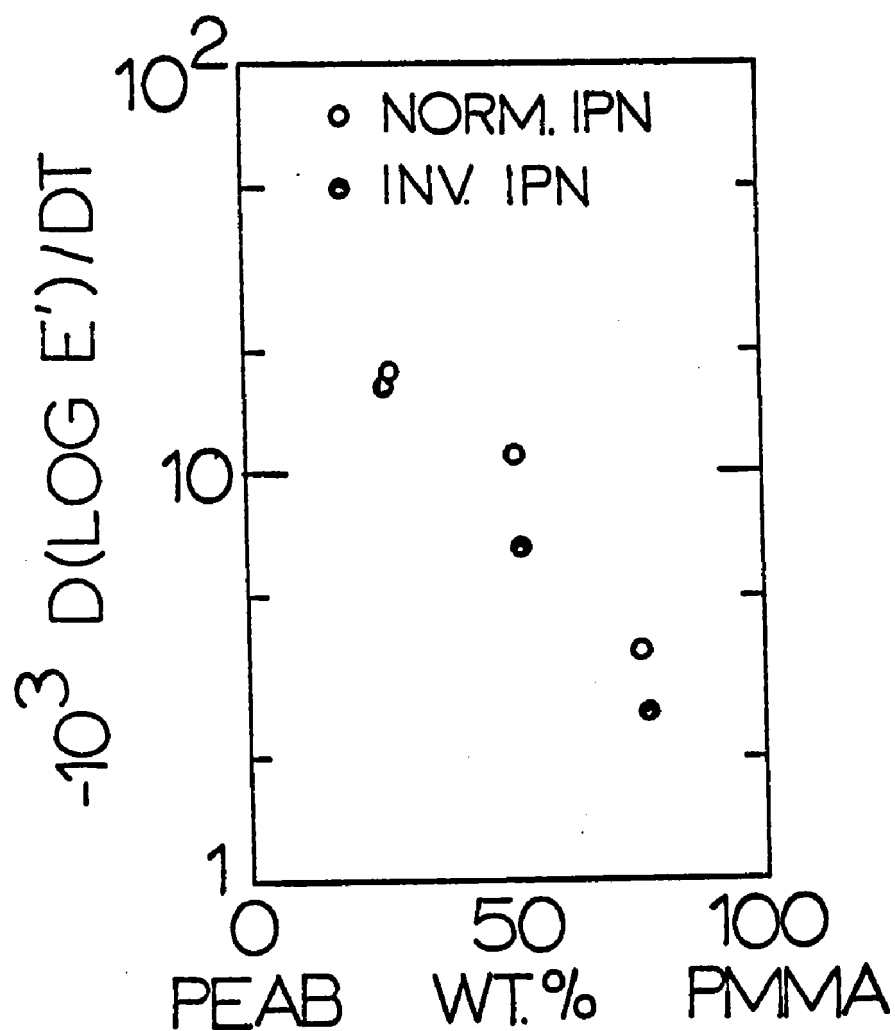


Figure 42. Slopes of intermediate E'-plateau regions for PEAB/PMMA IPN's

gies of the two IPN's I1 and I2 are displayed in Figures 22 and 35.

The prediction of the storage moduli for polyblends has been treated in several papers (28-30, 107-111). These calculations are based on mechanical models connected in series or parallel or by a combination of the two, and therefore the final results are very similar. The limiting types of phase morphology treated are:

- 1) one continuous matrix contains a dispersion of the discontinuous phase;
- 2) both phases are continuous.

BAUER and coworkers (28) give the following equations for two cases:

1a) plastic particles are dispersed in a rubbery matrix

(P in R):

$$E' = \frac{\varphi_P^{2/3} + E_{R'} / E'_P}{\varphi_P^{2/3} - \varphi_P - E_{R'} / E'_P} E'_{R'} \quad (\text{VI}, 7)$$

1b) rubbery particles are dispersed in a plastic matrix

(R in P):

$$E' = \frac{\varphi_R^{2/3} - (1 + E_{R'} / E'_P)}{\varphi_R^{2/3} - \varphi_R - (1 - E_{R'} / E'_P)} E'_P \quad (\text{VI}, 8)$$

with E' = storage modulus of the polyblend

E'_P, E'_R = storage modulus of the plastic and rubbery phase, respectively

φ_P, φ_R = volume fraction of the plastic and rubbery phase, respectively

These two equations are plotted in Figures 43 and 44 for the border composition IPN's PEAB/PS and PEAB/PMMA, respectively, at room temperature, $T_R = 25^\circ\text{C}$. The dashed lines in both figures represent the morphological type where both phases are continuous. The corresponding equation for both phases being continuous is very complex and cannot be expressed in explicit form. Therefore the values for the two dashed curves are taken from data by BAUER and coworkers (28).

At two compositions of the PEAB/PS IPN's (Figure 43) the E' -value of the normal IPN's is considerably below the E' -value for the inverse IPN's, indicating that the inverse composition is stiffer at room temperature. The normal leathery composition (sample 11) behaves similarly to a polyblend prepared by emulsion grafting (27), although the different methods of preparation will certainly result in a different morphology. The leathery polyblend prepared in this laboratory by a coprecipitation method has even a higher storage modulus than the leathery inverse IPN (sample 12).

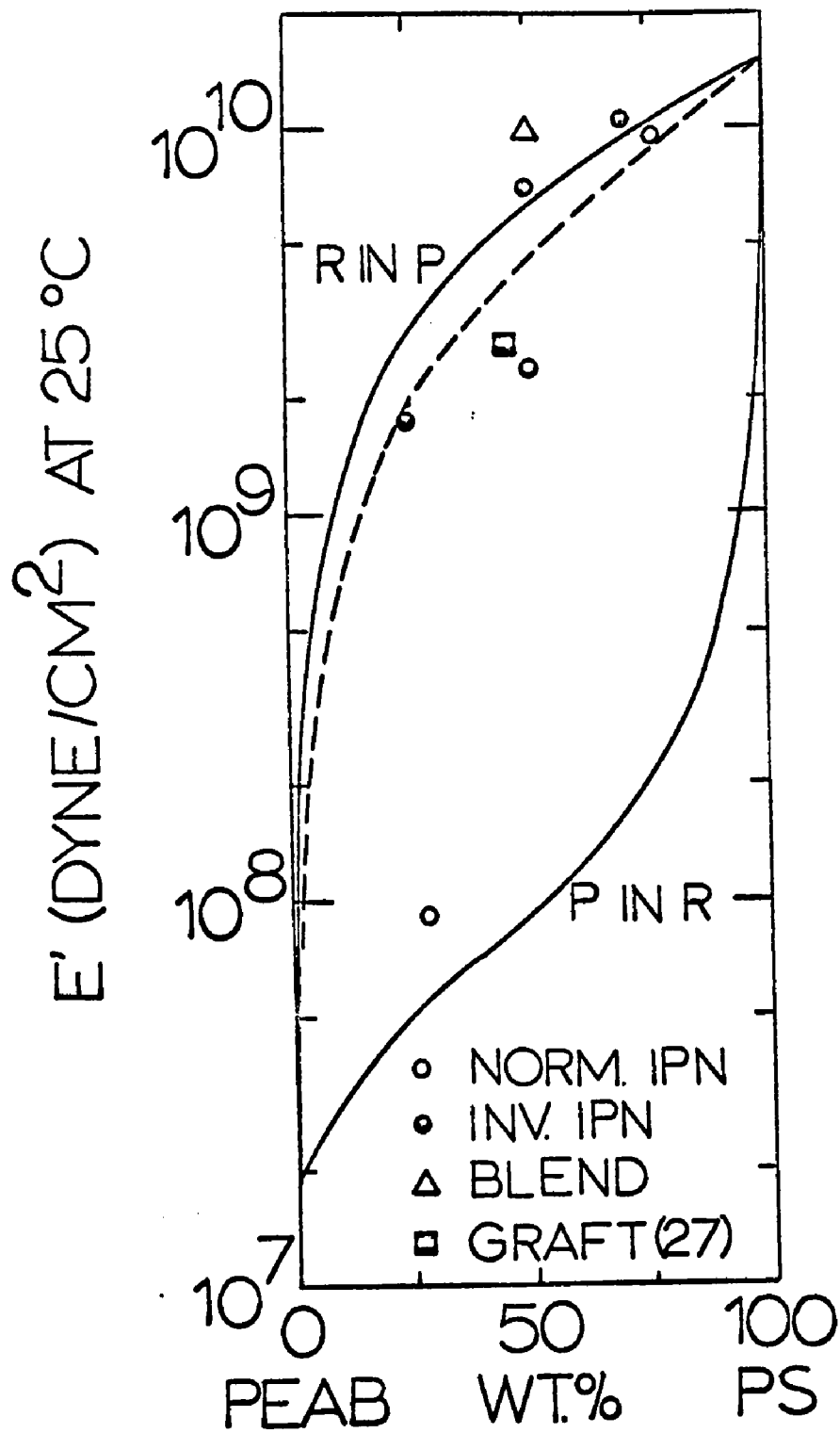


Figure 43. Storage moduli at 25°C for PEAB/PS IPN's

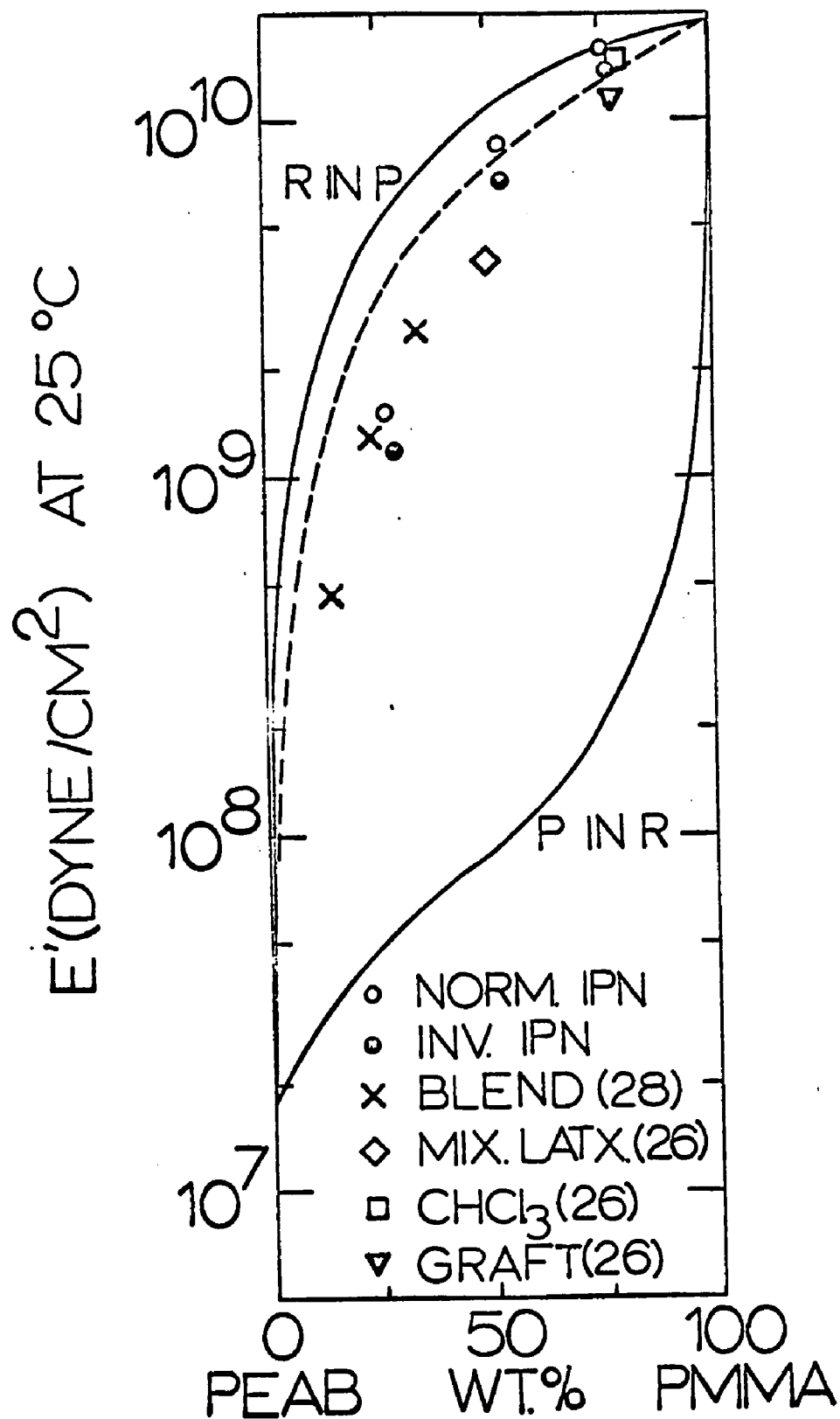


Figure 44. Storage moduli at 25°C for PEAB/PMMA IPN's

Three compositions are observed to fall outside the theoretically possible morphological range. Since the Rheovibron data showed very good reproducibility, ca. 10% deviation, experimental errors cannot account for this effect. Thus the reason has to originate from the generally made assumptions for the deviation of the theoretical curve. The most crucial ones are:

1. A homogeneous state of stress for the elements in series of the mechanical models;
2. A homogeneous state of deformation for the parallel elements of the mechanical models.

Many years ago VOIGT showed that both assumptions are not correct (112). Therefore it is obvious that the lines in Figures 43 and 44 are only good for approximate morphological estimations. It is reasonable to assume that with IPN's both phases are continuous. However, they certainly differ in the degree of continuity, i.e. one phase is more continuous than the other and thus influences the properties stronger than the other.

It is clear from these considerations that with the inverse IPN's the PS phase is the more continuous one as compared to the normal IPN's. This is in exact agreement with the electron micrographs of samples I1, I2 and I3 (Figures 35 through 37). The points in Figure 43 for samples I1 (Figure 36) and P1 (Figure 31) are supposed to exhibit two equally continuous phases.

The corresponding micrographs show, however, that PS is the more continuous phase. This might indicate that the line of equal continuity is at too high storage moduli values for the IPN's.

2. E'' -Considerations

Three aspects which influence the temperatures of the loss modulus peaks, $T(E''_{\max})$ include: The crosslink density, the frequency of dynamic mechanical testing and the degree of molecular mixing between the two components. The shift in the glass transition or in the loss peak temperature due to crosslinking depends strongly on the crosslinking agent used. If the crosslinking agent is very different in character from the monomer units, crosslinked polymers are formed which are, in a sense, copolymers (113). PMMA may serve as an example. Every increase of 10^{20} crosslinks per gram raises T_g of PMMA by 11°C if ethylene glycol dimethacrylate, EGDM, is used as crosslinking agent. However, employment of decamethylene glycol dimethacrylate, DMGDM, lowers T_g of PMMA by 23°C (114). Therefore it is a reasonable assumption that the raise of T_g due to TEGDM is somewhat smaller than 11°C at the same crosslink density.

TOBOLSKY and coworkers (115) derived an equation for the shear modulus of crosslinked polymers in dependency of the molecular weight between crosslinks, M_c . The value for M_c , which is inversely proportional to ΔT_g (116-118), controls

the shift in T_g . The proportionality constant depends on the polymer and on the assumption that the crosslinking agent is chemically similar to the monomer unit (e.g. PS and DVB or PMMA and EGDM). This assumption is not fulfilled for the IPN's using TEGDM.

The rise in T_g with frequency, w , depends on the activation energy, ΔH , and on the temperature according to the following equation (119):

$$\frac{W_e}{W_1} = \exp \frac{\Delta H}{R} \left(\frac{1}{T_{g1}} - \frac{1}{T_{g2}} \right) \quad (\text{VI},9)$$

In the present case only the total shifts in T_g -values are known. However, the experimental data do not allow distinguishing between the contributions of both effects, crosslink density and frequency.

| ml TEGDM | frequency | PEA | PS | PMMA | PMMA(β) |
|----------|-----------|-----|-----|------|-----------------|
| 0 | 1 | -22 | 100 | 105 | 36-50 |
| 0.5 ml | 110 | -12 | 125 | 136 | 100 |

Table 4. Glass transition temperatures ($^{\circ}\text{C}$) and maximum loss peak temperatures of the employed homopolymers.

Table 4 lists the maximum loss peak temperatures for the used crosslinked homopolymers as determined with the Rheovibron at 110 cps¹⁾. The different shifts indicate that the contributions

1) The dynamic moduli of the three homopolymers are given in Figures A1, A2 and A3 in the appendix.

from the crosslink density and the frequency are not the same for the three polymers. This becomes evident from the different rubbery plateau values, E_2 . If these values are used for calculating the molecular weights, M_c , between crosslinks (which is the reciprocal of the crosslink density) the following values for the pure homopolymers are obtained:

$$M_c(\text{PEAB}) = 4,430; M_c(\text{PS}) = 11,220; M_c(\text{PMMA}) = 5,160 \text{ g/mole}$$

The last column in Table 4 lists the shift in the secondary or β -transition of PMMA which is caused by motion of the carbonmethoxyl groups. Due to the small activation energy associated with the β -peak (considerably smaller than ΔH for the primary peak) the temperature at which this peak occurs depends much more on the method of investigation (119). Therefore β -peaks have been reported over a broad range of temperatures (120).

Since ΔH is small with secondary transitions their peaks are often hard to observe in polyblends. Therefore most dynamic modulus curves do not show the β -peaks. In some cases, however, secondary PMMA transitions are noticed with the loss modulus curves. Examples are the IPN's L6 at 75°C (Fig. 7) and I5 at 90°C (Fig. 20) as well as P5 at 95°C (Fig. 15) and I6 at 105°C (Fig. 21). It is noted that the β -peak temperatures are 10 to 15°C higher for the inverse samples than for the normal ones.

The effect of molecular mixing between the two IPN components upon the loss peaks is presented in Figure 45, where $T(E''_{\max})$ is plotted versus wt.% of the plastic network. It is observed that the extent of molecular mixing is in all cases higher with the normal IPN's than with the inverse compositions since the E''_{\max} -values are shifted more towards each other with the normal IPN's. This result is in agreement with the conclusion drawn from the slopes of the intermediate storage modulus regions.

The curves for the PEAB/PS IPN's (Fig. 45) pass through a maximum for the rubbery loss peaks at approximately 28 wt.% PS. The corresponding curves for the PS loss peaks exhibit a minimum at approximately 18 wt.% PEAB. It is noticed that the PEAB loss peaks for the PEAB/PMMA IPN's do not show a maximum up to 50% PMMA.

Four interesting damping curves have been selected for presentation in Figure 46: the normal and the inverse IPN's of the elastomeric samples E4, I4, E1 and I1. It is observed with the PEAB/PMMA IPN's a) that the damping remains approximately constant above 5°C, and b) that the damping for the normal and the inverse samples is almost the same. A material whose damping characteristics are invariant with temperature and whose loss tangent is relatively high has certainly useful application properties since it is able to dissipate mechanical energies

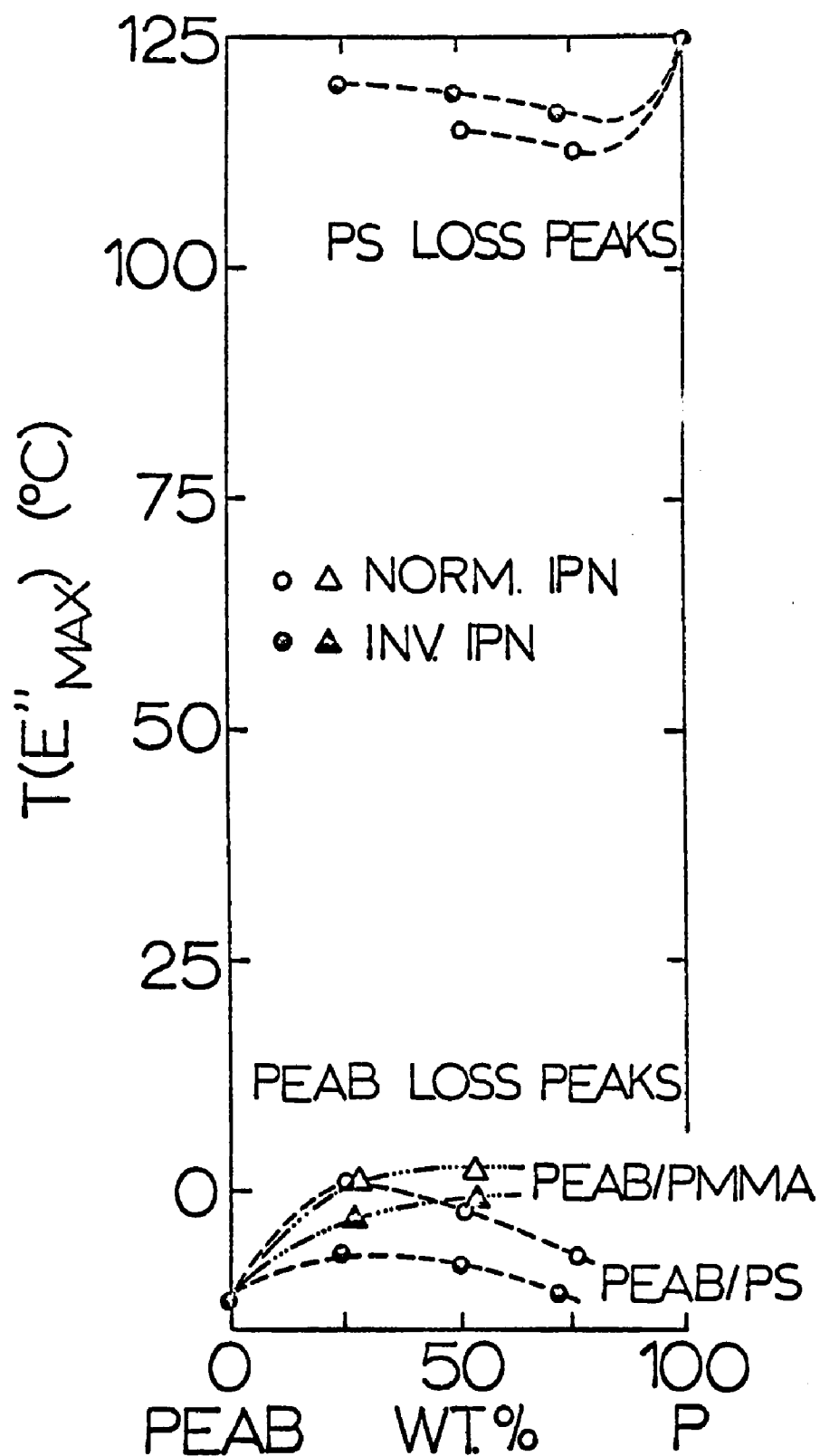
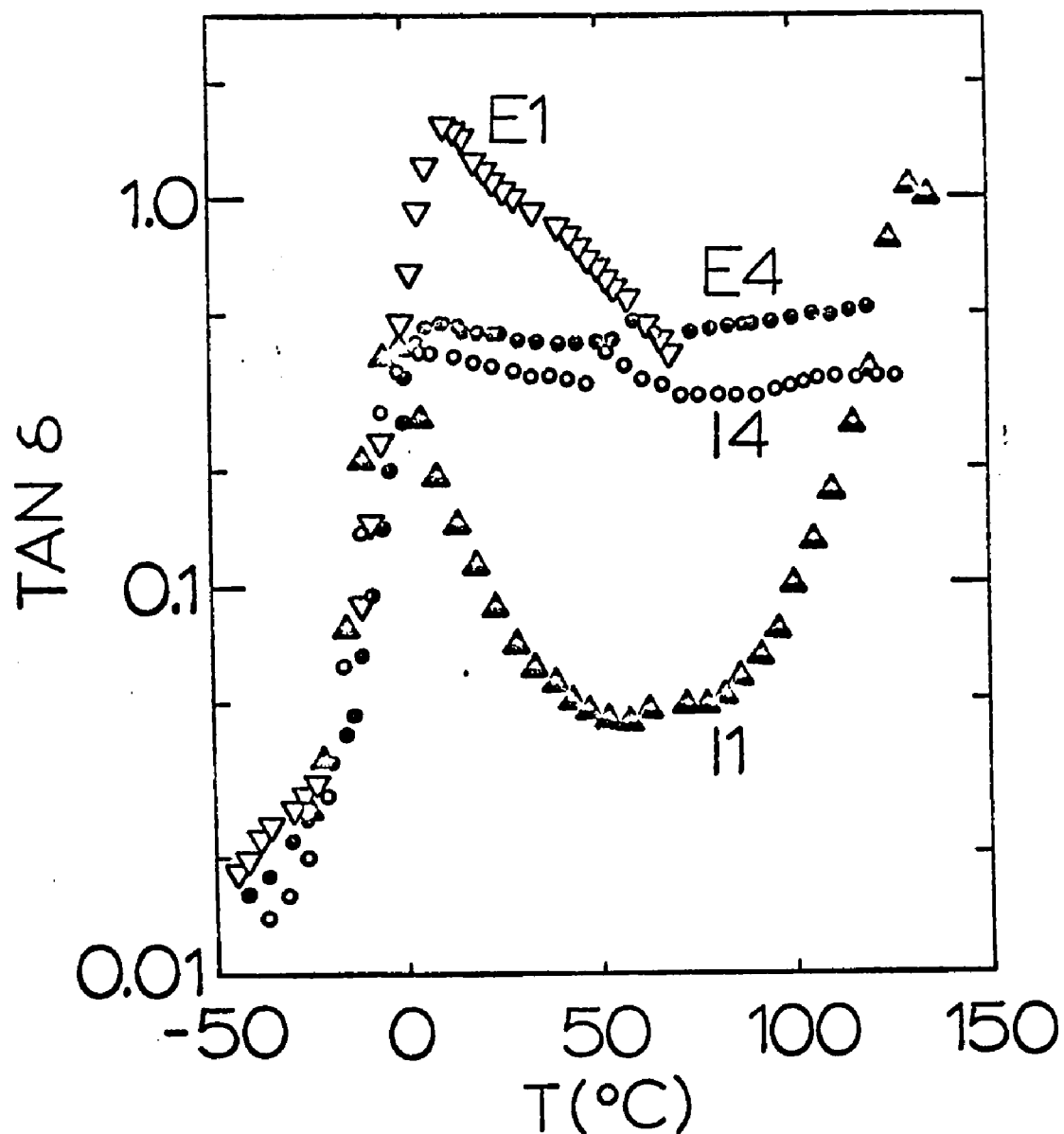


Figure 45. Dependency of the PEAB and PS loss peak temperatures on the plastic fraction in the IPN's



E1 74.4PEAB/25.6PS

E4 72.2PEAB/27.8 PMMA

I1 24.6PS/75.4PEAB

I4 27.0PMMA/73.0PEAB

Figure 46. Temperature dependence of $\tan \delta$ of four IPN's

over a wide temperature range.

Figure 47 shows how the PEAB and the PS damping maxima depend on the PS fraction in the IPN's. The $\tan\delta$ differences between the PEAB and the PS damping peaks are bigger with the inverse IPN's than with the normal ones in all cases. This means that equal damping maxima will be observed at a considerably lower plastic fraction with the inverse IPN's than with the normal materials. These compositions are read from the plot at the intersection of the two corresponding curves. They are at 14 wt.% and at 42 wt.% PS for the inverse and the normal IPN's, respectively. Equal damping values for the PEAB and the PMMA "peaks" are read from Figure 46 at ca. 27.4 wt.% PMMA, which is almost exactly the arithmetic mean of the two PS contents.

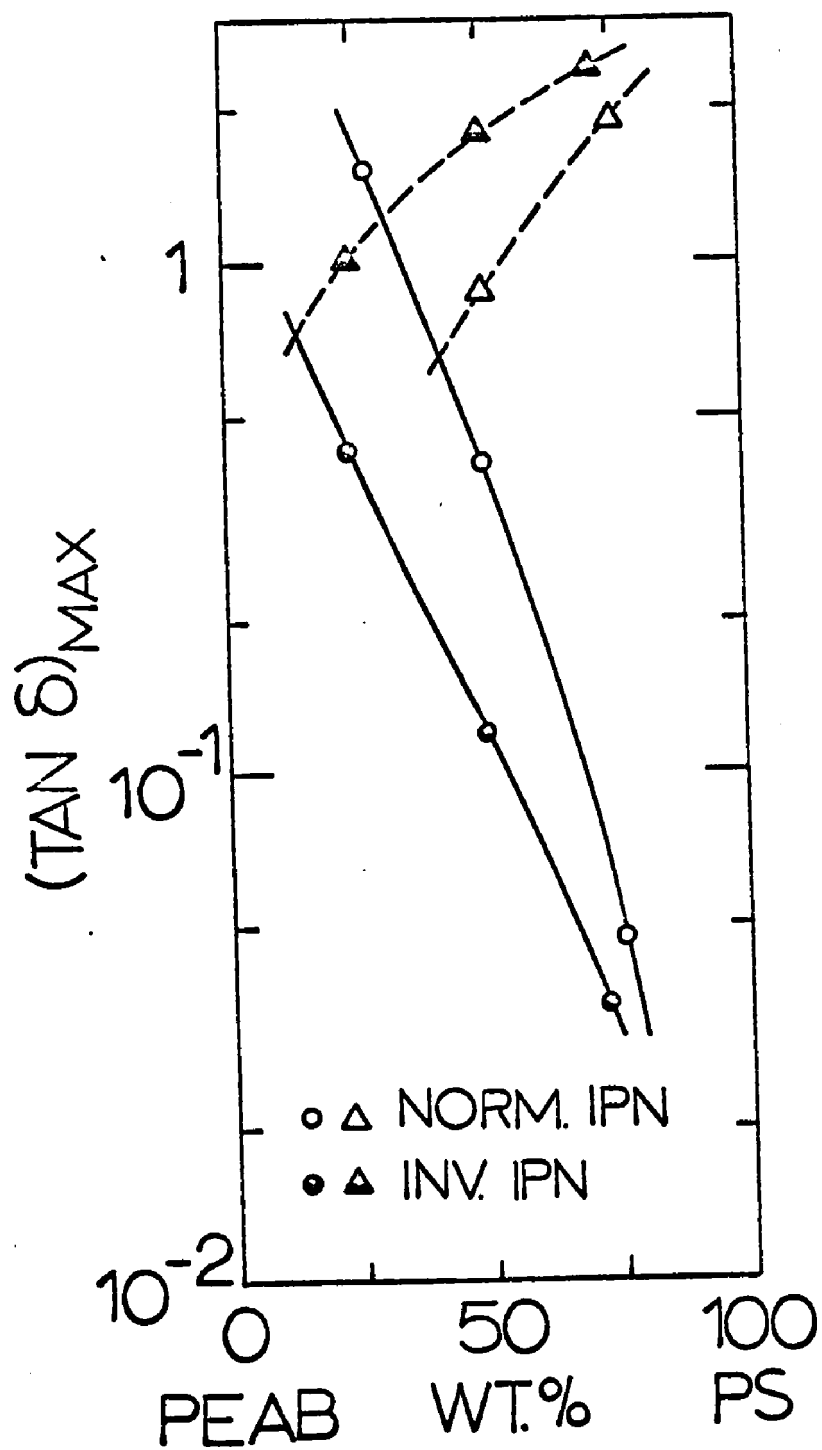


Figure 47. Temperature dependence of the PEAB and PS damping maxima on the PS fraction in the IPN's

E. Dynamic Mechanical Behavior-Structure Relationship

The dynamic mechanical behavior and the morphology are supplementary. Certain general correlations which exist between them will be treated here.

1. Compatibility

The only polyblend found to exhibit structures of the same order of magnitude as the investigated IPN's is a PVC/NBR blend studied by MATSUO and coworkers (31,32). The blends of PVC/NBR-30 (100/15) where the NBR phase contains 30% AN show a very fine dispersion of rubber particles of ca. 100 \AA inside the PVC matrix. The blend PVC/NBR-40 (100/15) with 40% AN in the NBR phase revealed this fine dispersion throughout the matrix. The estimated order of magnitude of the dispersed particles is in the sub 100 \AA range. This fine structure has also been observed with the IPN's E4, P5 and I6 (Figures 30, 34 and 38). The micrographs do not allow any definite distinctions between those four polyblends. The corresponding dynamic mechanical data reveal considerable differences. Sample E4 shows elastomeric features (Fig. 11), whereas samples P5 and I6 show E' and E'' curves indicative of a semicompatible polyblend. The PVC/NBR-40 blend is close to a homopolymer in its dynamic behavior. The transition is only slightly broadened.

The similarity of the electron micrographs and the differ-

ences in their dynamic mechanical behavior lead to the conclusion that domain sizes which individually affect the viscoelastic properties of a polyblend must be considerably below the 100 Å diameter dimension, perhaps as low as 10 Å.

The fact that blending by milling PVC and NBR-40 results already in micro heterogeneity illustrates the high degree of compatibility of this system.

YU (123) states that the term "compatibility as applied to polyblends cannot represent the state of homogeneous or nearly complete mixing. Conceptually, compatibility is a representation of how close the system can approach this ultimate state of molecular mixing as a limit. Phenomenologically, compatibility is a relative measure of the degree of heterogeneity of the polyblend, i.e. how fine is one polymer dispersed in another" (123).

CURTIUS (106,124) and this author tried to develop a general compatibility number, C.N., for polyblends. C.N. was developed from dynamic mechanical properties like the slopes of the storage modulus at the two transitions and at the intermediate plateau. Other attempts were made employing the maximum loss peak temperatures, $T(E''_{\max})$ of homopolymers and their shifts in polyblends or using the corresponding peak heights. However, all methods resulted in unsatisfactory equations. They indicated only trends, provided the method of preparation

was constant and the dynamic mechanical behavior of a polyblend is known prior to calculating C.N.

TURLEY (105) pointed out that such comparisons of polyblends must be made within a given system. This has been confirmed by KESKKULA and coworkers (75), by YU (123) and by BUCKNALL and HALL (125). "It is to be noted that compatibility of polyblends, being a relative attribute of the system, cannot be measured quantitatively" (123). MOLAU (70) and YU (123) mention the "compatibilizing" effect of block and graft copolymers from monomers whose polymers are not compatible in comparison with mechanical blends.

The results obtained for the normal and the inverse IPN's (in particular see Figure 17) and the information of chapter II stress the importance of the method of preparation with polyblends. Thus the compatibility of a two phase polymeric system is not clearly defined from its components, although one certainly can distinguish between systems which are generally more compatible than others.

These considerations support the idea of associating a compatibility range, C.R., rather than a compatibility number, C.N., with a certain polyblend. It has been shown via viscoelasticity and morphology that C.R. for the system PEA/PS is broader and generally less compatible than C.R. for the system PEA/PMMA. It was also pointed out that C.R. for the PVC/NBR-40

blend is narrower and generally more compatible than with the PEA/PMMA system. Since the compatibility for a polyblend in its phenomenological sense can be associated with a constant C.N. it is obvious that the method of preparation fixes C.N. within C.R. Figure 48 compares qualitatively C.R.'s for 3 polyblends.

2. Phase Inversion

The term "phase inversion" with IPN's means that the more continuous phase is inverted into the less continuous phase. Figure 43 predicts phase inversions for the PEAB/PS IPN's. These are read from the graph to occur between 55 and 75 wt.% PS for the normal IPN's and below 25 wt.% PS for the inverse IPN's. (For comparison: a mono-disperse spherical closest packing becomes continuous at 74.1%). The inversion range for the normal system is readily confirmed by the corresponding electron micrographs (Figures 22 and 31). IPN's for supporting evidence of the latter inversion have not been prepared. Samples P1 and I1 (Figures 31 and 36) which lie approximately on the curve show that even the predicted inversions from the more to the less continuous phase are at somewhat too high E'' -values, since both phases exhibit PS at the more continuous phase.

SPERLING and FRIEDMAN (6) predicted a phase inversion for PEA/PS IPN's between 40 and 60 wt.% PS. However, they obtained this result by considering inverse IPN's for high PS contents

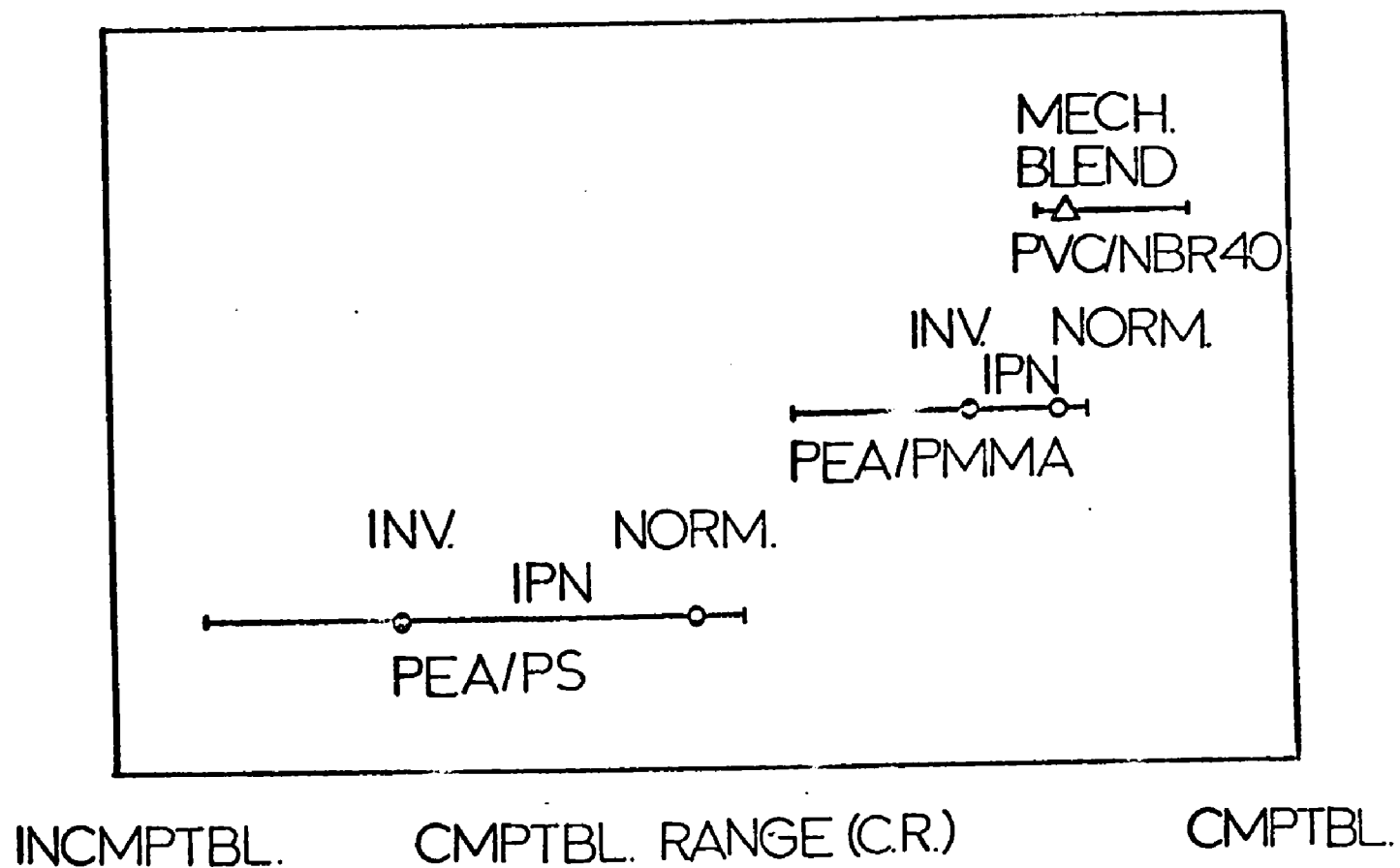


Figure 48. Compatibility ranges for three polyblend systems. The C.R.'s are not drawn on the base line for better distinction; there is no ordinate.

and normal IPN's for high PEA contents simultaneously in the same curve, whereas the gap in data (4-47% PS) had been extrapolated. The fact that they connected inverse and normal data results of course in a discrepancy to this authors findings. However, under those circumstances one would expect their predicted inversion range to fall between the ones found in this study which is the case. The phase inversion reported for the IEN's (85) at ca. 30 vol.% does hardly compare with the ones found for the IPN's, since with the IEN's both phases are not really continuous.

3. Evidence of Interpenetration

It is clear from the presentation and the discussion of the results that the in depth interpenetration of the two networks cannot really be proved. However, some points will be discussed briefly which are in supporting evidence of the fact that interpenetration does really occur.

The synthesis of an IPN produces a network with the first polymerization step. The second polymerization step produces a second network, which is chemically independent from the first one if one disregards grafting between the two networks, and which is physically pervading the first network. This reaction casuses both networks to be continuous within each other. This continuity does not change with the choice of the two polymers. However, if both components consist of chemically

distinct polymers, some degree of phase separation results without changing the independent continuity of the two networks. In a limiting case of high compatibility between both components, both networks are visualized as being interpenetrating even on a molecular scale.

Two dimensional electron micrographs of course cannot exhibit two continuous phases. However, all areas showing fine structures at the 100 \AA level of approximately equal continuity are indicative of double network formation and thus of interpenetration.

VII. Conclusions

This investigation employing dynamic mechanical experiments and electron microscopy showed that IPN's are a special type of polyblend. Conclusions from this research are presented below:

1. If one polymeric component is elastomeric and the other one is glassy at ambient temperature, the resulting IPN tends to behave synergistically, and depending on the predominating phase either a reinforced rubber, a leathery material or a toughened plastic result.
2. IPN's exhibit a very complex structure. The electron micrographs show a characteristic cellular morphology simultaneously with a fine structure with phase domains of the order of 100 \AA . The cellular envelopes disappear gradually as MMA mers replace S mers in the plastic component. Cocurrently, dynamic mechanical studies yielded two distinct loss peaks for the incompatible pair, PEAB/PS, and one very broad peak for the semicompatible pair, PEAB/PMMA.
3. The interpretation of the electron micrographs leads one to believe that, except for the orientation in the structural cellular domains, the morphology is independent of the plane of observation.

4. The sequence of preparation is of great importance since the network synthesized first tends to form the more continuous phase and thus controls the morphology and the dynamic mechanical properties of the IPN's. However, inverting the order of preparation does not result in an exact inversion of the morphology.
5. Inverting the sequence of preparation yields in all cases bigger differences (in dynamic mechanical behavior and morphology) for the PEAB/PS IPN's than for the PEAB/PMMA IPN's. This indicates a lower degree of compatibility and a broader compatibility range for the PEAB/PS system than for the PEAB/PMMS system.

VIII. RECOMMENDATIONS

The above investigation of the IPN's can be considered as a thorough endeavor to elucidate IPN's. However, numerous possible extensions of this treatise of IPN's may be conceived of. To be brief, only those which are directly related to and derived from this thesis will be recommended for further investigation.

1. From the lack of mechanical property investigations it is clear that no attempts were undertaken to optimize the IPN's with respect to mechanical properties such as impact resistance, ultimate tensile strength and damping. Such experiments should be carried out by varying a) the concentration, b) the polymer components, and c) the crosslink density.
2. Up to now the effects of annealing and quenching as well as pre- and post-swelling (126,127) on the morphology and thus on the properties are unknown.
3. It is of major interest to substantially decrease the amount of grafting between the two networks in order to produce an IPN whose components are approximately chemically independent. In order to compare those materials with the ones investigated here it is recommended to prepare identical IPN's except for the TEGDM. A suitable

crosslinking agent to be employed instead is 1.3 butylene diacrylate(95) which is known to result in low chain transfer.

4. A detailed understanding of molecular interpenetration and thus of the complex morphology is lacking. Although it is realized that a statistical thermodynamic theory is easily a complete thesis in itself, such a treatment would elucidate several raised questions.

IX. APPENDIX

Figures of the dynamic storage and loss moduli of the three homopolymers PEAB, PS and PMMA.

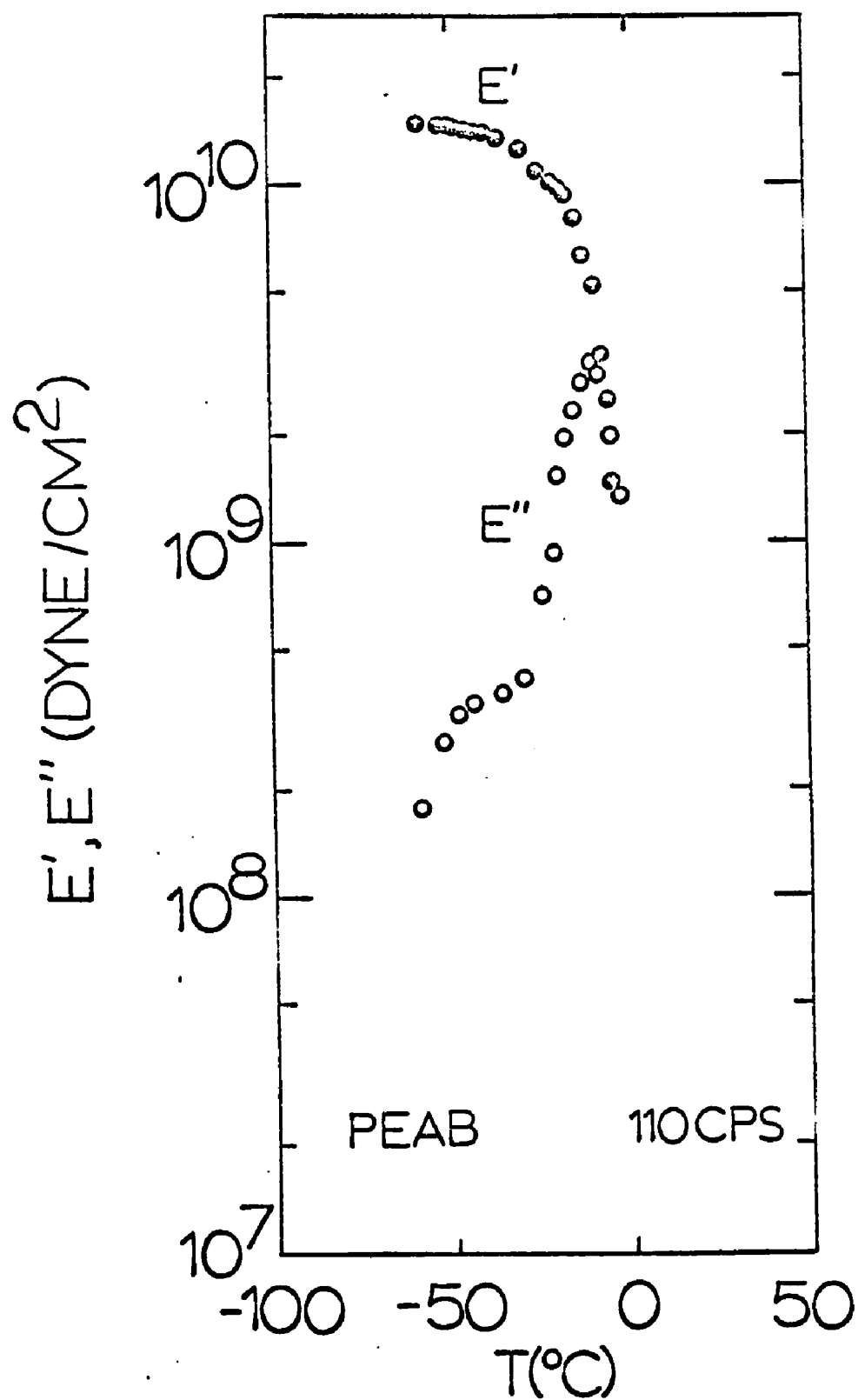


Figure A-1. Temperature dependence of E' and E'' of PEAB.

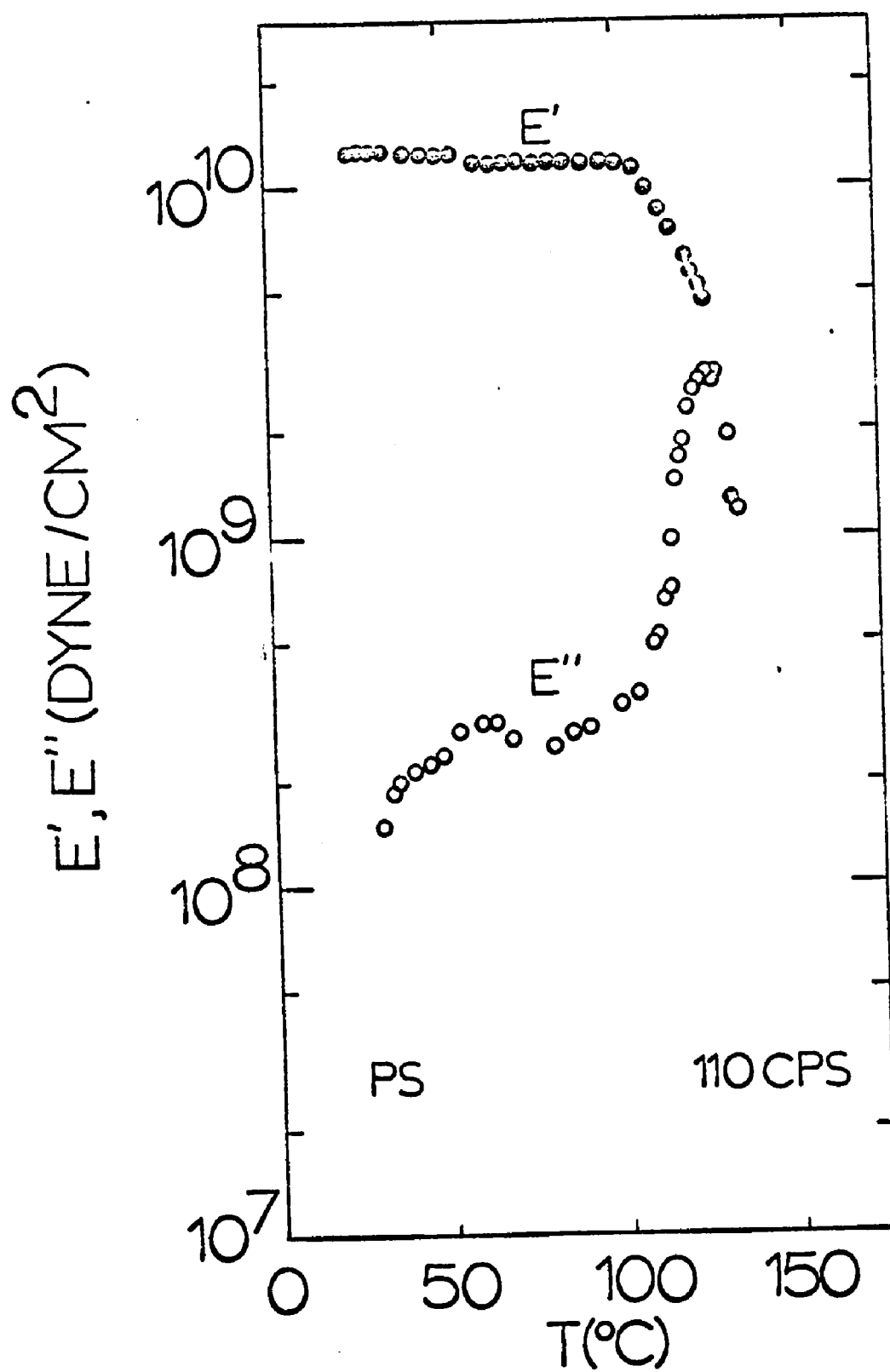


Figure A-2. Temperature dependence of E' and E'' of PS

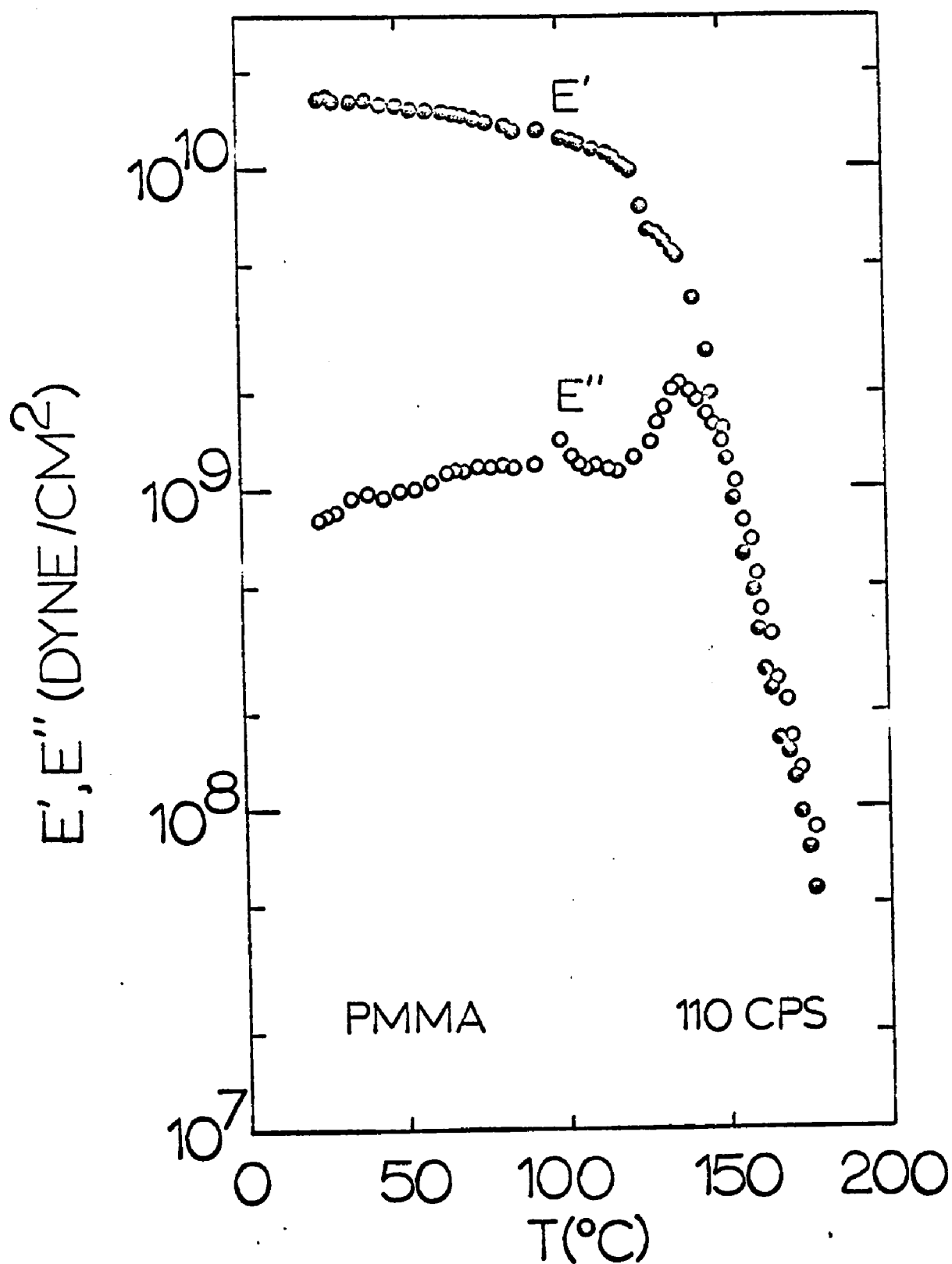


Figure A-3. Temperature dependence of E' and E'' of PMMA

X. BIBLIOGRAPHY

1. FETTES, E. M. and W. N. MACLAY, Appl. Poly. Symp., 7, 3 (1968)
2. MARK, H. F. and N. G. GAYLORD, eds., Encyclopedia of Polymer Science and Technology, Interscience Publ., New York, 1969, vol. 10, pp. 694-709
3. TOBOLSKY, A. V., Properties and Structure of Polymers, John Wiley & Sons, New York, 1960, p. 79
4. MILLAR, J. R., J. Chem. Soc., 1311 (1960)
5. SHIBAYAMA, K. and Y. SUZUKI, Kobunshi Kagaku, 23, (249), 24 (1966); Rubber Chem. Techn., 40, 476 (1967)
6. SPERLING, L. H. and D. W. FRIEDMAN, J. Poly. Sci., A-2, 7, 425 (1969)
7. FLORY, P. J., Principles of Polymer Chemistry, Cornell Univ. Press, Ithaca, 1953, Chapter XIII
8. HILDEBRAND, J. H. and R. L. SCOTT, Solubility of Non-Electrolytes, 3rd ed., Reinhold Publ. Corp., New York, 1950
9. ROSEN, S. L., Poly. Eng. Sci., 7, 115 (1967)
10. KERN, R. J., J. Poly. Sci., 21, 19 (1956)
11. BUCHDAHL, R. and L. E. NIELSEN, J. Poly. Sci., 15, 1 (1955)
12. SMITH, K. L., A. E. WINSLOW, and D. E. PETERSEN, Ind. Eng. Chem., 51, 1361 (1959)
13. WATANABE, W. H., C. F. RYAN, P. C. FLIESCHER, Jr., and B. S. CARRETT, J. Phys. Chem. 65, 896 (1961)
14. BOHN, L., Kolloid Z., 213, 55 (1966); Rubber Chem. Techn., 41, 495 (1968)
15. YOSHIDA, T., S. SAKURAI, T. OKUDA, and Y. TAKAGI, J. Am. Chem. Soc., 84, 3590 (1962)

16. POREJKO, S., W. GABARA, and J. KULESZA, J. Poly. Sci., A-1, 5, 1363 (1967)
17. BANK, M., J. LEFFINGWELL, and C. THIES, Bull. Am. Phys. Soc., 11, (15), No. 3, 351 (1970)
18. BUECHE, F., W. M. CASHIN, and P. DEBYE, J. Chem. Phys. 20, 1956 (1952)
19. BRESLER, S. Y., L. M. PYRKOV, S. Y. FRENKEL, L. A. LAIUS, and S. I. KLENIN, Hochmol. Verb. (Vysokom. Soed.), 3, 1072 (1961)
20. LENZ, R. W., Organic Chemistry of Synthetic High Polymers. Interscience Publ., New York, 1967, p. 711
21. KATO, K., Japan Plastics, 2, 6 (1968)
22. LENZ, R. W., Organic Chemistry of Synthetic High Polymers, Interscience Publ., New York, 1967, pp. 437, 719
23. AGGARWAL, S. L., ed., Block Polymers, Plenum Press, New York, 1970
24. MOACANIN, J., G. HOLDEN, and N. W. TSCHOEGL, eds., Block Copolymers, J. Poly. Sci., C, No. 26, 1969
25. REIMER, L., Elektronenmikroskopische Untersuchungs- und Präparationsmethoden, Springer Verlag, Berlin, 1967
26. HUGHES, L. J. and G. L. BROWN, J. Appl. Poly. Sci., 5 580 (1961)
27. HUGHES, L. J. and G. L. BROWN, J. Appl. Poly. Sci., 7 59 (1963)
28. BAUER, P., J. HENNIG und G. SCHREYER, Angew. Makromol. Chem., 11, 145 (1970)
29. TAKAYANAGI, M., H. HARIMA, and Y. IWATA, Mem. of the Fac. of Eng. Kyushu Univ., 23, (1), 1 (1963)
30. MANABE, S., R. MURAKAMI, and M. TAKAYANAGI, Mem. of the Fac. of Eng. Kyushu Univ., 28, (4), 295 (1969)
31. MATSUO, M., Japan Plastics, 2. (3), 6 (1968)

32. MATSUO, M., C. NOZAKI, and Y. JYO, Poly. Eng. Sci., 9, (3), 197 (1969)
33. BEECHER, J. F., L. MARKER, R. D. BRADFORD, and S. L. AGGARWAL, J. Poly. Sci., C, 26, 117 (1969)
34. HOLDEN, G., E. T. BISHOP, and N. R. LEGGE, J. Poly. Sci., C, 26, 37 (1969)
35. SMITH, T. L. and A. V. DICKIE, J. Poly. Sci., C, 26, 163 (1969)
36. COOPER, S. L. and A. V. TOBOLSKY, Text. Res. J., 36, 800 (1966)
37. SHEN, M., E. H. CIRLIN, and D. H. KAEUBLE, Polymer Preprints, 11, (2), 686 (1970)
38. HARPEL, G. A. and D. B. THRASHER, Polymer Preprints, 11, (2) 888 (1970)
39. NIELSEN, L. E., Mechanical Properties of Polymers, Reinhold Publ. Corp., New York, 1962, p. 163
40. STAVERMAN, A. J., Proc. Roy. Soc., A, 282, 115 (1964)
41. MORTON, M., J. E. MCGRATH, and J. F. HENDERSON, J. Poly. Sci., C, 26, 99 (1969)
42. BRUNWIN, D. M., E. FISCHER, and J. F. HENDERSON, J. Poly. Sci., C, 26, 135 (1969)
43. BERGEN, R. L. Jr., Appl. Poly. Symp., 7, 41 (1968)
44. KRAUS, G., K. W. ROLLMANN, and J. T. GRUVER, Macromolecules, 3, 92 (1970)
45. CHILDERS, C. W., G. KRAUS, J. T. GRUVER, and E. CLARK, Polymer Preprints, 11, (2), 553 (1970)
46. NIELSEN, L. E., Mechanical Properties of Polymers, Reinhold Publ. Corp., New York, 1962, p. 175
47. MORTON, M. and J. C. HEALY, Appl. Poly. Symp., 7, 155 (1968)

48. ROBINSON, R. A. and E. F. T. WHITE, in Block Polymers, S. L. AGGARWAL, ed., Plenum Press, New York, 1970
49. IKEDA, R. M., M. L. WALLACH, and R. J. ANGELO, in Block Polymers, S. L. AGGARWAL, ed., Plenum Press, New York, 1970
50. ESTES, G. M., D. S. HUH, and S. L. COOPER, in Block Polymers, S. L. AGGARWAL, ed., Plenum Press, New York, 1970
51. HARRELL, Jr., L. L., in Block Polymers, S. L. AGGARWAL, ed., Plenum Press, New York, 1970
52. WOLF, K., *Kunststoffe*, 41, 89 (1951)
53. PETERSEN, J. and B. RANBY, *Die Makromol. Chem.*, 133, 251 (1970)
54. PETERSEN, J. and B. RANBY, *Die Makromol Chem.*, 133, 263 (1970)
55. IOBST, S. A. and J. A. MANSON, *Polymer Preprints*, 11, (2) 765 (1970)
56. NIELSEN, L. E., *Mechanical Properties of Polymers*, Reinhold Publ. Corp., New York, 1962, p. 170
57. STOELTING, J., F. E. KARASZ, and W. J. MACKNIGHT, *Poly. Eng. Sci.*, 10, (3), 133 (1970)
58. MURAYAMA, T. and J. P. BELL, *J. Poly. Sci.*, A-2, 8, 437 (1970)
59. KATO, K., *J. Poly. Sci.*, B, 4, 35 (1966)
60. BROWN, W. E., *J. Appl. Phys.*, 18, 273 (1947)
61. BRADFORD, E. B. and E. VANZO, *J. Poly. Sci.*, A-1, 6, 1661 (1968)
62. MAHL, H., *Kunststoffe*, 54, 15 (1964)
63. MOLAU, G. E., *J. Poly. Sci.*, B, 3, 1007 (1965)
64. KATO, K., *Poly. Eng. Sci.*, 7, 38 (1967)

65. KATO, K., J. El. Micr., 17, (1), 23 (1968)
66. KATO, K., Plastics Age, Nov. 1969, p. 73
67. KATO, K., Kolloid Z., 220, 24 (1967)
68. MATSUO, M. and S. SAGAYE, Polymer Preprints, 11, (2), 384 (1970)
69. MATSUO, M. and S. SAGAYE, Colloidal and Morphological Behavior of Block and Graft Copolymers, G. E. MOLAU, ed., Plenum Press, New York, 1971
70. MOLAU, G. E., in Block Polymers, S. L. AGGARWAL, ed., Plenum Press, New York, 1970
71. INOUE, T., T. SOEN, T. HASHIMOTO, and H. KAWAI, in Block Polymers, S. L. AGGARWAL, ed., Plenum Press, 1970
72. MOLAU, G. E. and H. KESKKULA, J. Poly. Sci., A-1, 4, 1595 (1966)
73. MOLAU, G. E., J. Poly. Sci., A, 3, 1267 (1965)
74. SCOTT, R. L., J. Chem. Phys., 17, 279 (1949)
75. KESKKULA, H., S. G. TURLEY, and R. F. BOYER, J. Appl. Poly. Sci., 15 351 (1971)
76. KRAUSE, S., J. Poly. Sci., A-2, 7, 249 (1969)
77. KRAUSE, S., Macromolecules, 3, 84 (1970)
78. MEIER, D. J., J. Poly. Sci., C, 26, 81 (1969)
79. MEIER, D. J., Polymer Preprints, 11, (2), 400 (1970)
80. INOUE, T., T. SOEN, T. HASHIMOTO, and H. KAWAI, J. Poly. Sci., A-2, 7, 1283 (1969)
81. INOUE, T., T. SOEN, T. HASHIMOTO, and H. KAWAI, Macromolecules, 3, 87 (1970)
82. FRISCH, H. L., D. KLEMPNER, and K. C. FRISCH, J. Poly. Sci., B, 7, 775 (1969)

83. KLEMPNER, D., H. L. FRISCH, and K. C. FRISCH, J. Poly. Sci., A-2, 8, 921 (1970)
84. FRISCH, H. L. and D. KLEMPNER, Advances in Macromolecular Chemistry, vol. 2, Academic Press, London, 1970
85. MATSUO, M., T. K. KWEI, D. KLEMPNER, and H. L. FRISCH, Poly. Eng. Sci., 10, (6), 327 (1970)
86. SPERLING, L. H. and R. R. ARNTS, accepted, J. Appl. Poly. Sci.
87. RUMSHEIT, G. E. and P. BRUIN, U. S. Patent, No. 2,939,859 (1960)
88. TIFFAN, A. J. and R. S. SCHANK, U. S. Patent, No. 3,305,514 (1967)
89. SHIBAYAMA, K., Kobunshi Kagaku, 19, 219 (1962)
90. TOBOLSKY, A. V., Properties and Structure of Polymers, John Wiley, New York, 1960, pp. 68, 80
91. SPERLING, L. H., D. W. TAYLOR, M. L. KIRKPATRICK, H. F. GEORGE, and D. R. BARDMAN, J. Appl. Poly. Sci., 14, 73 (1970)
92. SPERLING, L. H., H. F. GEORGE, V. HUELCK, and D. A. THOMAS, J. Appl. Poly. Sci., 14, 2815 (1970)
93. SPERLING, L. H., V. HUELCK, and D. A. THOMAS, in Highly Crosslinked Network Polymers, S. NEWMAN and A. J. CHOMPFF, eds., Plenum Press, New York, 1971
94. Toyo Measuring Instruments Co., Ltd., Instruction Manual 17 for Rheovibron
95. WHITE, R. W., private communication, 1971
96. NIELSEN, L. E., Mechanical Properties of Polymers, Reinhold Publ. Corp., New York, 1962, p. 3
97. SPERLING, L. H., H. F. GEORGE, V. Huelck, and D. A. THOMAS Polymer Preprints, 11, (2), 477 (1970)
98. FERRY, J. D., Viscoelastic Properties of Polymers, Wiley, New York, 1961, pp. 71, 72

99. NIELSEN, L. E., Mechanical Properties of Polymers, Reinhold Publ. Corp., New York, 1962, pp. 89-92
100. TOBOLSKY, A. V. and J. J. AKLONIS, J. Phys. Chem., 68, 1960 (1964)
101. TOBOLSKY, A. V., J. Poly. Sci., C, 9, 157 (1957)
102. ROUSE, P. E., J. Chem. Phys., 21, 1272 (1953)
103. BUECHE, F., J. Chem. Phys., 22, 603 (1954)
104. BLANCHARD, A. F. and P. M. WOOTON, J. Poly. Sci., 34, 627 (1959)
105. TURLEY, S. G., J. Poly. Sci., C, 1, 101 (1963)
106. CURTIUS, A. J., M. S. Thesis, Lehigh Univ., Bethlehem, Pa. 18015, 1971
107. KERNER, E. H., Proc. Phys. Soc., B, 69, 808 (1956)
108. HASHIN, Z., J. Appl. Mech., 29, 143 (1962)
109. TAKAYANAGI, M., Plastics (Japan), 13, 1 (1962)
110. TAKAYANAGI, M. S. UWMURA, and S. MINAMI, J. Poly. Sci., C, 5, 113 (1964)
111. FUGINO, K., Y. OGAWA, and H. KAWAI, J. Appl. Poly. Sci. 8, 2147 (1964)
112. VOIGT, W., Lehrbuch der Kristallphysik, Leipzig, 1910
113. MILLER, M. L., The Structure of Polymers, Reinhold Book Corp., 1966, p. 293
114. LOSHAEK, S., J. Poly. Sci., 15, 391 (1955)
115. TOBOLSKY, A. V., D. W. CARLSON, and N. INDICTOR, J. Poly. Sci., 54, 175 (1961)
116. UEBERREITER, K. and G. KANIG, J. Chem. Phys., 18, 399 (1950)
117. FOX, T. G. and S. LOSHAEK, J. Poly. Sci., 15, 371 (1955)

118. NIELSEN, L. E., J. Macromol. Sci., C 3, 9, 69 (1969)
119. NIELSEN, L. E., Mechanical Properties of Polymers, Reinhold Publ. Corp., New York, 1962, p. 161
120. GALL, W. G. and McCRUM, J. Poly. Sci., 50, 489 (1961)
121. SPERLING, L. H., private communication, 1971
122. KAEMPF, G. and H. SCHUSTER, Angew. Makromol. Chemie, 14, 111 (1970)
123. YU, A. J., Polymer Preprints, 11, 354 (1970)
124. CURTIUS, A. J., M. J. COVITCH, D. A. Thomas, and L. H. SPERLING, to be published
125. BUCKNALL, C. B. and M. M. HALL, J. Mater. Sci., 6, 95 (1971)
126. SHIBAYAMA, K. and M. KODAMA, Kobunshi Kagaku, 24, 1 (1967)
127. SHIBAYAMA, K. and M. KODAMA, Kobunshi Kagaku, 24, 104 (1967)
128. MORAWETZ, H., Macromolecules in Solution, Interscience Publ., New York, 1965
129. THOMAS, D. A., private communication, 1970/71
130. American Society for Testing Materials, ASTM, D 1053-61

VITA

Volker Huelck was born on January 19, 1940 in Gelsenkirchen, Germany, the son of Heinz and Luise Huelck. He received his matura (Abitur) from the Mathematisch-Naturwissenschaftliches Gynmasium Herten, Germany in February 1960.

From November 1961 to April 1967 he studied at the University of Karlsruhe, Germany in the Department of Chemical Engineering (Verfahrenstechnik). He received the degree Diplom-Ingenieur in April 1967. Upon winning an exchange fellowship from the University of Karlsruhe to Lehigh University, he pursued his studies in the fall of 1967 and received the degree Master of Science in Chemical Engineering in 1969.

The author is a member of the American Chemical Society and of the Society of Sigma Xi. He is the author of four papers.

He is married to Wiltrud D. H. Huelck-Freese of Konstanz, Germany.